Paleoenvironmental Analysis of the Mangere Formation, Mangere Island, Chatham Islands, New Zealand

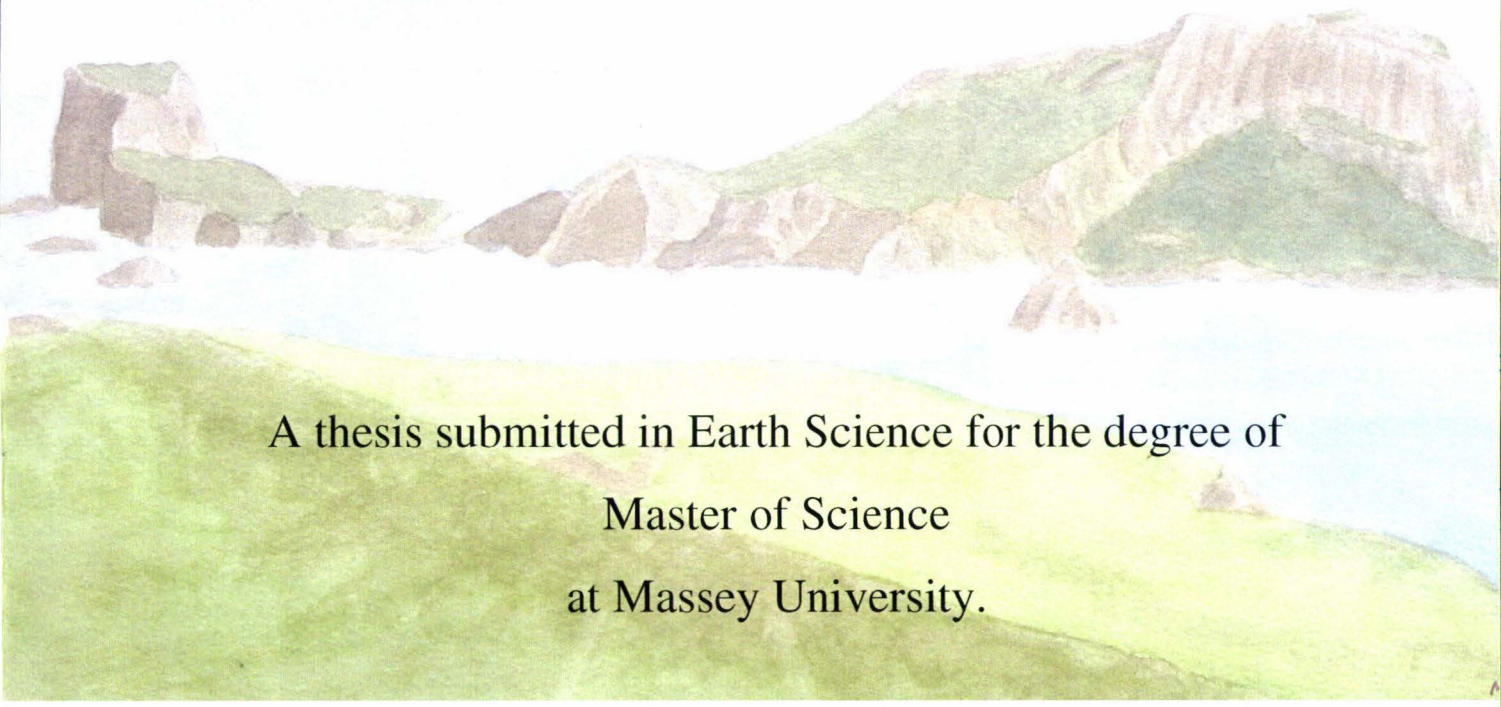

A thesis submitted in Earth Science for the degree of
Master of Science
at Massey University.

George Sydney Fletcher Davies

2006

Abstract.

Mangere Island consists almost entirely of alkali basalt of the late Miocene early Pliocene Rangiauria Formation (Campbell et al., 1993) with outcrops of the sedimentary Tupuangi Formation on the east coast and the Mangere Formation (Campbell, et al., 1993), a sedimentary remnant, mainly lacustrine but also partly marine, lying between the northeastern and southwestern groups of volcanic vents of Mangere Island:

As a result of the present work the sedimentary Mangere Formation of Campbell *et al.* (1993) has been divided into two formations, Mangere Formation and the overlying Parakeet Formation. Mangere Formation consists of (1) a Basal member (32m of mudstone), and (2) a Cyclic member (12.6m of alternating sandstones and mudstones). Parakeet Formation has (1) a Carbonaceous member (0.6m 0f organic rich mudstones), (2) a Skua member (16.8m of tuffaceous siltstone), and (3) a capping rhyolitic tephra. The Basal member of the Mangere Formation is underlain by a breccia that is texturally extremely variable (Bag End breccia).

A sedimentary outcrop on the eastern coast of Mangere Island is lithologically and mineralogically identical to Tupuangi Formation on Pitt Island as well as having the same Cretaceous pollen suite. Thus it is inferred that, at the time of Rangiauria volcanism, Tupuangi Formation and its overlying Tertiary strata extended from Pitt Island at least as far as Mangere Island.

An arm of the sea between two Mangere Island volcanic centres extended towards Waihere Bay, Pitt Island. At some time in the late Pliocene, volcanic debris avalanches from the northeast and southwest groups of vents formed a debris dam that blocked off the seaward side of the sea arm, resulting in the formation an oligotrophic fresh water lake. As a result of a low energy regime and vegetated slopes, the lake filled to *ca.* 30m with very fine sediment (the Basal member) from both the volcanics of Mangere Island and the quartzofelspathic Tupuangi Formation of Pitt/Mangere Island.

Following this a debris dam, formed by volcanic debris avalanches, was breached by a rising sea. Local marine influence in storms destablised the slopes surrounding the then shallow lake resulting in the influx of coarse sands which alternated with mudstones deposited during quieter periods (the Cyclic Member).

At the end of this period there was a eustatic fall of sea level or tectonic uplift or both, probably resulting in subaerial erosion and an unconformity between the Cyclic and Carbonaceous Members.

A second shallow fresh water lake (the Carbonaceous member) was established on the top of the Cyclic member. This lake was later overwhelmed by wind-blown material derived from a deposit of Paleocene Red Bluff Tuff exposed probably by a falling sea level or marine erosion. The reworked Red Bluff Tuff was later covered by a layer of rhyolitic tephra probably from the Taupo Volcanic Zone (TVZ), North Island, New Zealand.

The distinctive jointing pattern seen in the sandstone units of the Cyclic member resulted from doming with a principal stress directed northwest-southeast. This probably correlates with tectonic uplift in the Castlecliffian.

The lack of any positive time markers makes dating the formation rather indeterminate, but the Basal and Cyclic members (Mangere Formation) are probably upper Mangapanian and the Skua member probably Quaternary. The sequence is generally lacking in fossils, except for palynomorphs which occur throughout, and ostracods which occur only in the Cyclic member. Neither proved useful for dating the sequence.

The pollen diagrams show a consistent coastal plant association of small trees, shrubs, herbs and ferns throughout the history of the sequence, with the implication that climate during this time did not vary greatly from a mild, moist, equable mean.

Acknowledgments.

My grateful thanks to my supervisors, Prof. V.E. Neall and Dr. Clel Wallace, for their patience, support, and helpful discussions. Thanks also to the Marsden Grant and the Chatham Emergent Arc Research Survey (ChEARS), without which this study could not have been undertaken.

My thanks also to Alison Davies and the staff of DOC on Chatham Islands for their unfailing interest, cooperation, and help both on Mangere Island and with the loan of equipment. Thanks also to Bill Carter for making his residence freely available to me.

Special thanks to Juliet Cox and the Soil and Earth Sciences secretary, Moira Hubbard, for cheerfully and adroitly steering me through my computer problems; to Michael Turner for microprobing the tephra and hornblendes; to Kat Holt for discussions and resources related to the Chatham Islands; to Kevin Butler for his valuable and cheerfully given help with palynology; and to Tristan Davies for help with Paintshop Pro.

My thanks also to the technicians Carolyn Hedley, Ian Furkert, Bob Toes, Glenys Wallace and Anne West for their help, friendliness and advice in the laboratory. Thanks to my fellow students, Juliet Cox, Kim Martelli and Seth Laurenson for an interesting year of discussions, help and friendship. Special thanks to fellow student Deborah Crowley, who has been a good friend and colleague.

Finally my grateful thanks to my wife, Megan, for her patient support, advice, proof reading, and the water colour of Mangere Island on the title page.

Contents

Figures.

Tables.

Chapter 1.

Introduction.

1.0.0 Aims.

The primary aims of this study were to:

- Provide a detailed description of the stratigraphy of the Mangere Formation (as defined by Campbell *et al.* (1993).
- Determine the areal extent of the Mangere Formation
- Determine the provenance of the Mangere Formation
- Explain the palaeohistory of the Mangere Formation
- Determine the palaeoclimate at the time of deposition of the Mangere Formation, using palynology and other microfossils
- Determine the time of deposition of the Mangere Formation.

1.1.0. Thesis structure.

This thesis comprises five chapters. Chapter 1 is an introduction to the study area. It covers the aims of the study, and the location of the study area, together with notes on the history and physiography of Mangere Island, plus some background on Mangere Island's conservation importance. The regional geology of the Chatham Islands, and especially Pitt Island, is briefly covered as this is relevant to the Mangere Island study. Finally, in Chapter 1, previous geological work on Mangere Island is covered. Chapter 2 details and explains the methods of field and laboratory work used in the study. Chapter 3 details the results of field and laboratory work and includes stratigraphic columns of the Tupuangi and Mangere Formations on Mangere Island. Chapter 4 discusses the results of field and laboratory work given in chapters 2 and 3, and reconstructs the palaeohistory of the Mangere Formation as a series of maps. Chapter 5 details the conclusions of the study and relates them to the Haq *et al.* (1987) sea level curve.

1.1.1. Location of the study area.

The Chatham Islands are located approximately 850 km east of Christchurch (Fig. 1). The main economic activity is fishing (blue cod, crayfish, paua) and sheep farming for wool. The islands were originally inhabited by the Moriori. In the mid-

nineteenth century they were settled by Europeans and in 1835 the Moriori were largely displaced as a result of a Maori invasion from mainland New Zealand (King, 1990).

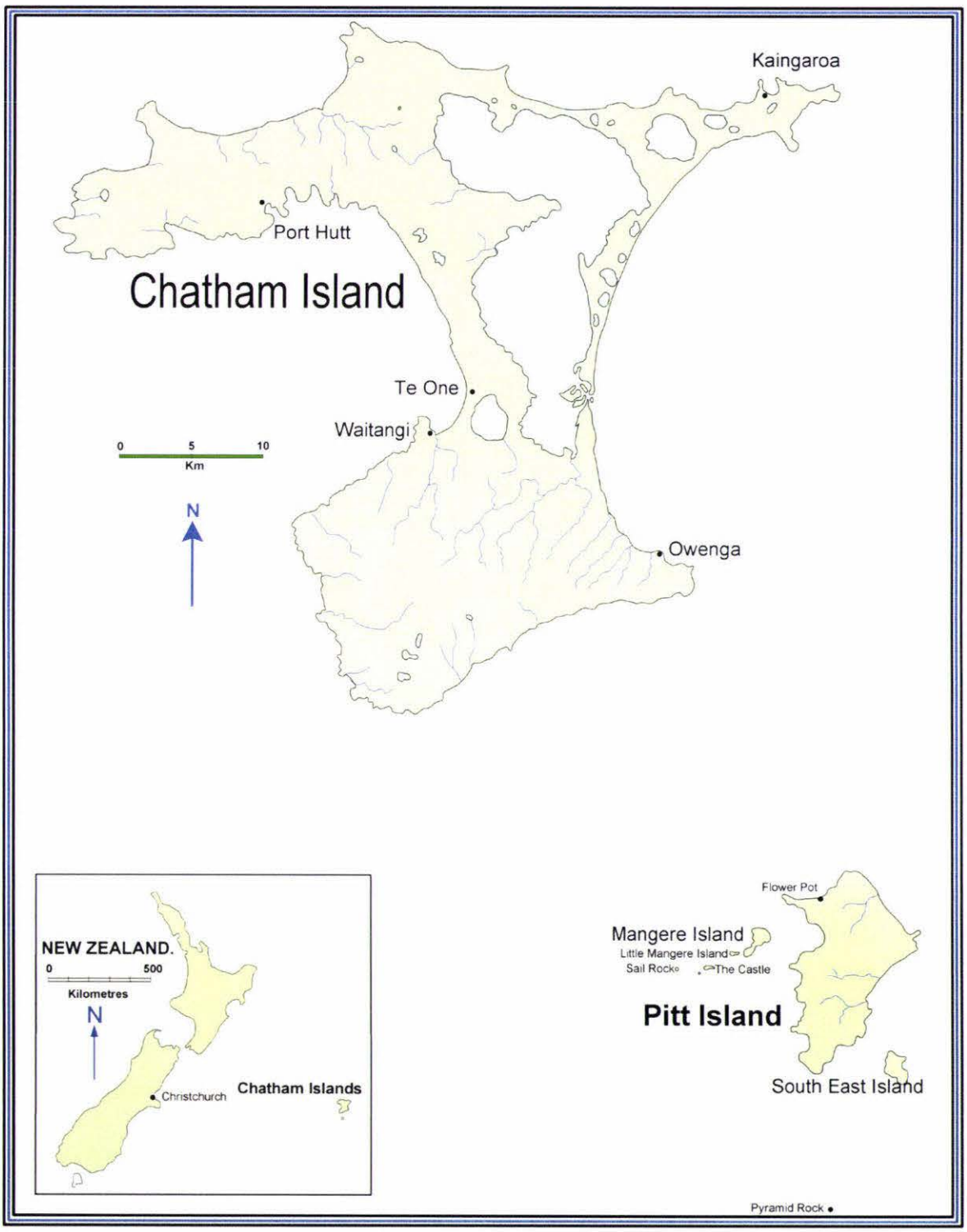

Figure 1. Chatham Islands location map.

The largest island is Chatham Island, over 50% of which is covered in blanket peat, followed in order of decreasing size by Pitt Island, South East Island, and Mangere Island (the object of this study), as well as many smaller islands, rocks, and reefs.Mangere Island lies 2.3 km off the west coast of Pitt Island. It is approximately 2.3 km long and 1.2 km at its widest (Fig. 2). Associated with it are a number of smaller islands, the most prominent of which are Little Mangere Island, The Castle, Pyramid Rock, and Sail Rock (Fig. 1), as well as a number of small rocks and reefs. These islands and rocks are all volcanic and of Late Miocene or Early Pliocene age, except for the sedimentary Tupuangi (Cretaceous) and Mangere Formations (upper Pliocene) on Mangere Island.

1.1.2. Mangere Island, historical and biological background.

Mangere Island was largely forested until the 1890's when the forest was cleared for sheep farming which continued until 1966 (Atkinson 2003). The island was made a nature reserve in 1967 (Atkinson, 2003), and an extensive reafforestation programme of mainly Chatham Island akeake (*Olearia traversii*) was initiated. The present vegetation is broadly, akeake forest, koromiko scrub, flaxland, herbfields, and introduced grasses. Between 1970 and 1989 (Atkinson 2003) Chatham Island snipe, black robins, shore plover, and Chatham Island tomtits were reintroduced. The Island is also important for several threatened species of invertebrate; the Rangatira spider, the coxella weevil which lives on the last remaining area of Dieffenbach's speargrass found only on Mangere Island, the giant click beetle (*Amychus candezei*) as well as a flightless carabid beetle (*Mecodema alterans*), a nocturnal flightless stag beetle (*Geodorcus capito*), plus a number of moths. Skinks are abundant on the island. In addition to the above mentioned birds there are sooty shearwaters, fairy prions, broad billed prions, black-winged petrels, blue penguins, Chatham Island oyster catchers, Pitt Island shags, red-billed gulls and white-fronted terns. Land birds include brown skua, Forbes parakeet, and Chatham Islands warblers, tuis, and parakeets.

1.1.3. Mangere Island Physiography (Figs.2 and 3).

The Island can be divided into 3 major topographic units:

1. A top plateau to the north, bounded on its northern and western sides by 200 metre-high cliffs of massive resistant breccia which rise almost vertically from the sea. The eastern side of the plateau falls precipitously to Black Robin Bush where huge blocks fallen from the cliff above are scattered on a colluvial footslope that extends to the shoreline.
2. To the south, the top plateau gives way to the more gently sloping Douglas Basin and this merges into:
3. A long narrow, generally steep sided southwest-trending peninsula with a central ridge attaining a height of no more than 100 m. The lowest part of this peninsula is occupied by the Mangere Formation (as defined by Campbell *et al.* 1993), a flat lying sedimentary sequence, 350 metres long and averaging about 175 metres wide with the highest point at 72 m.a.s.l.(metres above sea level) (Figs. 2 and 3). The lower part of the formation is a skirt sloping away from a layered sequence at about 40° (Figs. 4 and 5). The cliff face of the layered sequence slopes at about 60° and the upper part is near vertical.

Although the prevailing wind direction is southwest, northwesterlies are frequent. The western side of the island is thus subject to a high frequency of rough seas which account for the steep cliffs of the indurated northern massif of Mangere Island and Little Mangere Island, as well as wave-cut platforms which occur only on the southwest-trending peninsula and are also partly a consequence of its much less consolidated lithology.

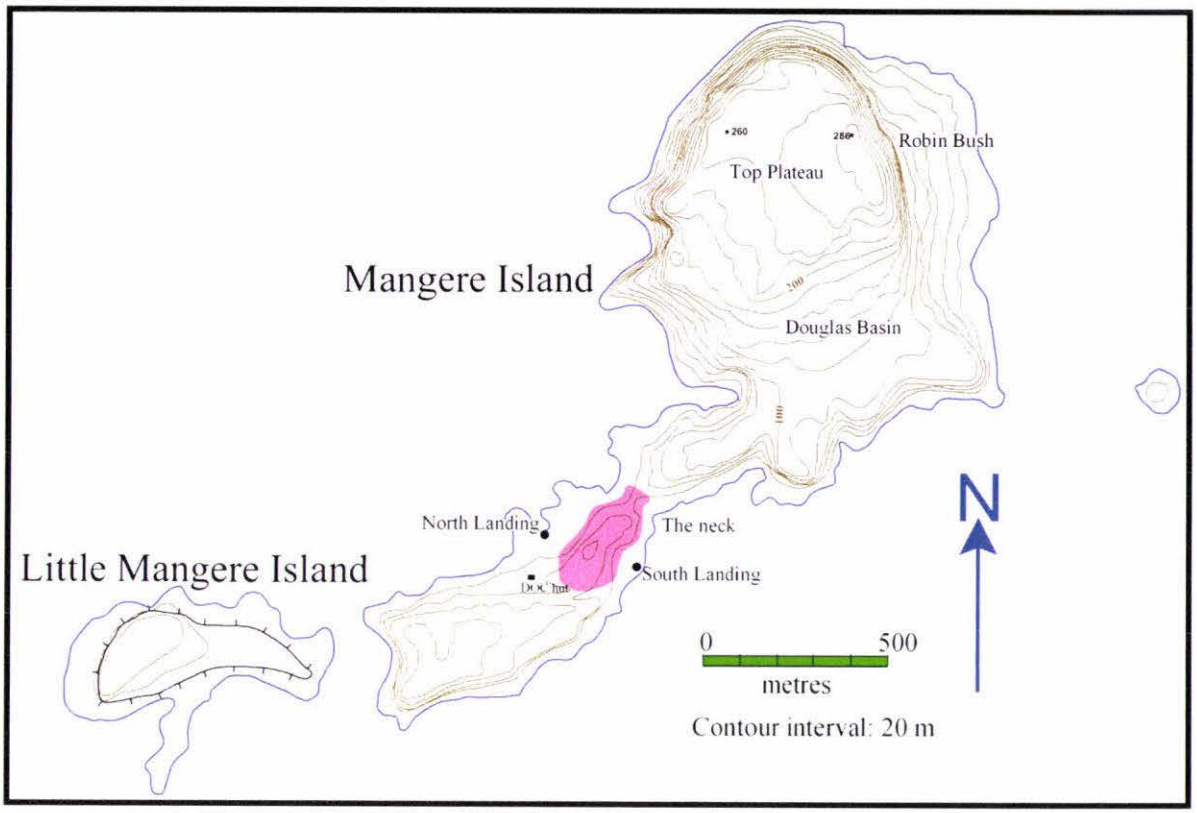

Figure 2. Location map for Mangere Island showing the extent of Mangere Formation (maroon colour). The place names on Mangere Island are informal names used by local people and the Department of Conservation.
The "tick" symbol on little Mangere Island indicates a vertical rock face.

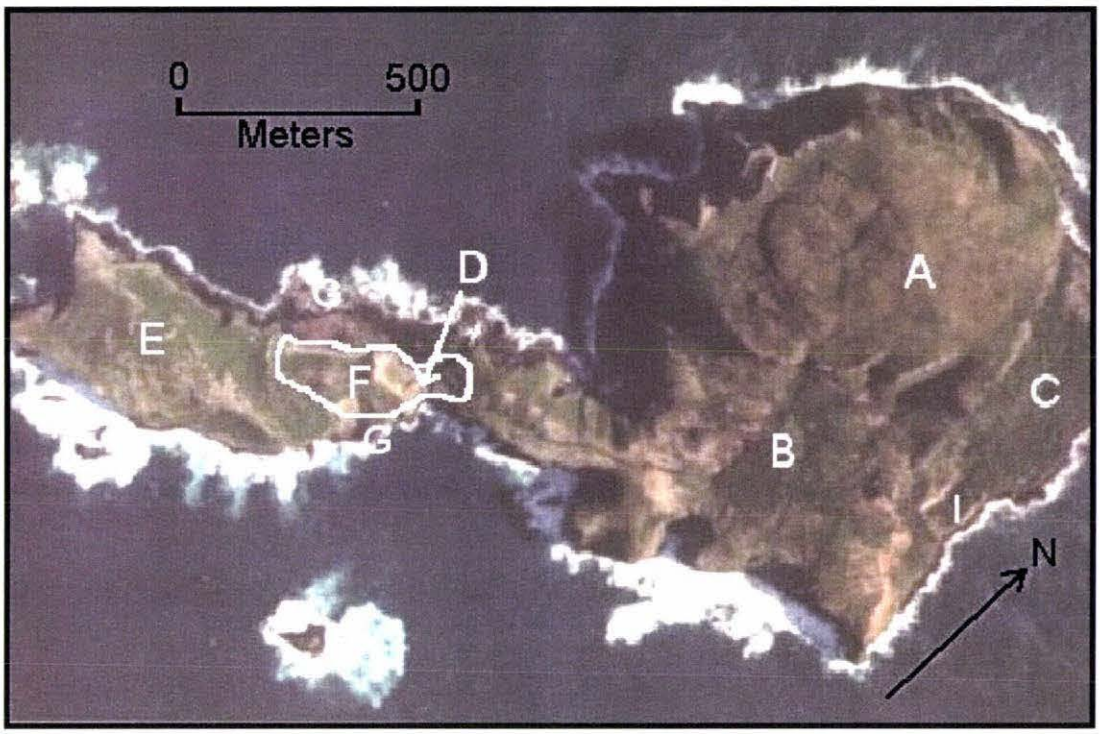

Figure 3. Aerial photo of Mangere Island showing: A; Top Plateau, B; Douglas Basin, C; rockfall footslope (covered by Robin Bush), D; The Neck, E; the lower peninsula, F; the extent of the Mangere Formation, G; wave cut platform, I; Tupuangi Formation. The green lines on the Top Plateau and the lower peninsula are akeake hedges planted as part of a Department of Conservation (DOC) reafforestation programme. Photo: Dept. of Lands and Survey.

Figure 4. View of Mangere Formation taken from the North Landing. The DOC hut is the white object at the extreme centre right of the photograph and The Neck is at the extreme left. The North Landing is marked by the "X"at centre foreground. The South Landing is opposite this on the other side of the Mangere Formation. The photograph was taken from the seaward edge of the wave-cut platform.

Figure 5. View of Mangere Formation taken from Douglas Basin looking southwest along the lower peninsula. The Mangere Formation remnant is the hill in the centre of the photograph. The North Landing is marked with an "X" at the end of the inlet in the wave-cut platform just below the hut at the centre right. The South Landing, "Y", is on the wave-cut platform at the centre left of the photograph. Little Mangere Island is at the top right hand corner. (Photo: Mark Bellingham).

1.2.0. Regional Geology.

Introduction.

The Chatham Islands lie on the easternmost emergent structural high of the Chatham Rise. The Chatham Rise is a shallowly submerged (to about 400 m along its crest) block of continental crust which was probably formed at the edge of the proto-Pacific plate when it was Gondwana (Campbell *et al.* 1993, p. 29). Structurally the Chatham Rise extends about 250 km to the east of the Chatham Islands and 950 km west to the Alpine Fault and is about 100 km wide. The Rise was originally part of Gondwana and probably adjacent to Antarctica. The Rise is bounded to the north by

the Hikurangi Plateau and to the south by the Bounty Trough. The Mernoo Gap at the western end of the Rise is part of a foreland basin which includes the Canterbury Plains and shelf and which developed during Late Miocene time (Fig. 6). The Chatham Islands is the only emergent area on the Rise. There is no satisfactory explanation for this at present although the Islands themselves may be the result of thermal uplift associated with Late Cretaceous volcanism. In the past the Veryan and Mernoo Banks may have been emergent as there is evidence of erosion on them (Campbell *et al.* 1993).

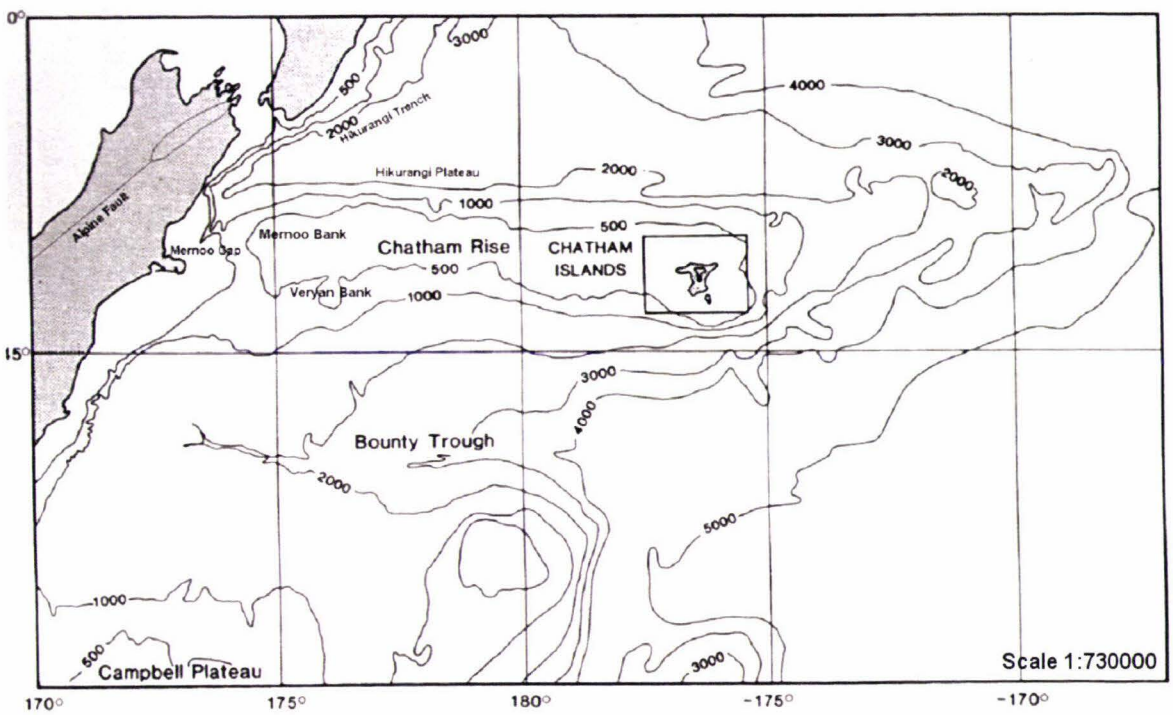

Figure 6. Regional bathymetry and tectonic features of the Chatham Rise (adapted from Wood and Anderson 1989: p. 269).

A useful way of visualising the geology of the Chatham Islands is given in Figure 7 from which it is clear that the geology of the Chatham Islands is subject to many hiatuses. The stratigraphic abbreviations used in the text refer to the geological map (Campbell *et al.* 1993) of the Chathams and its key (Figs. 8 and 9). A number of minor stratigraphic units which do not occur on either Pitt Island or Mangere Island will be only briefly discussed for completeness. Much of what follows is adapted from Campbell *et al.* (1993).

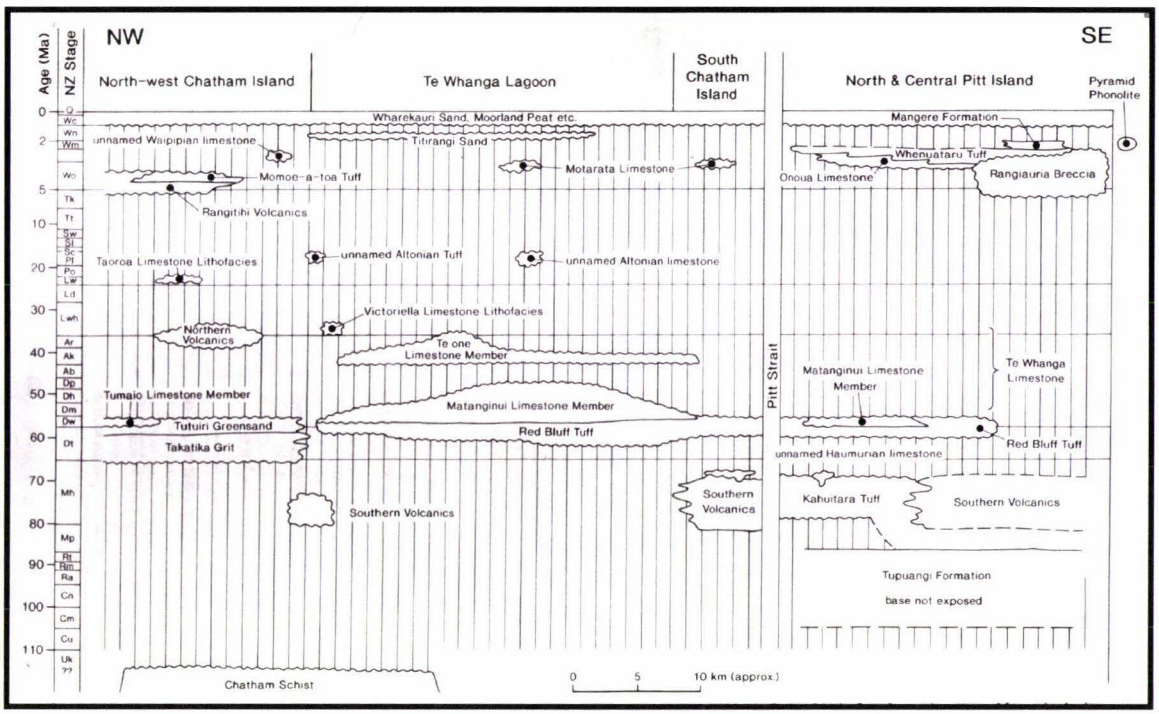

Figure 7. Space-time diagram showing the general relationships of known stratigraphic units in the Chatham Islands. (From Campbell *et al.* 1993, p12).

Chatham Schist (bc).

During the Permian and Triassic (perhaps earlier), volcanic and quartzofeldspathic sediments were deposited in a deep marine environment on the margin of the proto-Pacific plate where burial transformed them into greywacke and argillite. During the Mid-Jurassic (*ca.* 164 Ma) they were largely metamorphosed to schist (Adams and Robinson 1977, p. 296) as a result of a major collision between these quartzofeldspathic Torlesse terrain sediments and the Caples/ Aspiring and Murihiku terrains thus forming the future basement of the Chatham Rise and Chatham Islands. This basement also underlies Mangere Island as is demonstrated by schist xenoliths in the Rangiauria Breccia.

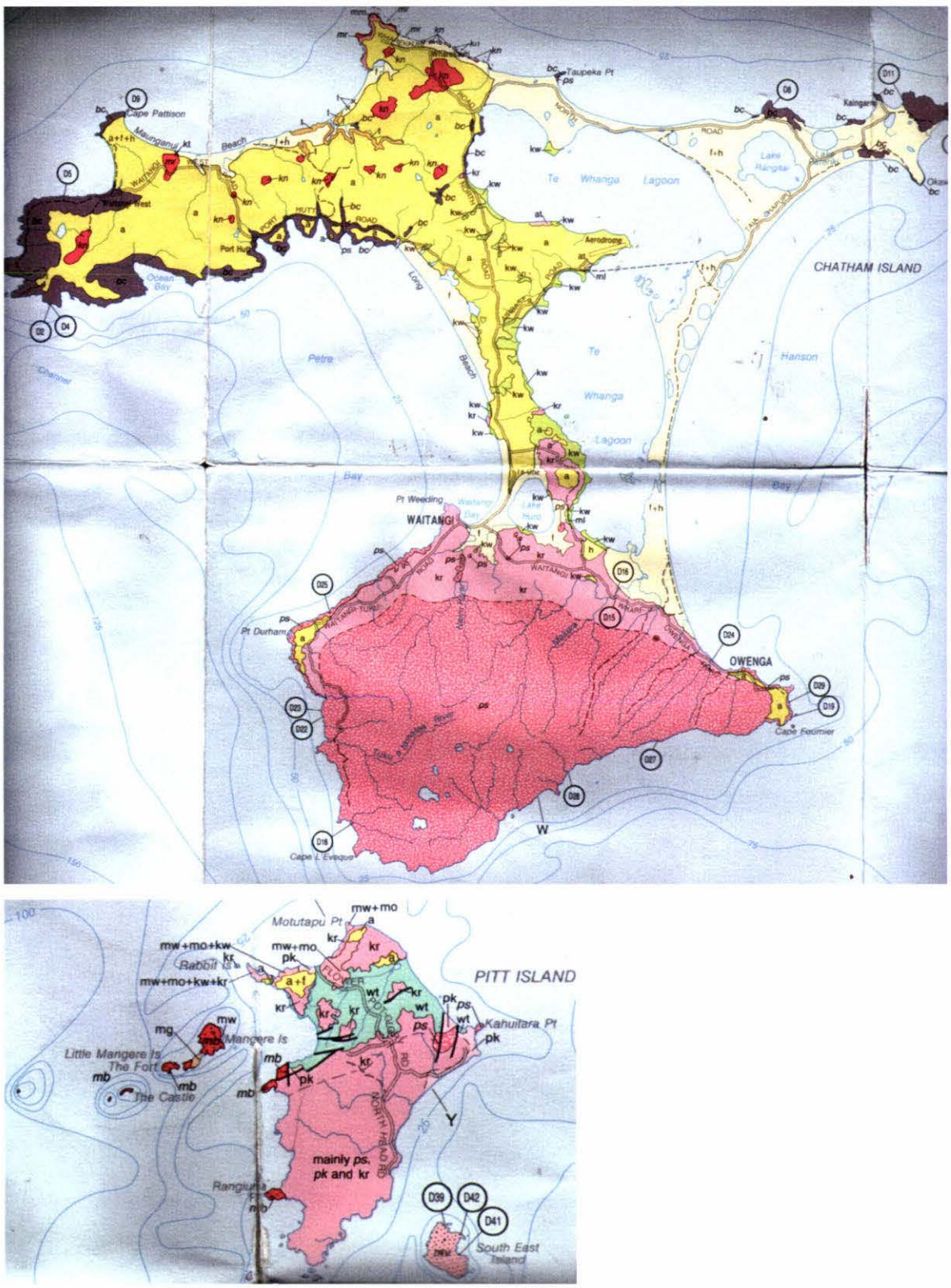

Figure 8. Geological map of the Chatham Islands. (from Campbell *et al.* 1993).

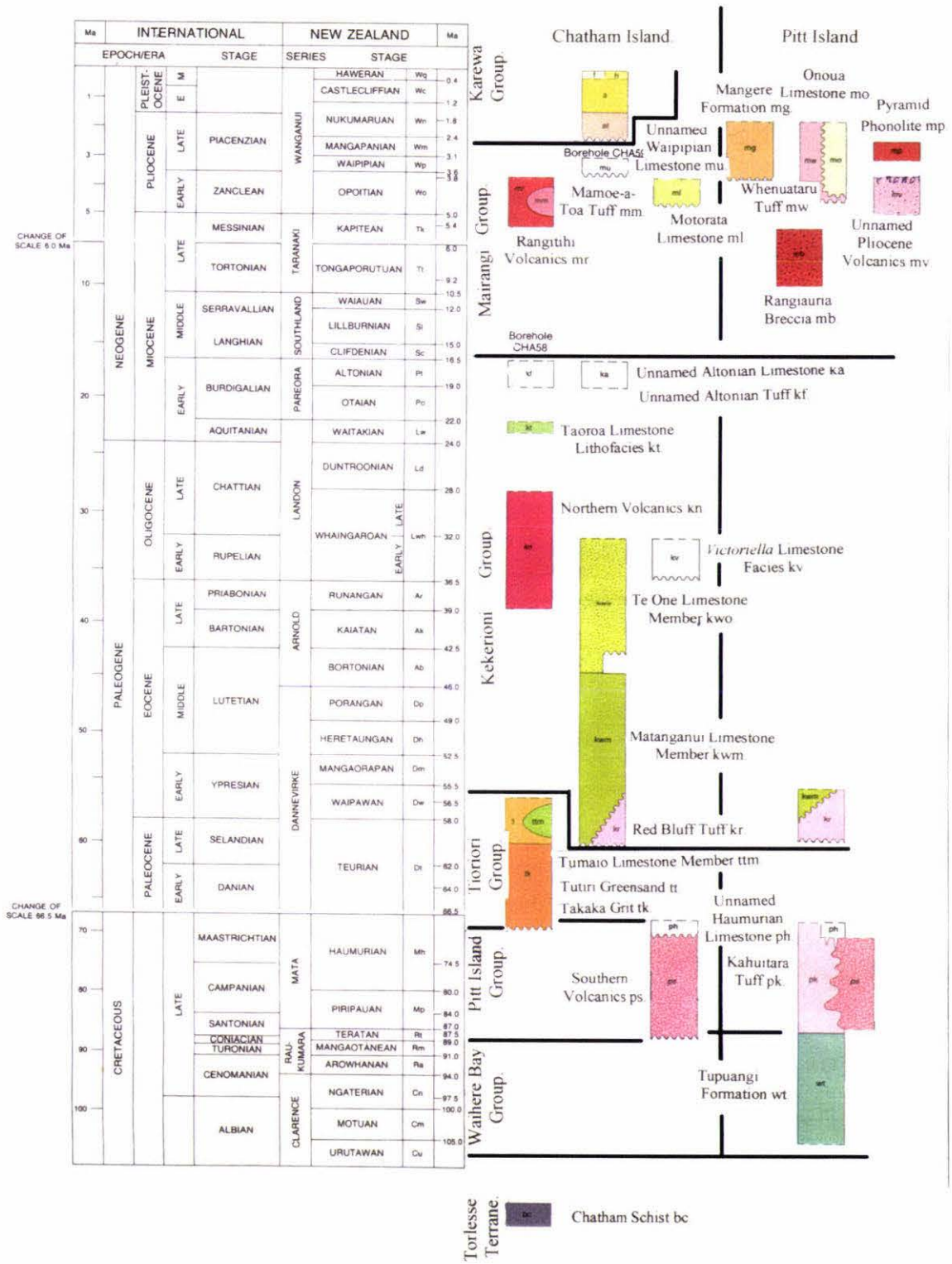

Figure 9. Key to geological map of Chatham Islands (Fig. 8). (modified from Campbell *et al.* 1993).

Based on an assumption that there is no fault in Pitt Strait and with a uniform dip of 1° of the schist surface from Chatham Island, Campbell *et al.* (1993, p 128)

estimated the schist would be 830-900 m below sea level at Mangere Island. However, the situation is more complicated at Pitt and Mangere Islands since (a) the well exposed Tupuangi Formation on Pitt Island suggests there is a fault in Pitt Strait and (b) as a result of faulting and doming in the Pitt/Mangere area, the Tupuangi Formation dips generally somewhat less than 20° to the southeast on Pitt Island and 14° to the northwest on Mangere Island. Further, the Tupuangi Formation on Mangere Island is faulted with an unknown downthrow to the south where it underlies the Mangere Formation. Thus, under the northern part of Mangere Island the schist is probably considerably nearer the surface but dipping to the west, and under the southern part of the island the schist is an unknown amount deeper, but presumably with a similar attitude.

It is probable that the whole Chatham Rise has always been proximal to the Pacific Plate boundary (Campbell *et al.*, 1993, p 29). There is seismic reflection evidence that the basement of the Hikurangi Plateau may dip beneath the Chatham Rise with the possibility that it was once a convergent margin (Bradshaw *et al*, 1981, Campbell *et al.*, 1993, p 30). However this is not upheld by King (2000) who shows no convergence along the northern margin of the Chatham Rise in his series of reconstructions of the New Zealand area. The southern margin of the Rise borders the Bounty Trough which was formed by rifting in mid-to-late Cretaceous times (105 to 75 Ma), (Wood *et al.*, 1989, p 281) accompanied by rifting and tensional crustal thinning. This tension, in turn, resulted in east-west horst and half-graben structures on the eastern Rise which are major controls on the present geology of the Chatham Islands. The rifting which began in the Lower Cretaceous resulted in the separation of the New Zealand continental area from Gondwana in the Upper Cretaceous (85 to 87 Ma). The Chatham Rise, as part of the Pacific Plate, began its rotation to its present position at this time.

Waihere Bay Group (w).

While still part of Gondwana the half grabens were mainly filled (87 to 105 Ma) with horizontal quartzofeldspathic sediments of Tupuangi Formation which now dip gently south to southeast (Fig. 8). Tupuangi sediments are generally grey to dark grey and poorly consolidated with an estimated thickness of at least 700 m (Campbell *et al.*, 1993, p 37).

They are best exposed as a series of fault blocks in Waihere Bay opposite Mangere Island. The sediments include conglomerate with discoid pebbles near the base, silty sandstones, sandy siltstones and lignite with some basalt and rhyolite volcaniclastics. They are generally rich in pollen, leaves, and wood with rare macrofossils at the base. They are tuffaceous near the top and gradually grade into the massive Kahuitara Tuff. From palaeocurrent trends (Campbell *et al.* 1993) the sediments appear to have been derived mainly from the slowly prograding delta of an emergent landmass the north northeast (Fig. 10). These sediments appear to have come from a Permian–Triassic source, as reworked Permian–Triassic palynomorphs are found in both the Tupuangi Formation and the Kahuitara Tuff (Mildenhall and Crosbie 1981 pp.2-23; Mildenhall 1983 p.165). At this time it is thought that much of the Rise was emergent (Campbell *et al.* 1993 pp. 29, 41, 43). The Tupuangi Formation is nowhere exposed on Chatham Island and its base is not exposed on Pitt Island. Offshore seismic evidence and velocity data (Austin *et al.* 1973; Wood and Ingham 1981; Campbell *et al.* 1993 p. 35) suggest that older unexposed sedimentary sequences of inferred Cretaceous age underlie the Tupuangi Formation and may be the provenance from which the lowest units of the Tupuangi Formation are partly derived. These studies also show that there is an unconformity between these units and the Chatham Schist. The Tupuangi Formation is shown in this study to be present on Mangere Island.

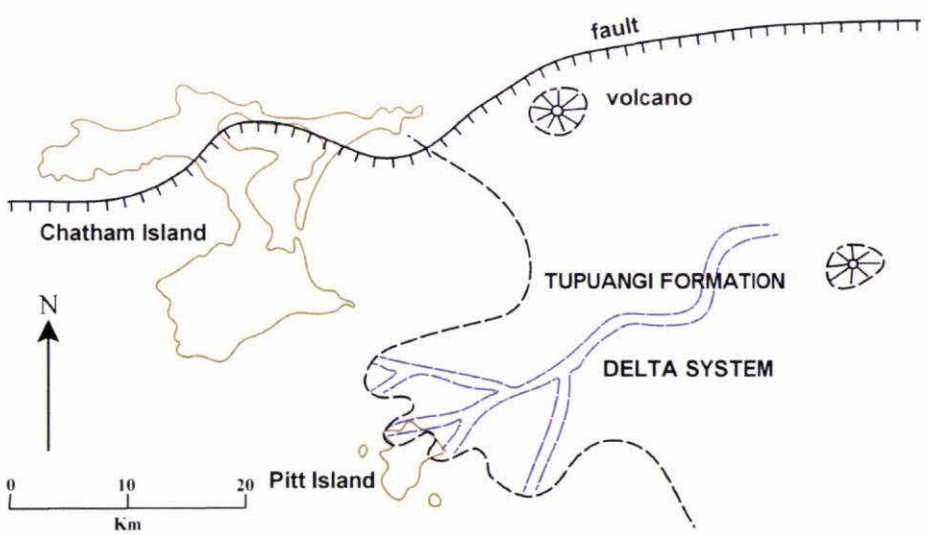

Figure 10. Paleogeographic reconstruction of the Chatham Island area during Tupuangi time (from Campbell *et al.* 1993 p. 41). This study shows that Tupuangi Formation extended at least as far west as Mangere Island.

Pitt Island Group (p).

Introduction.

The Pitt Island Group immediately, and mainly conformably, followed the deposition of the Tupuangi Formation. It represents a prolonged episode of volcanism which occurred from *ca.* 87 to 70 Ma in the Upper Cretaceous (Campbell *et al.* 1993, p. 54). It consisted of basaltic flows together with the deposition of Kahuitara Tuff and an unnamed Haumurian limestone. These lithologies consist of the southern portions of Chatham Island and Pitt Island and probably underlie or extend out towards Mangere Island. It was at this time that crustal extension finally separated the New Zealand continental area from Gondwana. Thermal uplift from late Cretaceous volcanism resulted in the raising and emergence of fault blocks. Evidence for this includes the basement horsts which are exposed in Chatham Schist, northwestern Chatham Island, and graben fill on Pitt Island. Graben filling ceased during latest Cretaceous time with minor folding, peneplanation, thermal subsidence and eruption of the Southern Volcanics in the form of several large alkaline volcanoes (Campbell *et al.* 1993 p. 29). Following this there was a period of widespread mild tectonism in the Palaeocene/Eocene when Cretaceous normal faults were reactivated, especially to the west, and the clastic Red Bluff Tuff was deposited. Through most of the Tertiary, periods of limestone deposition (xenoliths from some of these are common in the Rangiauria Breccia on Mangere Island), alternated with periods of volcanism interspersed with prolonged periods of non-deposition or erosion between episodes as is shown in Figure 7. Little appears to be known of what happened during these non-depositional periods.

Kahuitara Tuff (pk).

There are no known outcrops of Kahuitara Tuff on Chatham Island. The Tuff is brown-grey and massive to well bedded. It consists of volcaniclastic sandstone, scoriaceous conglomerate, and lapilli tuff of basaltic composition, with bombs in the basal units. Its thickness is *ca.* 225 m and it is unconformable with the Tupuangi Formation to the northeast but is conformable in northwestern Pitt Island (Campbell *et al.* 1993 pp. 50,55). Fissure fill of an unnamed Haumurian limestone contains foraminifera of outer shelf depth (100 – 200 m). The Kahuitara Tuff contains macrofossils and a shallow water (5 to 50 m) foraminifera fauna which indicates

deepening in Haumurian time (Strong and Edwards 1979 p. 615; Campbell *et al.* 1993 p. 50). Faulting in the tuff is probably associated with the late Miocene/early Pliocene volcanism that produced Mangere Volcano, and Waihere and Rangiauria Heads (Campbell *et al.* 1993 p. 53). At eastern Pitt Island, deposition of Kahuitara Tuff was interrupted at *ca.* 80 Ma (middle Piripauan; early Campanian) by the extrusion of a thick olivine basalt (Southern Volcanics). In northwestern Pitt Island deposition of Kahuitara Tuff continued contemporaneously with the extrusive volcanism, both ceasing at about 70 Ma (late Haumurian; early Maastrichtian) (Campbell *et al.* 1993 p. 55).

Southern Volcanics (ps).

Extensive areas of Southern Volcanics are found in the south of Chatham Island where they attain a thickness of 300 m, and also to the south and east of Pitt Island where they attain a thickness of at least 150 m. The volcanics consist essentially of alkaline olivine basalt hawaiites, (Morris, 1985a, p 255) dominated by flows 5-10 m thick on Chatham Island, and 5-20 m thick on Pitt Island, where tuff and scoria deposits alternate with the flows. Columnar jointing, pillow basalt, agglomerate, breccia, hyaloclastite, trachyte and basalt dikes are common. There is no fossil content (Campbell *et al.* 1993 p. 57). This unit is of Haumurian age, and is subaerial and shallow marine. Volcanism ceased at about 70 Ma (late Haumurian) and a period of non-deposition or erosion that lasted 4 m.y. ensued (Campbell *et al.* 1993 p. 57). The source of the Kahuitara Tuff and Southern Volcanics is in southern Chatham Island or beneath Pitt Strait. This has been determined from flow sequences (Hay *et al.* 1970; Morris 1985a p. 254) and magnetic survey data (Austin *et al.* 1973; Yakunin and Schoernharting 1971 (quoted in Campbell *et al*, 1993); Campbell *et al.* 1993 p. 57 Strong and Edwards 1979 p. 615). Associated with the tuff are the carbonate minerals dolomite, ankerite and siderite. Its age is late Haumurian.

Tioriori Group (t).

Introduction.

This group is not related to Pitt or Mangere Island stratigraphy but is mentioned briefly for completeness. The Tioriori Group is Haumurian to early Waipawan in age and includes Takitika Grit, Tutuiri Greensand, and Tumaio

Limestone Member. It is restricted to northwestern Chatham Island and rests unconformably on Chatham Schist. It consists essentially of a thin sequence of non-tuffaceous, quartzofelspathic, schist-derived very coarse sandstone, sometimes rich in authigenic minerals, and includes minor bioclastic limestone bodies (Campbell *et al.* 1993 p. 60).

Kekerione Group (k).

Introduction.

Kekerione Group (represented on Mangere Island as xenoliths in Rangiauria Breccia) is "...a widespread but discontinuous, essentially volcaniclastic succession of fossiliferous marine palagonitic tuff, tuff breccia, minor basalt flows, and associated bioclastic limestone which ranges in age from Paleocene to Oligocene. The group includes nine units: Red Bluff Tuff; TeWhanga Limestone with at least two members- Matanginui Limestone and Te One Limestone; Northern volcanics; two restricted limestone lithofacies lenses – *Victoriella* Limestone and Taoroa Limestone; an unnamed Altonian tuff and an unnamed Altonian limestone" (Campbell *et al.* 1993 p. 73).

Red Bluff Tuff (kr).

Red Bluff Tuff is at least 100 m thick and covers large areas of Chatham and Pitt Islands. It is fossiliferous and largely marine. It was possibly derived from Surtseyian-type volcanism (Campbell *et al* 1993 p. 88) and this study shows that it may have supplied material to the Mangere Formation as defined by Campbell *et al.* (1993). It is essentially a calcareous tuff of basaltic composition containing beds of lapillistone and tuff-breccia. It is generally a yellow-brown to brick-red colour but basal parts are dark green and grey-brown. It is generally well bedded with cross bedding and graded bedding indicative of water sorting. Red Bluff Tuff unconformably overlies the Southern Volcanics and Kahuitara Tuff and is unconformably overlain by all units younger than the Matanginui Member. Fossil evidence shows it to be coeval with Tutiri Greensand. Its age is late Paleocene to early Eocene. It has a rich fossil content of spores, pollen, foraminifera, calcareous nanofossils, sponges, corals, bryozoans, brachiopods, bivalves, nautiloids, echinoderms, teeth, and trace fossils from many localities, giving an age of late

Teurian to late Waipawan. Cross-bedding is common suggesting shallow marine deposition with a northeast-southwest current regime. On the other hand the fossil evidence suggests a mid-shelf to bathyl environment (Campbell *et al.* 1993 pp. 74, 75, 88).

Te Whanga Limestone (kw).

Introduction.

Te Whanga Limestone includes Matanginui Limestone Member, Te One Limestone Member and Undifferentiated Te Whanga limestones (some outcrops are undifferentiated and cannot be assigned to either member).

Matanginui Limestone Member (kwm).

Matanginui Limestone is, "... a soft, white, poorly bedded bryozoan-echinoid-formaminiferal-bivalve packstone" (Campbell *et al.* 1993 p. 89). It is at least 35 m thick and is the lower member of Te Whanga Limestone. It is conformable, or interfingers with Red Bluff Tuff and is disconformable with overlying units. It was deposited in the Waipawan-Bortonian in moderately deep oceanic water, although the presence of *Asterocyclina*, a warm relatively shallow water species in some beds may indicate changes in water depth (Campbell *et al.* 1993 p. 95). On Mangere Island it appears as large xenoliths in the Rangiauria Breccia.

Te One Limestone Member (kwo).

Te One Limestone Member is a pale, soft, massive, porous bryozoan grainstone. It is pale yellow to medium orange-grey and is found only on Chatham Island. It was deposited in the Kaiatan to early Whaingaroan and is greater than 25 m thick. It disconformably overlies the Red Bluff Tuff and the Matanginui Limestone. It is also disconformably overlain by Motorata Limestone and the Karewa Group. The fossil assemblage is mid-to-outer shelf and includes vertebrate bones and teeth, bryozoans, brachiopods, bivalves, barnacles, and echinoderms (Campbell *et al.* 1993 pp. 88, 89, 95, 98, 102).

Northern Volcanics (kn).

This group is not directly related to Pitt or Mangere Island but is briefly mentioned for completeness.

Northern volcanics are made up of cones up to 140 m high standing directly on the Chatham Schist, and are overlain by Karewa Group sediments. The cones are made up of massive, extrusive, limburgitic basalt, plus extrusive agglomeritic and scoriaceous deposits. The massive flows are pale grey to black when unweathered but are usually weathered to brown. Accompanying volcaniclastic deposits are strong reds and browns. The deposits are unfossiliferous but radiometric dating shows them to be of Eocene- Oligocene age. The volcanic products suggest Strombolian type episodic flow and diatreme volcanism (Morris 1985b; Campbell *et al.* 1993 p. 107).

Mairangi Group (m).

Introduction.

Mairangi Group is largely volcanic limburgitic basalt with richly fossiliferous volaniclastics and tuffs as well as some bioclastic limestone. The group includes Rangitahi Volcanics, Momoe-a-toa Tuff, Rangiauria Breccia, Mangere Formation, Whenuataru Tuff, Onoua Limestone, Motorata Limestone, Pyramid Phonolite, an unnamed Waipipian limestone and unnamed Pliocene volcanics.

Rangitihi Volcanics (mr).

The limbugitic, basaltic, Rangitihi Volcanics are composed of massive extrusive and intrusive rocks with associated agglomerate, scoriacious and tuffaceous deposits. They are at least 100 m thick and were initially submarine, with later pyroclastic deposits above sea level. The unit is unfossiliferous. Radiometric ages range from $4.54^{\pm}$ 0.3 Ma to $5.3^{\pm}$ 0.4 Ma (Campbell *et al.* 1993 p.117) and average 5 Ma. Thus the unit is Late Miocene to Early Pliocene in age.

Momoe-a-toa Tuff (mm).

Momoe-a-toa Tuff is made up of dark grey, medium yellow-brown and medium red-brown hornblende-rich, fine to coarse volcaniclastic sandstone and

limburgitic basalt tuff. It appears to be greater than 120 m in thickness, is marine and richly fossiliferous. It rests unconformably on the Rangitihi Volcanics and is disconformably overlain by Rangitihi Volcanics and/or Kawera Group sediments. The macro-and micropaleontological evidence suggests a mid-to-inner shelf environment of deposition (Campbell *et al.* 1993).

Rangiauria Breccia (mb).

Rangiauria Breccia is found at Rangiauria and Waihere Heads, and at the south end of Pebbly Beach on Pitt Island and on Mangere Island. The Breccia is Late Miocene and comprises hard, dark grey-brown massive to crudely bedded, poorly sorted, coarse, pyroclastic breccia of limburgitic basalt composition. It contains very large crystals of hornblende and has an abundant xenolith component of igneous, metamorphic and sedimentary lithologies derived mainly from the Waihere Bay, Pitt Island, Kekerione, and Mairangi Groups. On Mangere Island it is the source of much of the material making up the Mangere Formation. Grain size is from large boulders to fine sand with highly vesicular smaller basalt clasts. Thickness is greater than 300 m. It is unconformable with all older units and is disconformably overlain by Whenuataru Tuff and units of the Quaternary Karewa Group. Often the clasts are set in a matrix of finely comminuted debris but elsewhere the clasts are surrounded by limburgite. It contains some wood fossils and fossiliferous limestone xenoliths Campbell *et al.* (1993).

Motarata Limestone (ml).

Motarata Limestone is early Pliocene in age and is pale yellow-brown, massive, soft, well sorted, sandy fine foraminiferal grainstone with a basal layer of phosphorite pebbles. It is more than 5 m thick and rests disconformably on Red Bluff Tuff. Fossil evidence shows it was deposited on the mid-to-outer shelf Campbell *et al.* (1993).

Onoua Limestone (mo).

Onoua Limestone, early (?) to late Pliocene, is a white to pale yellow, massive, soft, porous, well sorted, glauconitic fine bryozoan grainstone, composed of

bryozoans, foraminifera, brachiopods, bivalves and echinoderm fragments. It is at least 26 m thick and is unconformable with the Red Bluff Tuff and Matanginui Limestone, but is conformably and gradationally overlain by Whenuataru Tuff and in places interfingers with it. It was deposited on the outer part of an oceanic platform at depths of mid-to-outer shelf (Campbell *et al.* 1993).

Whenuataru Tuff (mw).

Whenuataru Tuff is Early to Late Pliocene in age, brown-grey to red-brown, massive to well bedded, volcaniclastic sand, silt and palagonite tuff of limburgitic basalt composition with large hornblende crystals. It is marine, fossiliferous and some beds contain blocks and bombs. It is up to 50 m thick and overlies either Onoua Limestone conformably or Red Bluff Tuff unconformably. Whenuataru Tuff is very fossiliferous with abundant macro-and microfossils and was deposited between the outer and inner shelf. On Mangere Island the Tuff is thought to form part of the low-lying, northeastern coastal strip where it conformably overlies Rangiauria Breccia and is conformably overlain by Mangere Formation (Campbell *et al.* 1993 p. 136). On the northwestern shore of Mangere Island, in the vicinity of the North Landing, the "...Rangiauria Breccia is overlain, apparently conformably, by about 7.5 m of coarse tuffaceous sandstone with thin lensing beds of well stratified Whenuataru Tuff which in turn is overlain by the Mangere Formation...On the evidence available the tuff was laid down immediately after the formation of the Rangiauria Breccia on Mangere Island following collapse of the central part of the volcano and incursion of the sea" (Campbell *et al.* 1993 p. 148). (In this study the unit underlying the Mangere Formation is not considered to be Whenuataru Tuff and has been renamed "Bag End Breccia" from the name of an informal site in Black Robin Bush).

Mangere Formation mg. (as defined by Campbell *et al.* 1993).

Mangere Formation is of Late Pliocene age and is made up of flat-lying, well bedded, well sorted, generally fine-grained sediments of partly volcaniclastic and tuffaceous limburgitic basalt, and partly terrigenous quartzofeldspathic composition. The Formation is fossiliferous, non-marine and thought to occur only on Mangere Island although, according to Campbell *et al.*, (1993, p 149), a thin poorly exposed tuffaceous sandstone on the summit of Kaingaroa Hill, Pitt Island, may belong to the

Formation. It conformably overlies Bag End breccia (Campbell *et al*'s. 1993 Whenuataru Tuff) and is approximately 60 m thick. The Formation contains fossil wood fragments, spores, pollen, dinoflagellates and acritarchs especially in the lower part, which is also concretionary. To date no foraminifera, calcareous nanofossils, diatoms or sponge spicules have been found (Campbell *et al.* 1993 p. 149). Most of the pollen and dinoflagellates are reworked and derived from the Tupuangi Formation. The extinct Mangapanian pollen, *Rhoipites alveolatus*, puts an upper limit on the age of the Formation (Mildenhall in Campbell *et al.* 1993 p. 150) though it is not clear exactly where in the Formation *R. alveolatus* was found. Also the possible occurrence of *Epilobium* (again, it is not clear exactly where in the Formation this was found) puts a lower limit on the Formation of Opoitian age (Campbell, *et al.* 1993 p.150). Only reworked marine fossils have been found in this Formation suggesting that most of the Formation was deposited under terrestrial conditions in the collapsed crater of the Mangere Volcano with periods of lacustrine deposition. It is thought that the formation is a remnant that was once spread over part of the area west of Pitt Island (Campbell *et al.* 1993 p. 150).

Pyramid Phonolite (mp).

Pyramid Phonolite is a hard dark green-grey fine grained alkaline rock. It forms a single plug 9 km south of Pitt Island rising to 174 m above sea level and radiometrically dated at 3.9 Ma Campbell *et al.* (1993).

Unnamed Pliocene volcanics (mv).

These occur on South East and Round Islands as a result of submarine eruptions. They are bedded, dark pyroclastic rock of basaltic composition and dominated by lapilli tuff breccia with xenoliths of Southern Volcanics and Te Whanga Limestone. Their thickness is more than 150 m Campbell *et al.* (1993).

Karewa Group (a).

These are all Late Pliocene to Recent deposits and consist of sands, peat, shell beds and tephra. They occur almost entirely on Chatham Island although small areas are found in the vicinity of Kaingaroa and Moffett trig on Pitt Island.

1.3.0. Previous work on Mangere Island.

Prior to this study very little geological work had been done on Mangere Island and even less on the Mangere Formation. The geology was first described in Hay *et al.* (1957) who made "...two visits of a week each to Pitt Island, and a brief landing on Mangere..." (p 7). They recognised two formations on Mangere Island: the Rangiauria Agglomerate, (named after the precipitous "hard, dark massive agglomerate" at Rangiauria and Waihere Heads on Pitt Island as well as at the southern end of Pebbly Beach and the Mangere Agglomerate (on Mangere Island only) which made up, "...the low lying south-west part of Mangere Island." (Fig. 11).

Hay *et al.* (1970 p. 42) described the Whenuataru Tuff from Pitt Island as beds consisting of "...brown calcareous palagonite tuff with occasional pillow lava near the base. The tuff is richly fossiliferous, displays prominent current bedding and contains abundant hornblende crystals." No mention is made of Whenuataru Tuff on Mangere Island. Campbell *et al.* (1993 p. 136) describes it as, "...brown-grey to red-brown, massive to well bedded volcaniclastic sand, silt and palagonite tuff (crystal, lithic) of limburgitic basalt composition. Some beds are calcareous. Some are locally coarse, containing blocks and bombs. It is richly fossiliferous, marine, and restricted to Pitt Island and its adjacent islets."

Watters (in Campbell *et al.* 1993 p. 148) reports, "Whenuataru Tuff is believed to form part of the low-lying coastal strip in the northeastern part of Mangere Island...(and)... Along the northwestern shore of the narrow part of Mangere Island, the Rangiauria Breccia is overlain, apparently conformably, by about 7.5 m of coarse tuffaceous sandstone with thin (<20 cm) lensing beds of well stratified tuff." This in turn is overlain by the Mangere Formation. Watters (in Hay *et al.* 1970 p. 71) interpreted the volcanism as explosive and short lived, noting that there were no lava flows. He gave a detailed account of the petrography of these formations (Hay *et al.* 1970 pp. 69-71) and the relationship between the two agglomerates was interpreted as "...the low lying Mangere Agglomerate" being "the collapsed central portion of a wide volcanic vent, the outer part of which is represented by the two high remnants of Rangiauria Agglomerate forming Little Mangere Island and the high north-east part of Mangere." (Fig. 12). It is noteworthy that Hay *et al.* (1970 p. 69) did not

recognise the Mangere Formation (Campbell *et al.* 1993) in the lowest part of Mangere Island as being distinct from the Mangere Agglomerate.

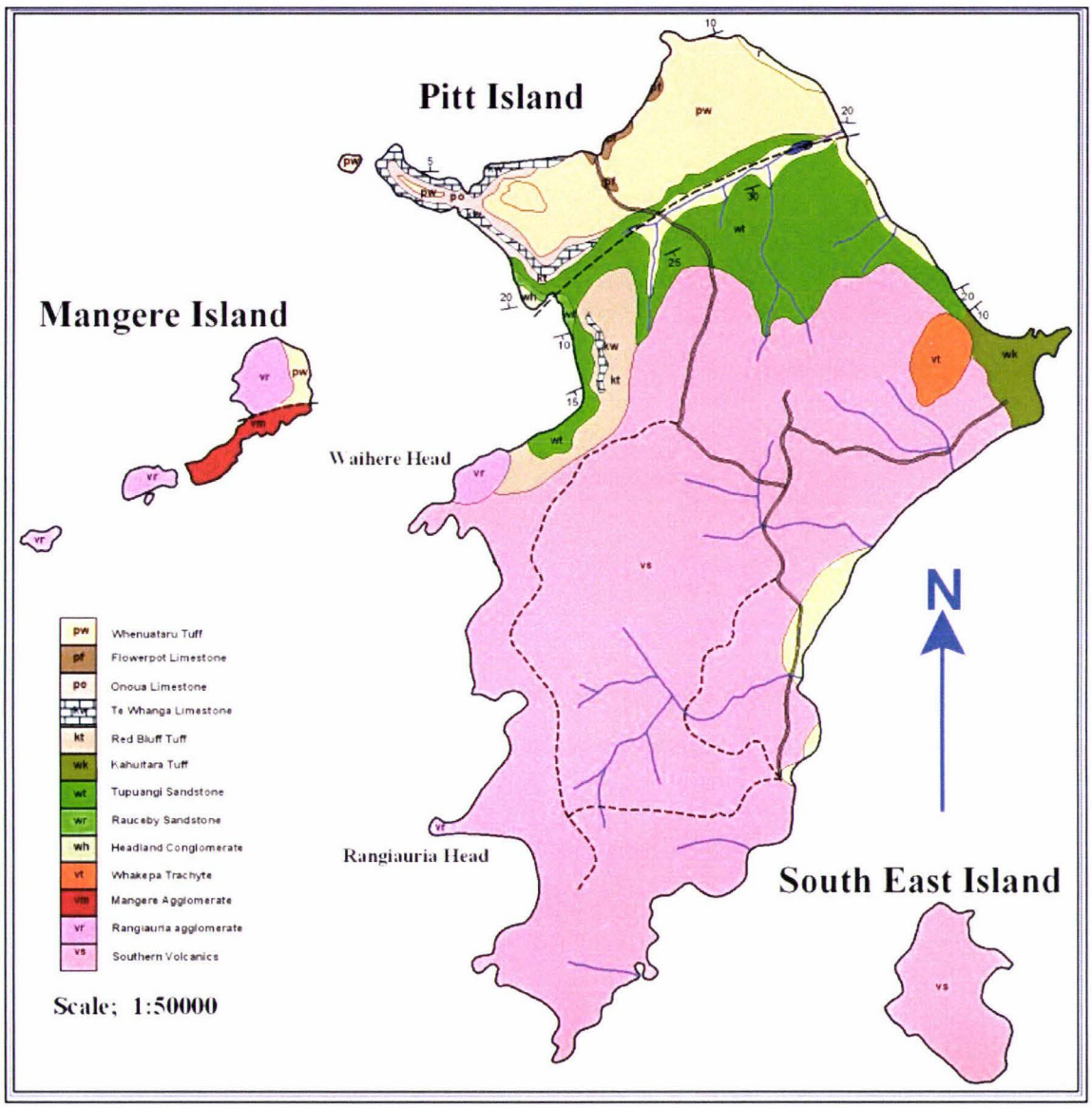

Figure. 11. Map of Pitt and Mangere Islands redrawn from Hay *et al.* 1970. The Headland Conglomerate, and the Tupuangi and Rauceby Sandstones are now assimilated in the Tupuangi Formation and the Mangere Agglomerate is assimilated in the Rangiauria Formation (Campbell *et al.* 1988).

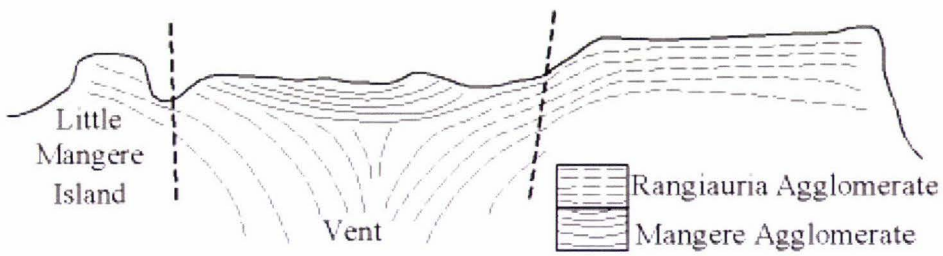

Figure 12. Diagram of Hay *et al's.* 1970 model "...showing the relationship between Rangiauria and Mangere Agglomerates at the suggested single volcanic vent at Mangere and Little Mangere Islands." (Drawn from Hay *et al.* 1970 p. 69).

The Mangere Agglomerate of Hay *et al.* (1970) was renamed as Mangere Beds by Watters (1978). Mildenhall and Wilson (1978) altered Mangere Agglomerate to Mangere Formation without change of definition. Campbell *et al.* (1988, 1993, p. 149) redefined Mangere Formation as consisting of, "flat lying, well bedded, well sorted generally fine grained sediments of partly volcaniclastic and tuffaceous limburgitic basalt composition and partly terriginous quartzofeldspathic composition. Some siltstone and claystone is concretionary. The formation is fossiliferous, non-marine, and thought to be restricted to southwestern Mangere Island (from which it is named), although thin, poorly exposed tuffaceous sandstone on the summit of Kaingaroa Hill, southwest of Flowerpot Harbour, Pitt Island may belong to the Mangere Formation or may be a correlative of it." This is the first detailed definition of the formation.

The type section of the Mangere Formation is given as CH/655194-CH/659198, Sheet 2, 1981. (All further grid references in this study refer to Land Information New Zealand Topographic Map 260, Edition 1 Sheet 2, 1998).

In November 1957, Watters collected four samples from the Mangere Agglomerate (Geological Survey Fossil serial numbers f 247 to 250). The actual location of these was in the above described sedimentary sequence, i.e. the Mangere Formation (though the precise localities could not be ascertained from the reports). In March 1977 Fleming and Billing collected ten samples from the same locality (Numbers f 445 to 553). All of the above samples were processed for pollen and dinoflagellates by Mildenhall and Wilson (1976b, 1977, 1978, 1981, 1994). They

found abundant well preserved Cretaceous pollen and rare poorly preserved Pliocene pollen. Dinoflagellate cysts and acritarchs are, "... moderately abundant and diverse" (1978, p 661). Both Cretaceous taxa indicate a mid-to late Cretaceous age (1978). The Pliocene pollen gave an age of Opoitian to Mangapanian. The presence of the abundant Cretaceous palynomorphs showed "Clearly the source rocks for these fossils are the Waihere Bay group sediments of Pitt Island..." (Mildenhall and Wilson 1978 p. 661).

Several of Hay *et al's.* (1970) group and formation names were subject to revision by Austin *et al.* (1973); Mildenhall and Wilson (1978); Grindley *et al.* (1977), and finally by Campbell *et al.* (1988 and 1993) when revisions relevant to Mangere Island were made; i.e. Rangiauria Agglomerate and Mangere Agglomerate were subsumed under Rangiauria Formation, and Tupuangi Sandstone, Rauceby Sandstone and Headland Conglomerate became Tupuangi Formation.

This is summed up by (Fig. 13) showing the development of the stratigraphy of Mangere Island. (The changes in nomenclature shown in the right hand column have been adopted throughout the rest of this study. They are explained in Chapter 4).

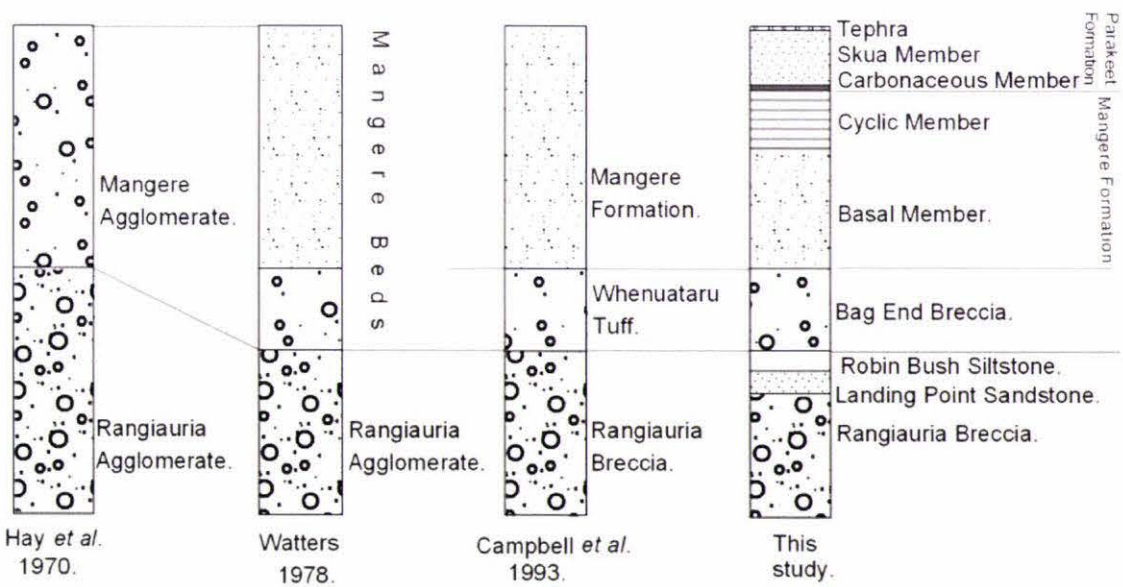

Figure 13. Comparison of stratigraphic columns for Mangere Island, 1970 to the present. (Not to scale).

In January/February 2005 G. Davies, V.E.Neall and R.C.Wallace visited Mangere Island to complete mapping for this project. Neall spent considerable time

investigating the volcaniclastics under the Mangere Formation and, from the disposition of the bedding and types of deposits, was able to show that, rather than one vent on Mangere Island, there were at least eight vents (V.E.Neall, pers.com.). The general situation is illustrated in Fig 14. Further, Dr Neall named Robin Bush Siltstone and Landing Point Sandstone and recognised them as separate members within the Rangiauria Breccia (Neall, 2005).

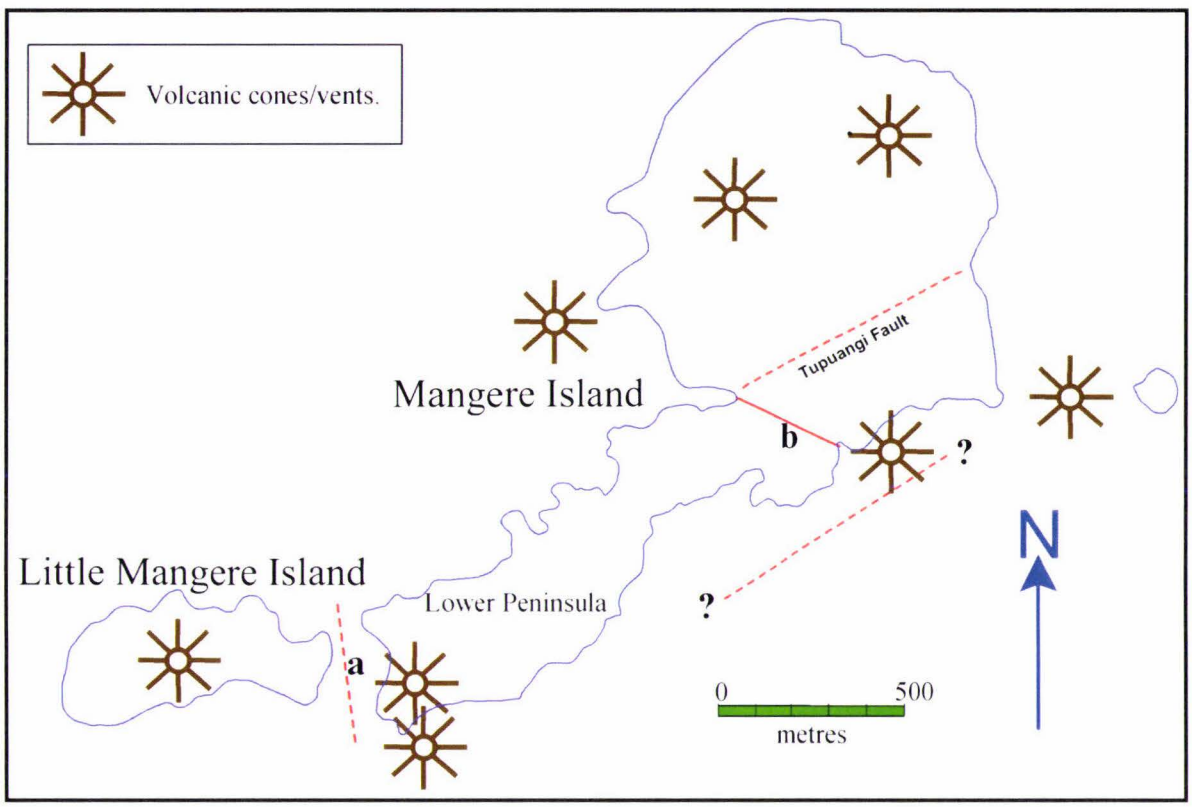

Figure 14. Sketch map showing inferred locations of a number of volcanic vents on Mangere Island (V. E. Neall, pers. com. 2005).

Chapter 2.

Methods.

2.0.0 Fieldwork.

Mangere Island is isolated in two respects; it is two hours by fishing boat from Chatham Island and it is a DOC reserve that requires special permission and quarantine provisions to enter. It can be entered only if there is a DOC employee in residence. There is one hut on the island with a capacity for eight persons. Landing is by rubber dingy (Naiad) directly onto the shore platform and several trips from fishing boat to shore are necessary to transport everything ashore. All food and equipment must be taken to the island and provision must be made for enforced stays resulting from storms and/or high seas. All non-organic rubbish is removed when one leaves. Organic rubbish is dumped in the sea.

To some extent the isolation puts constraints on fieldwork (especially on my first trip when I was working alone) because methods and resources that might be accessible in New Zealand (such as a ladder to make access to very steep faces easier) are not available.

Fieldwork on Mangere Island was carried out between 10-3-04 to 15-3-04 and 28-2-05 to 6-2-05. It consisted initially of measuring stratal thicknesses, describing, photographing, and taking samples of the different lithologies within the Mangere Formation for laboratory analysis of grain size, diagenesis and fossil studies. Samples were described *in situ* for contacts, colour, induration, sedimentary structures, sorting, grain size and cementation. A careful search for evidence of unconformities was also made. In the process possible scenarios to explain the origin of the formation were considered. This was combined with a careful study of published maps (topographic, geologic and bathymetric) of the Pitt-Mangere Island area.

A number of stratigraphic names have been altered or introduced in this study. They will be explained as they occur in the text.

The areal extent of the Mangere Formation (as defined by Campbell *et al.*, 1993) was determined by walking its boundary with the Rangiauria Breccia and Whenuataru Tuff (in this study renamed Bag End Breccia). However, this was hampered especially at the northwestern end of the Mangere Formation by

continuous grass and herb cover and at the southeastern end by tall, thick *Hebe*. This not only made finding the exact boundary difficult but also made it impossible in these places to determine the exact nature of the contact with Rangiauria Breccia (*ie*. whether the Mangere Formation strata lapped directly on to the Rangiauria Breccia or onto steeply dipping strata as is common on lake edges or onto a faulted contact.

The area of the lower southeastern peninsula (Fig. 3, E) was walked over to determine whether any remnants of the formation existed. Again a dense cover of flax over much of the area made this difficult, but no evidence was found of such remnants.

Access to the upper western face of the formation was not possible because of its steepness. As a result the stratigraphic column had to be compiled from several sites as explained in chapter 3. Because of the difficulty of gaining access to the upper parts of the formation and the need to gather as much information as possible, I resorted to studying blocks from the upper two members that had fallen onto the steeply sloping Basal member and beach. Where data are derived from this source I acknowledge it in the text.

The stratigraphic column was drawn and labelled in the field on card with a pre-printed grid at a scale of 100mm equalling 1 (2mm) division.

Samples were placed in labelled self-sealing plastic bags and then double bagged to obviate the danger of the label rubbing off in transit in the pack or carton. The inner bag was labelled with prefixes B, Bm, C, Cm and Sk for Bag End Breccia, Basal, Cyclic, Carbonaceous, and Skua Members respectively, and numbered serially together with the date of collection. Details of the sample and collection site were recorded in a field notebook and its position marked on the stratigraphic column. A grid reference for each group of fossils collected was also recorded.

2.0.1 Height and thicknesses of the formation.

The height of the Mangere and Parakeet Formations from sea level (including Rangiauria Breccia and Whenuataru Tuff (Bag End breccia)) is 72 m as determined from the contour map of RNZAF (sortie 197), Aerial Plan 1074, 1974, 1:12000, Photogrammetric Branch, Department of Lands and Survey. To determine the thickness of each major unit a photograph (Fig. 17) taken face on to the

Formation from about 700 m out to sea was used. This involved measuring on the photograph the height of the Formation and each unit thickness in millimetres and then applying these ratios to the known height to give the true unit thicknesses. Two checks were used on this; (1) a pocket altimeter measurement of the height to the junction of the Basal and Cyclic Members, Mangere Formation, was averaged from three measurements taken by climbing the Basal member three times in a stable atmosphere and returning immediately to sea level and, (2) using DOC laser range finding binoculars (with a geological compass clinometer taped on parallel to the optical axis) from the edge of the extensive wave cut platform to get the distance and angle to each major unit and calculating each height/thickness from that. The thickness of the individual strata of the Cyclic Member and some Parakeet Formation units was determined by tape and this also confirmed the Cyclic member unit thickness.

2.0.2 Note.

The bathymetry map in Knox (1957) has omitted Mangere Island. As this map will become important in chapter 4, the Land Information 260, 1998 map of the Chatham Islands was scanned and Pitt/Mangere Island reduced to the exact scale of the Knox map. The shape and exact position of Mangere Island was then traced through onto Knox's map. The relevant portion of Knox's map appears in chapter 4 (See Fig. 62).

2.0.3 Fossils.

A search of all units produced sparse fragmental macrofossils in Bag End breccia (Campbell et al's. 1993, Whenuataru Tuff) and very small fragments, mainly bryozoa, together with some ostracods and the odd small bivalve shell, in a number of the units of the Cyclic member.

All units were also checked for microfossils. Collection sites for calcareous microfossils were taken from mudstone units determined by testing the site with hydrochloric acid. These sites also produced samples for possible siliceous microfossils. In each case before taking the sample, the weathered surface was cleaned above and below the site to expose unweathered rock and to avoid

contamination from surrounding material. Once taken, the sample was cleaned with a knife in the case of soft sediments or chipped from the centre of indurated rocks.

2.1.0 Laboratory Work.

2.1.1 Preparation of microfossils.

The methods used were mainly those of Brasier (1980).The samples were completely disaggregated by scrubbing with a firm bristle brush, soaking, boiling, or by gentle crushing of soft samples. Hard samples were crushed to disaggregate individual grains where applicable, or disaggregated acoustically, or by boiling with washing soda. Specimens that proved too hard to disaggregate were examined in thin section with a petrological microscope. Following disaggregation the samples were sieved to sizes appropriate to each microfossil size and then treated as follows according to whether they were calcareous or siliceous fossils:

(a) Siliceous fossils, diatoms and radiolaria:

Two grams of sample were taken and placed in a 100 ml test tube to which 20 ml of 27% hydrogen peroxide was added. The samples were then placed in a water bath at 80°C with regular stirring until all reaction had ceased. At this stage 32% hydrochloric acid was added to remove all carbonate. The samples were then centrifuged at 3000 rpm for three minutes and the supernatant liquid decanted off. Distilled water was added to each sample and the samples were centrifuged to wash out the added chemicals. This was repeated three more times. The samples were then vigorously shaken for 15 seconds and then left to stand for 45 seconds when the supernatant liquid was decanted into clean test tubes, the residue being discarded. This eliminates any sand. Any remaining clay was then removed by stirring the mixture vigorously and centrifuging it at 1800 rpm for three minutes and then gently pouring off the cloudy supernatant liquid. This step was repeated until the liquid became clear. The liquid was then concentrated to approximately 5 ml by evaporation. At this stage temporary mounts in water on microscope slides were made by placing a drop of the liquid on a microscope slide coverslip and inverting it onto a glass slide. Six

slides for each sample were examined. As the slides did not contain siliceous microfossils, permanent slides were not made.

(b) Calcareous fossils:

The disaggregated (as above) samples were sieved to <32μm, (for coccoliths), 63-125μm and 125-250μm (for foraminifera) and 125-250 and 250-500μm (for ostracoda). Temporary mounts in water (as above) were made of the <32μm coccolith fraction, but a search of six slides for each specimen with a petrological microscope under high power with highly condensed (conoscopic) light found none. The samples above 125μm were then scanned under a binocular microscope and the fossils picked out and transferred to a Franke slide. Ostracods, bryozoa, a fragment of echinoderm spine and rare small bivalves, but no foraminifera, were found.

(c) Pollen. (This will be dealt with in section 2.3).

2.1.2 Particle size analysis.

Sand, silt and clay fractions were determined for the Tupuangi Formation and Basal member of the Mangere Formation. Full particle size analyses were obtained for units of the Skua and Cyclic members. These were dry sieved through 500, 250, 125, 63 and 32 μm sieves to obtain percentages of sand, silt and clay. The 63- 32μm and <32μm fractions were obtained by wet sieving. Sieving was carried out at the base, top, and along the length of units 26 and 28c of the Cyclic member, to determine whether there is a grain size gradient in these units which would give an indication of direction of their origin. Sieving was inappropriate for some of the sandstone units of the Cyclic member as they are too indurated to break down completely. Microscopic estimation of grain fraction sizes based on thin sections was therefore used here. The grain sizes of the mud units of the Cyclic, and the whole of the Basal member, are all less than 63μm and very largely less than 32μm. Separation of heavy and light minerals and volcanic glass was carried out at the same time using sodium metatungstate. Graphical statistical calculations for graphic mean, inclusive graphic standard deviation, and inclusive graphic skewness (Folk and Ward, 1975) were computed. Kurtosis was not included as there is no good evidence for this parameter having any geological significance.

2.1.3 Microprobing of hornblendes and tephra.

Although altered volcanic glass is ubiquitous in this Formation there is only one primary tephra. It occurs at the top of the Skua member. This was microprobed in order to identify its chemical composition. Hornblendes are also ubiquitous throughout the Formation. Eight samples of these, extracted by heavy liquid separation were extracted and microprobed to ascertain whether there was more than one population, *i.e.* an expected population derived from the Rangiauria Breccia and its numerous xenoliths with possibly another population derived from the Red Bluff Tuff of Pitt Island.

In preparation for microprobing, epoxy cylinders of 3 cm diameter and 1 cm thick were drilled with one central and seven radial 5 mm holes. These holes were then numbered and a small amount of each sample was placed in each hole taking care not to contaminate adjacent holes. A record was kept of which sample was in which hole. The holes were then filled with epoxy and stirred with a long pin to ensure that the hornblende was wet and properly spread. When the epoxy had dried the cylinder face was ground successively with 400, 600 and 1000 grit to prepare the hornblende crystals for a final polishing to optical flatness (so that surface roughness would not affect the microprobe results), using a Streurs Planopol- 3 polisher. The sample was then given a coating of carbon to allow a path to earth for the impinging electron beam.

The instrument used for this study is an energy dispersive electron microprobe (JEOL JXA-840A) fully computerized system at the University of Auckland. The analyses were collected using a Princeton Gammatech Prism 2000 Si(Li) EDS x-ray detector, a 2μm focussed beam, an accelerating voltage of 15 kV, a current of 600 pA and 100 second counting time.

2.2.0 Optical Microscopy.

This study uses both low power reflected light stereomicroscopy as an aid to finding microfossils and for studying the coarser textural features of samples, and high power polarizing microscopy in which individual particles coarser than about 20 μm may be identified optically using a polarizing microscope. Petrological examination enabled minerals to be identified and textural relationships to be studied

as well as providing a check on XRD results. The instruments used were a Leica Wild M28 binocular microscope and a Nikon Model Eclipse E400 POL petrological microscope.

2.2.1 Temporary and permanent microscope mounts.

For temporary mounts, grains were sprinkled on a microscope slide and covered with a coverglass. The grains were then immersed in clove oil (with a refractive index of 1.53-1.54) which is injected under the coverglass. (Quartz and most of the plagioclase feldspars have refractive indexes higher than clove oil while the potash feldspars have lower). Permanent whole grain mounts were made as above but using epoxy resin instead of clove oil. Permanent thin grain mounts first require the setting of the grains in epoxy resin (EPO-TEK, 301. R.I. = 1.539) in small (1cm diam.) lids. The resulting disk was then released from the lid and the surface containing the grains was ground flat with 400 and 600 grade carborundum powder. The disk was then attached with epoxy to a standard petrological slide, grain side down. When set, the disk was cut through leaving a thin slice on the slide. This was then ground down to 30μm for microscopic examination. Permanent whole rock slides were made similarly but with an oblong slice of the sample cut to fit the microscope slide.

2.2.2 Counting of mineral grains.

Counting of mineral grains was done as an aid to correlation and provenance of relevant units. Three hundred mineral grains were counted along the cross-hairs of the eyepiece with successive moves on the relevant slides. Samples that could not be disaggregated, were also estimated by counting and assigning grains to between 63, 125, 250 and 500μm fractions. An estimate of the <63μm fraction (the matrix) was then made using Andrews (1982, Figure 18, p.52)

2.3.0 Palynology.

2.3.1 Sampling Proceedure.

Sampling for pollen and dinoflagellates was done in the hope of obtaining some time constraints on the time of deposition of the Mangere and Parakeet

Formations and also to gain potential information on the palaeoclimate, palaeogeography and conditions of sedimentation.

Spot samples were taken from every fine-grained unit in the Mangere and Parakeet Formations. The sample site was cleared to a depth of about 15 cm (as erosion here generally exceeds weathering it was considered that 15 cm was ample depth). The sample was then dug out with a clean spatula and bagged as described below. In the case where a series of samples was taken for 1.6 m above and below the contact between the Basal and Cyclic members at grid ref.657194, sampling began by using a spade to cut a clean strip 40 cm wide from the top of the section down to its base and, at the same time, cutting back about 15 cm. A tape measure was then hung down the cut and securely anchored at the top. Sampling began at the base of the section at 1.6 m below the contact. A spatula with a 6 cm wide blade was forced horizontally for ca. 40 mm into the mudstone at the base of the section and then another one inserted 1 cm above this. The sample was then withdrawn between the spatulas and placed directly into a self sealing plastic bag labelled with the locality identification and sample depth. All samples were later double bagged to prevent the labels rubbing off. The spatulas were then washed in a bucket of water and cleaned and dried with a fresh paper towel ready for the next sample. The position of the next sample was measured 200 mm up the tape from the base of the previous sample. This procedure was repeated every 200 mm until the top of the sequence was reached at 3.2 m. No sample was taken at the actual contact.

2.3.2 Sample preparation.

The method used was that of Faegri and Ivensen (1964) but using Erdtman's acetolysis. Details are as follows:

- 1 cm^3 of material from each sample was taken by filling a standard 1cm^3 cylinder with the sample material and then transferring it to a plastic test tube which was then filled with water and left for a week for the contents to soften.
- The samples were then treated with HCl to eliminate all carbonate.
- The samples were centrifuged and washed twice.

- The samples were treated for 2 min. with equal parts of KOH and 0.1 Mol. $Na_4P_2O_7$ in a hot block set at 95°C to deflocculate clays and remove humic acids.
- Following this the samples were wet sieved with distilled water though 180μm mesh terylene cloth to eliminate any larger detritus. The detritus was kept for macrofossil examination.
- The samples were centrifuged and decanted several times until all humic acids had been removed.
- To remove water the samples were washed with HCl.
- The samples were treated in the fume cupboard with 40%HF in a hot block for 3 minutes to eliminate silicates. Following this an equal volume of 10% HCl was added to remove any fluoride accretions that might have formed. The sample was then lidded, centrifuged and decanted, and washed three times with distilled water.
- To remove any remaining clay the samples were treated with sodium pyrophosphate in a hot block for 4 min. The samples were then centrifuged and the water decanted.
- Erdtman's acetolysis was then used in the fume cupboard to remove cellulose from the samples. First the samples were dehydrated using glacial acetic acid and then treated with 9 parts of acetic anhydride to 2 parts concentrated H_2SO_4.
- The slides were then checked under the microscope. A few still contained too much detritus. These samples were oxidized to remove the remaining lignin by treatment with glacial acetic acid to which 5 drops of sodium chloride solution and 1ml of conc. HCl were added. This produced a violent reaction which was stopped after several seconds by pouring the contents of the sample tube into a beaker of distilled water. The beaker contents were then progressively centrifuged and decanted until only the cleaned sample wass left. This was then washed and centrifuged with distilled water. These samples were then re-acetolysed to darken the now bleached pollen grains.
- The samples were then sieved at 6 μm in a Sartorius vacuum apparatus to further concentrate the pollen.

- At this stage the samples were dehydrated prior to mounting on microscope slides. The samples were washed in industrial alcohol, centrifuged and decanted. This step was repeated with absolute alcohol and followed by immersing the samples in a 50:50 mixture of absolute alcohol and tertiary butyl alcohol (TBA).
- Following this the samples were washed in pure TBA, transferred to labelled 10 ml vials containing TBA and silicone oil and centrifuged to separate the TBA which was then evaporated off in a 50°C oven. The samples were then sealed ready for mounting on microscope slides.

2.3.3 Slide preparation.

- Two slides were made for each sample.
- All glass slides and coverslips were first cleaned.
- The slides were placed on a hot plate and warmed. The vial contents were thoroughly stirred with a glass rod. The glass rod was then used to place a few drops of the sample on the centre of the slide.
- Some time was allowed for the sample to spread out and for air bubbles to disperse before a cover slip was placed over the sample.
- With a fine nozzled pipette hot wax was injected under the cover slip to seal off the sample.
- The surplus wax was then scraped off and the slide cleaned with white spirit.

2.3.4 Counting.

The slides were counted using a magnification of 500x on a Zeiss Axiophot microscope. Two slides were counted for each sample to minimise errors which might arise from incomplete mixing of pollen with the silicone oil. One hundred and fifty non-aquatic pollen grains were counted on each slide – a total of 300 grains per sample. Slides that were sparse in palynomorphs were near or totally scanned in the counting. Slides that were rich in palynomorphs were counted by traversing in the vicinity of the across-stage diameter.

2.3.5 Identification.

It was difficult to positively identifying some species as no complete checklist of Chatham Island pollen, past and present was available. References used were: Large and Braggins (1991); Moar (1993); Mildenhall (1994). The *Nothofagus* pollens are divided into *Fuscospora* (McGlone *et al.* 1996) and *Nothofagus menziesii* as the pollens in the *Fuscospora* group are very difficult to differentiate.

2.3.6 Charcoal.

Since charcoal, often in significant amounts, occurs in all members of the Mangere Formation, it was counted with the pollen samples. As Boyd (1982a and b) showed, there is difficulty in distinguishing fire-derived charcoal from carbonised vegetable matter in that charcoal-like particles can be produced without fire in a subsurface position as a result of an oxidation or coalification process. Thus the larger fragments were counted only if they were totally opaque and had at least one straight side and the smaller only if they were totally opaque (on the assumption that they were charcoal rather than lignified or coalified vegetable matter). Blackford (2000) showed that large-sized charcoal is abundant where the fire has burned and that unburned areas have mostly fragments of the smallest size. Clark (1988), and Patterson *et al.* (1987) show that charcoal fragments <20 μm ascend thermally from a fire and are dispersed regionally, while particles >50 μm, because of their greater terminal velocity, settle close to the originating fire. That fine charcoal fragments can disperse on a planetary scale is shown by Butler (in press). Counting was therefore done in sizes 0-20 μm, 20- 50 μm and >50 μm in the hope of distinguishing local fires from distant, wind-borne charcoal.

2.4.0 X-Ray Diffraction (XRD): Introduction.

X-ray diffraction is used in this study, in conjunction with optical microscopy, to help determine the mineralogy of the various units of the Mangere Formation, and as an aid to determining provenance. XRD is non-destructive and requires only small amounts of material.

2.4.1 Instrument.

The x-ray diffractometer used is a Philips 4 kVa, PW 1710 micro-processor-controlled instrument with a PW 1050/80 goniometer and PW 1775 (42 sample) sample changer. It is operated by broad focus cobalt target tubes operating at 40kV and 60mA.

In general, instrument settings for routine analysis were always kept the same except that recorder sensitivity could be varied according to the crystallinity and type of minerals present in the sample.

2.4.2 Processing of samples for XRD.

The technique employed here is that of Whitton and Churchman (1987). This technique, together with Differential Thermal Analysis (DTA) and optical microscopy, is a method of analyzing for the mineral and clay content of the units making up the Mangere Formation (as defined by Campbell et al. 1993). It also enables approximate quantitative measures of mineral and clay proportions from the samples. In order to obtain some quantitative results the samples are first treated as outlined below (see also Fig. 15).

2.4.3 Calcium Removal.

First calcium (exchangeable or carbonate) is removed as any calcium present during the peroxide treatment in step 2 may precipitate insoluble calcium oxalate which will interfere with identification of the minerals present in the clay fraction. Approximately 10 g of sample is put in a centrifuge tube with *ca.* 50 ml of water and 1 drop (or more if the colour is difficult to see) of bromophenol blue indicator. 1:1 HCl is added dropwise until the colour changes to yellow. The final pH of the solution should be 3.5. If there is much calcium carbonate present, a vigorous reaction will occur with frothing. All the calcium carbonate may not be completely removed but the acid treatment should remove the small particle-sized material, leaving the coarse, less-reactive, particles to be identified in the sand fraction. Centrifuging is carried out for 10 minutes at 1500 rpm to sediment the sample. The supernatant liquid and any floating plant debris is poured off.

2.4.4 Organic matter removal.

Approximately 10 ml of 27% hydrogen peroxide is added to the test tubes, together with 10 ml of distilled water. They are then stirred and left to stand overnight. Any tubes that froth excessively are transferred to 600 ml breakers. After standing overnight tubes and beakers are placed in a water bath and heated until the water bath is boiling. They are kept at this temperature and stirred occasionally until all frothing ceases. Samples with high organic matter contents may need extra H_2O_2 to be added to completely destroy any organic matter present. When all frothing has ceased, the tubes are filled with water and stirred. The tubes are then centrifuged for 15 minutes at 1500 rpm and the clear (though often coloured) supernatant liquid is discarded. If clay remains in suspension a few drops of saturated NaCl is added and the samples centrifuged again.

2.4.5 Removal of iron and aluminium oxides and oxyhydroxides

30 ml of citrate reagent (0.26 M) and 5 ml of 1M sodium bicarbonate are added after the removal of organic matter to each tube and stirred. They are then placed in a water bath at 90-100°C. When hot, the tubes are again stirred and approximately 1 g solid sodium dithionite is added to each tube with gentle stirring. Excessive frothing is damped down by a squirt of cold distilled water. The test tubes are left in the water bath for 15 minutes and stirred at intervals. They are then centrifuged for 15 minutes at 1500 rpm, and the clear, though often coloured, supernatant liquid is decanted and discarded. If solutions are cloudy they are flocculated by adding 1ml or more of saturated NaCl solution, stirred, and centrifuged again. This step is repeated until any reddish or brownish colouration disappears and the liquid is clear. Any aggregates or iron-cemented concretions are crushed at this stage with the end of a glass rod. The tube contents are then rinsed by adding 30 ml of citrate reagent, stirred and heated in a water bath for 15 minutes. They are then centrifuged and the clear supernatant solution is discarded.

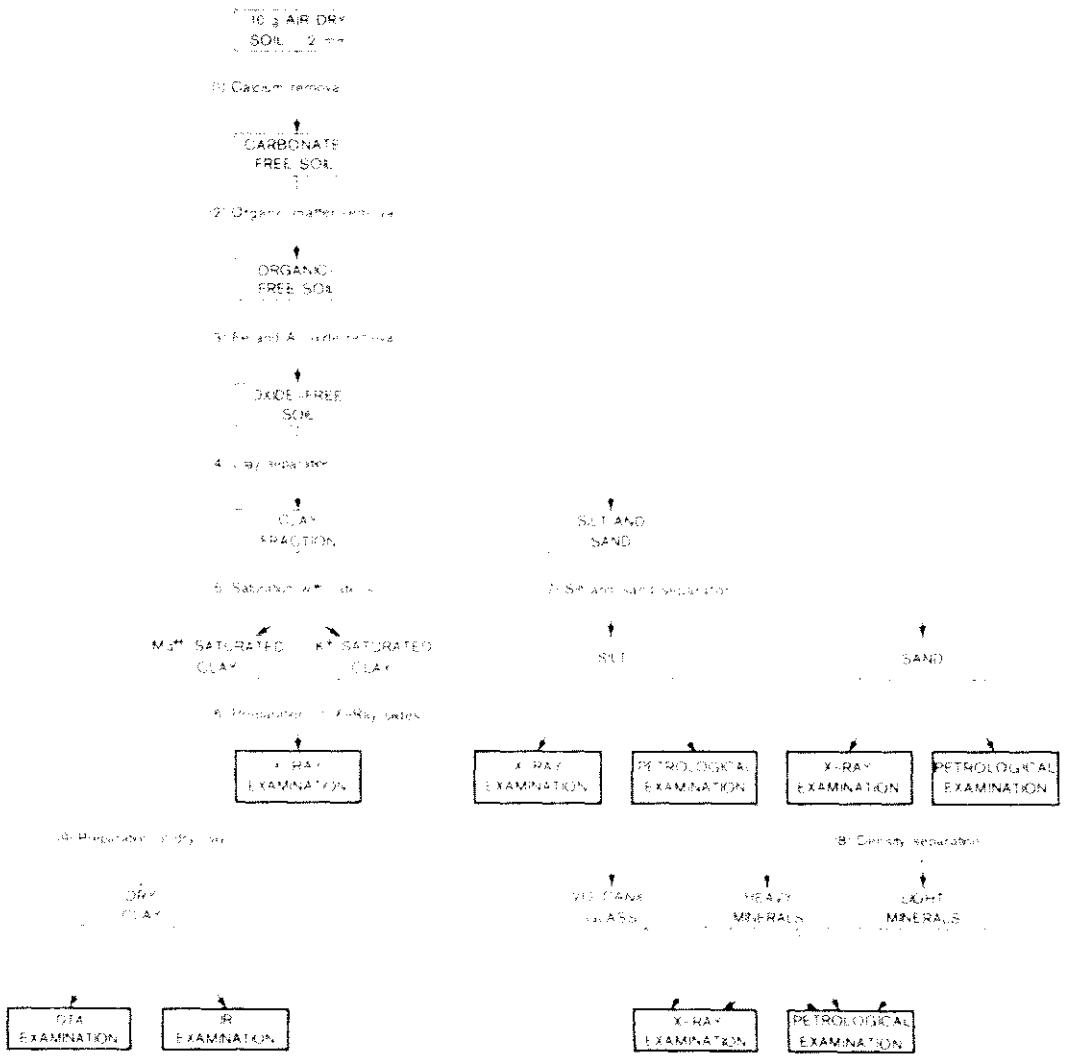

Figure 15. Flow diagram for XRD processing and determining the mineral content of samples (from Whitton and Churchman 1978).

2.4.6 Clay separation.

Distilled water was added to the tubes to the 10 cm mark and the suspensions stirred thoroughly with a motorized stirrer. They were then centrifuged at 500 or 800 rpm for the appropriate time from Table 1 of Whitton and Churchman (1987) according to the ambient temperature. If the samples have a high clay content then the first two of these separations should be carried out at higher rpm and longer time to ensure that all of the silt and sand has settled to the bottom of the tubes. The supernatant clay suspension was poured into a beaker of 600-1000 ml capacity and

the separation repeated until the supernatant liquid remained almost clear (usually 5 or 6 times). The sand and silt fractions remain in the test tubes.

2.6.7 Saturation with cations.

About 10 ml aliquots of clay suspension were transferred to 15 ml centrifuge tubes and saturated with potassium ions by adding, without shaking, 3ml of 1M KCl to the clay suspension in the tubes. The clay was allowed to flocculate and settle under gravity overnight. The clear supernatant liquid was then vacuum drawn off and a further 10ml of KCl was added, the tubes shaken, and the clay again allowed to flocculate overnight. The clear supernatant liquid was drawn off, the K^+ saturated clay suspension was washed with distilled water and centrifuged at 1500 rpm for 15 minutes and the clear supernatant liquid discarded. Washing and centrifuging was repeated three times, or until the clay began to disperse, *i.e.* the suspension remained cloudy following centrifuging.

To the remaining bulk of the clay suspension, 10 ml of saturated $MgCl_2$ was added, followed by 1 drop of bromophenol blue indicator and then 1:1 HCl dropwise until the colour turned yellow. The beaker was filled with distilled water and the clay suspension allowed to flocculate overnight. The clear supernatant liquid was then drawn off, the beaker refilled with distilled water, and the clay again allowed to flocculate overnight. The clear supernatant liquid was drawn off and the washed Mg^{++}-saturated clay retained for x-ray slide preparation.

2.4.8 Preparation of x-ray slides.

A clean dry glass slide (approximately 25mm x 25mm) was covered with as much finely ground sand, silt, or clay suspension in water as can be held on the slide (1-2 ml) and allowed to dry in air. This gives time for some of the the particles to orientate themselves to the 001 face as they sink. For clays, two or three slides were prepared in this manner, one each of: Mg^{++}-saturated clay, K^+-saturated clay, and, if necessary Li^+-saturated clay. After X-ray diffractograms were obtained, using the air-dried slides as prepared above, the slides were further treated as follows: (a) Mg^{++}-saturated slides were sprayed with a 10% glycerol in water solution. Each slide was allowed to dry overnight giving time for the glycerol to react. This glyceration step

may need to be repeated to achieve the complete expansion of some smectites. The slides were then re-examined by x-ray diffraction (XRD). (b) After the diffractogram for the Mg^{++}-glycerol sample had been obtained the slide was heated to 550°C for 2 hours, cooled and another diffractogram obtained.

2.4.9 Silt and sand separation.

Silt was separated from the residue remaining in the centrifuge tube after step 4 (Fig. 15) by filling the tubes with distilled water to the 10cm mark, stirring and allowing them to stand for the appropriate time as given by Table 2 in Whitton and Churchman, (1987). The suspension contained only silt at the end of the time and was poured into a 600m beaker. This step was repeated until no further silt remained in suspension (usually 4-5 times). The silt in suspension in the 600 ml beaker was allowed to settle out overnight and the supernatant liquid drawn off next day. The silt was washed with distilled water, air-dried, and stored in vials for x-ray and optical examination. The sand fraction, which was the residue remaining in the tubes after silt separation, was dried by heating the tubes in an oven at 110° C overnight and stored in vials.

2.4.10 Sand fraction density separation for heavy and light minerals and volcanic glass.

The sand fraction was then separated into glass, light and heavy fractions. Using sodium polytungstate (SPT) of density 2.45 g cm^3.This separates out the glass from the light and heavy mineral fraction, and a density of 2.85-2.90 g cm^3 separates the light from the heavy minerals. The separation was accomplished by placing 0.5 g of sand in a 10 ml centrifuge tube having a narrow stem and 5-6 ml of the lower density SPT was added. The tube was gently stirred to disperse sand grains and break up any aggregates. It was then allowed to settle. If there was much fine sand it was necessary to centrifuge at 1000-1500 rpm for 10-15 min to obtain a complete separation. A glass rod with a button on one end was pushed down through the light floating fraction (taking care that none of the light material is carried down with the button) until the button sealed the narrow stem which contained the heavier fraction. The SPT above the seal, together with the very light fraction, was poured into a filter

paper in a glass separating funnel. The tube was washed with SPT to remove any sand adhering to the glass rod or tube, care being taken during this washing step to avoid breaking the seal and thus contaminating the heavy separate. The remaining fraction was washed with SPT into a second filter paper. Each filter paper was labelled with sample number and heavy-plus-light or light fraction etc. for future identification. The two filter papers were then washed with distilled water and allowed to air-dry in a fume cupboard, and further dried in an oven at 110°C also in a fume cupboard, and stored in vials for x-ray and optical examination. The heavy plus light fraction was similarly separated to get heavy and light (quartz, feldspar *etc.*) mineral fractions using SPT of 2.85g cm^3.

2.4.11 Preparation of dry clay.

The remaining suspension of Mg^{++}-saturated clays was air-dried in a petri dish in preparation for differential thermal analysis (DTA). Each sample was then analysed by DTA to establish the quantities of gibbsite and kandite present.

2.5.0 XRD procedure: oriented samples.

X-ray slides prepared as detailed above were placed in sample holders, stacked in the sample magazine, loaded into the sample changer and an x-ray diffractogram obtained using the appropriate programmes for the PW 1710 instrument. These were programme 222 for Mg^{++} saturated clay in air, and programme 223 for Mg^{++} saturated and glycerated samples, K^{+}saturated samples, and 550°C heated samples.

For heavy and light mineral samples, a few milligrams of the sample were finely ground using an agate mortar and pestle. The samples were then mixed to a slurry with acetone or water and evenly distributed over the whole slide. The acetone was allowed to evaporate and the slides were then placed in sample holders, loaded into the sample changer and the machine started. X-ray diffratograms were obtained using programme 211 for heavy minerals or programme 210 for lights.

2.5.1 Interpretation.

Sand, silt, clay and whole soil samples are analysed using powder x-ray diffractograms to estimate the kinds of minerals present. This was done in two steps.

Step 1: x-ray powder diffractograms were compared to cards on which the principal XRD peaks for each of the commonly occurring minerals had been marked.

Step 2: any remaining peaks not identified above were then be identified using standard reference books of XRD data and/or the ASTM index and data file.

The quantities of minerals present were qualitatively estimated from peak height intensities (which represents counts/sec.) of each of the minerals present. This was carried out using graphs of peak height intensity against concentration, which had been prepared, using pure mineral standards, for each of the common minerals. Graphs were available for quartz, feldspar (albite), mica (muscovite and biotite), chlorite, hornblende, cristobalite and calcite. Other less common minerals were dealt with by reference to standard tables. Some minerals *e.g.* chlorite, are subject to enhancement of peak intensity due to orientation effects. Others such as epidote have poor peak intensities compared to other minerals. Therefore, in the estimation of these minerals chlorite intensities are halved and epidote intensities doubled. These calculations were checked using counting techniques and optical microscopy for some samples in each group of samples analysed. At the same time the presence of significant minor components not detected by XRD could be recorded.

2.5.2 Determination of clays.

In XRD, clays are distinguished by the basal (001) spacing of minerals. Clay minerals are classified into 1:1, 2:1 and 2:2 layer spacing corresponding (in XRD) to repeat spacing of $\geq$ 7.2Å (kaolinite, dehydrated halloysite), 10Å (micas, illites, vermiculite, smectites) and, 14Å chlorites respectively.

- 1:1 clays. Dehydrated halloysite was distinguished by treatment with glycerol which expands the layer spacing to 11Å.
- 2:1 clays. The 10Å peaks of illite and mica cannot be distinguished from each other and both are classed as mica. Vermiculites were distinguished by replacing the interlayer cations or by heat treatment around 550° C. Vermiculites, in which all the interlayer spaces have been replaced by K^+, have 14Å spacing and, with Mg^{++}, the separation

between layers is 10Å. In the case of $Al(OH)_3$, heating to 550°C is needed to collapse the spacing to 10Å. In the presence of glycerol, magnesium-saturated smectites have a basal spacing of *c.*18 Å, while K^+ saturated smectites have a basal spacing of 10 Å. This distinguishes the smectites.

- 2:2 layer clays. Chlorites are similar to kandites and are difficult to distinguish with XRD but are distinguishable with DTA which gives the quantity of kandite (kaolin/halloysite). Clays were identified from the tables on page 12 of Whitton and Churchman, (1978) which gives the interlayer spacing for clays after treatments with Mg^{++} in air and glycerol, K^+ and heating to 550° C.

2.5.3 Quantitive analysis of minerals and clays.

Semi-quantative analysis is possible on all minerals by measuring the main peak of each mineral and clay and applying the formulae given in Whitton and Churchman (1987, p13). Tables of estimated errors for the clay and mineral values are given on pages 23 and 24 of Whitton and Churchman (1987)..

2.5.4 Determination of allophane content (Basal and Skua members).

The presence of allophane in the very glassy Skua member was determined by atomic absoption (AA) using acid – oxalate- extractable Al_o and Si_o values and pyrophosphate-extractable Al_p values. The Al/Si ratio was calculated from Al_o-Al_p/Si_o and then the allophone/imogolite content was calculated by multiplying Si_o by the given factor in the table on page 18 of Whitton and Churchman (1987) appropriate for the Al/Si ratio. For the Basal member a simple field test was used. This consisted of adding NaF to the sample on filter paper that had been treated with phenolphthalein. The NaF reacts with the OH and OH_2 to give NaOH and AlF. If allophane is present the pH is raised to 9-10 and this turns the phenolphthalein pink

2.6.0 Differential Thermal Analysis (DTA).

The DTA instrument used was a Du Pont 99 micro-processor controlled DTA using a high temperature (up to 1200°C) furnace.

Differential thermal analysis (DTA) involves the simultaneous heating of two samples; the unknown sample and, in this machine, aluminium which is inert and maintains the same temperature as the furnace. Thus the difference between these two, measures endothermic and exothermic reactions in the sample relative to the standard (Al) which occur when a sample is either heated or cooled. These reactions are a result of, for example, water loss, oxidation of organic matter, recrystallisation, and crystal inversions. As a mineral undergoes these reactions it will become hotter or cooler than the reference sample (Al). The difference in temperature between the two, measured by a differential thermocouple is plotted against the furnace (*i.e.* the Al) temperature. This curve is reproducible for most minerals. In this study it was used to ascertain the amount of kandite (kaolinite plus halloysite) in the samples. As compared with values from XRD, those from DTA are more precise and subject to less variation from differences in crystallinity and particle size of the clay minerals. Values obtained for gibbsite and kandites from DTA are also less affected by overlap of characteristic peaks of different minerals in XRD.

The temperature difference (detected by thermocouples attached to the crucibles and wired in opposition) between the two materials is continuously recorded as they are heated or cooled. When the temperature of the sample equals the temperature of the reference material the two thermocouples produce identical but opposed voltages and the net voltage is zero. When the sample and reference temperature differ, there is a proportional voltage differential and a peak then develops on the curve of temperature differential against temperature. An example of such a peak is shown diagrammatically in Figure 16. Along the line AB no reaction is occurring and the temperature difference is zero but at B an endothermic reaction starts, giving rise to the peak BCD. When point D is reached the sample is again at the same temperature as the reference material and the temperature difference remains zero until another reaction occurs. The position of the peak temperature at point C is usually characteristic of the minerals present and peak area (BCD) or peak height (h) is proportional to the amount of the reacting material.

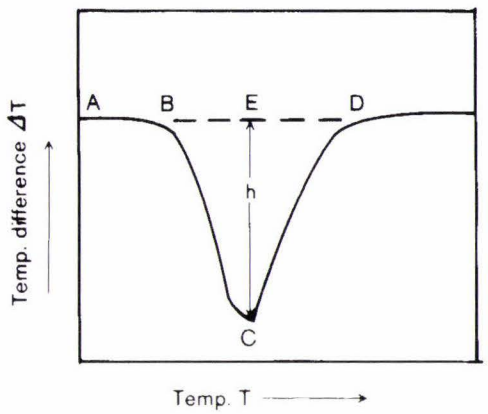

Figure 16. Graph illustrating temperature differential peak discussed in text (from Whitton and Churchman 1987).

2.6.1 Procedure.

Representative samples of clay or whole soil were finely ground and packed into the sample holder. Fifty mg of Al_2O_3 was firmly packed into the platinum liner of the macro cup (the larger of the two available cups) and the cup containing the reference Al_2O_3 was placed on top of the right hand thermocouple. Fifty mg of sample was similarly packed into a second cup and placed on the left-hand thermocouple. The furnace was then closed and the thermogram run.

2.6.2 Interpretation.

Once the thermogram had been obtained it was compared with the thermograms run using standard pure mineral specimens. A quantitative estimate of gibbsite and kandites was made by measuring peak heights or areas under characteristic endothermic peaks at temperatures of 280-330°C for gibbsite and 520-560°C for kandites, and obtaining the concentration of the minerals present from standard graphs.

2.7.0 Loss on Ignition.

Loss on ignition was carried out on the Basal and Carbonaceous members to determine the amount of carbon in these units. The procedure was first to check for, and eliminate any calcite with dilute HCl and then to dry the samples in a 100° C oven for 24 hrs. The samples were then weighed and placed in weighed crucibles and heated in a furnace to 700° C for 7 hrs. The crucibles were placed in the furnace in a recorded order to obviate later misidentification of samples. After 7 hrs the crucibles were extracted from the furnace and allowed to cool enough (to avoid uptake of atmospheric water before weighing) for them to be weighed. The final weight was; (weight of crucible + sample) – weight of crucible. The percentage of organic carbon is: (original weight of sample – final weight of sample) / original weight of sample * 100 %

2.8.0 Experiment to simulate ripples found on the bases of several sandstone units of the Cyclic member.

Near symmetric ripples of very short wavelength averaging 4- 5 mm (ripple index = 3.5- 4 approx.) were found on the bases of several sandstone units in the Cyclic member, Mangere Formation. Calculation of the various ripple and ripple symmetry indices (Reinech and Singh, 1980 p. 35) gave indeterminate results as to whether the ripples were wind or current generated (though the ripple index makes them definitely wave ripples). However Reinech and Singh (1980 p. 35) also state that ripples smaller than 4.5 mm are known only as assymetrical wave ripples. None of the standard texts I consulted dealt satisfactorily with such short wavelengths. For this, and reasons discussed in Chapter 3, I assumed them to be wind generated and Dr. Clel Wallace and I attempted separately to simulate them in large troughs. Fig 38 shows the result obtained.

Chapter 3.

Results.

3.0.0 Introduction.

Mangere Island is essentially volcanic but in two restricted areas quartzofeldspathic sedimentary sequences are found. These are the Tupuangi and Mangere (Campbell, et.al. 1993) Formations.

3.1.0 Tupuangi Formation.

As part of this study the Tupuangi Formation (formerly known only on Pitt Island) is found at the southwestern end of Black Robin Bush (Fig. 3, C). Although not a formal part of this project, a stratigraphic section was measured and described (Fig. 20) because finding it on Mangere Island has implications for the palynology and provenance of the Mangere Formation. Furthermore this identification considerably extends its distribution beyond Pitt Island. Also its strike and dip are significantly different between Pitt and Mangere Islands suggesting that there is some form of structure between the two islands. The Tupuangi Formation on Mangere Island consists of siltstones and silty sandstones and is lithologically indistinguishable from its counterpart on Pitt Island. No other outcrops of Tupuangi Formation were found on Mangere Island.

3.1.1 Mangere sedimentary sequence.

The Mangere sedimentary sequence is found in the central low part of the island between the North and South Landings (Fig. 17). It rests on, and is surrounded by, the Rangiauria Breccia. This sequence comprises six distinctive units:

- At the base is the 7 metre-thick Bag End Breccia (formerly the Whenuataru Tuff- see discussion in chapter 4).
- A massive, 32 metre-thick mudstone sequence, here named the Basal Member.
- A central 12.55 metre-thick sequence of alternating sandstones and mudstones, here named the Cyclic Member.

- A dark organic rich unit of 0.575 metres maximum thickness here named the Carbonaceous Member.
- An upper 16.8 metre-thick strongly tuffaceous sequence here named the Skua Member.
- A 0.6 metre-thick tephra cap.

All but the first of these units formerly made up the Mangere Formation of Campbell *et al.* (1993). These units are shown in Figure 17.

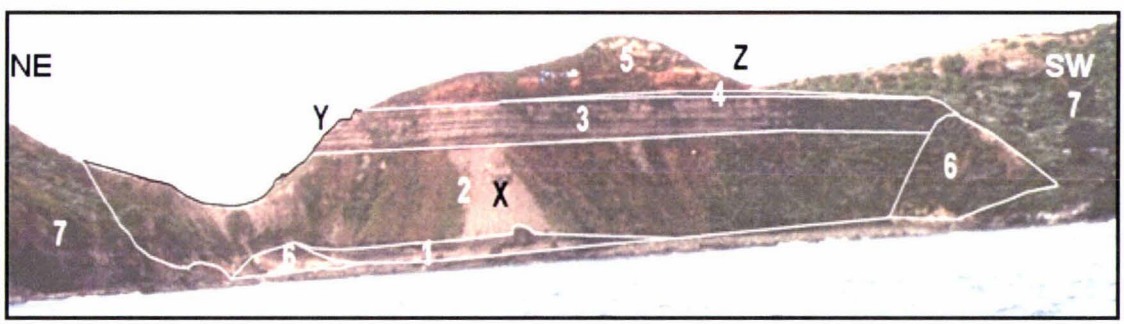

Figure 17. View of the western side of Mangere, Parakeet, and Rangiauria Formations to show the following stratigraphic units (vertical exaggeration 1.5):

(A) Rangiauria Formation: 6. Robin Bush Siltstone member. 7: Rangiauria Breccia.

(B) 1.Bag End Breccia.

(C) Mangere Formation: 2: Basal Member, 3: Cyclic Member.

(D) Parakeet Formation: 4:Carbonaceous Member, 5: Skua Member with tephra cap.

The letters X Y and Z on the photograph locate the sites from which the stratigraphic column was compiled. (Photo: R.C. Wallace).

The stratigraphic column of the Basal Member of the Mangere Formation was compiled from the vegetation free skirt marked "X" on Figure 17; the Cyclic Member was compiled from the north-eastern end of the sequence at "Y". The Carbonaceous and Skua Members and tephra of the Parakeet Formation were measured from the southwestern end of the formation along the cliff edge at "Z" to the top of the sequence. A continuous section down the centre of the formation was

not possible because the upper sections are close to vertical and either inaccessible or heavily vegetated.

Campbell *et al.* (1993 p. 149) suggested that there might be an outcrop of Mangere Formation or its correlative on the summit of Kaingaroa Hill, Pitt Island. I visited Kaingaroa Hill and the area around it, but found no signs of units resembling the Mangere Formation.

Figure 18. View of the Mangere and Parakeet Formations looking towards the northeast from the ridge immediately north of the hut, showing the Basal member (A), the Cyclic member (B), and the Skua member capped by a 0.6 m thick tephra (C). Two thick, prominent sandstone units can be seen in the lower half of the Cyclic member. The lowest of these is informally named the ripple unit. Two more thick sandstone units appear, partly obscured by vegetation, at the upper right of the Cyclic member. These pinch out in the vegetated area. Just above the Cyclic member is the thin black Carbonaceous member (arrowed). The white unit (D) at the lower right is Robin Bush siltstone. It dips away from the ridge on both sides and forms the southwestern boundary of the Basal member and the lower half of the Cyclic member.

Figure 19. View of Mangere and Parakeet Formations on the eastern (South Landing) side of the island showing the Basal (A), Cyclic (B), and Skua (C) (entirely vegetation covered), Members. Note the two prominent sandstone units in the Cyclic Member which completely cross the lower half of the member (the lower unit is the ripple layer). The Bag End Breccia (D) is seen to the right immediately below the Basal Member. Below this and across the photo is the light yellow-brown Robin Bush Siltstone (E) and below this, at sea level is the Rangiauria Breccia (F). Note that the Bag End Breccia "rides" up over the Robin Bush Siltstone at the extreme right. A brownish Rangiauria Breccia megaclast (G) in the Bag End Breccia is seen just to the right of centre. The Carbonaceous Member is obscured by vegetation in this photograph. The pinched out unit (arrowed) at the bottom right of the Cyclic Member is unit 28c, a turbidite. Northeast is to the right.

3.2.0 Stratigraphic Columns.

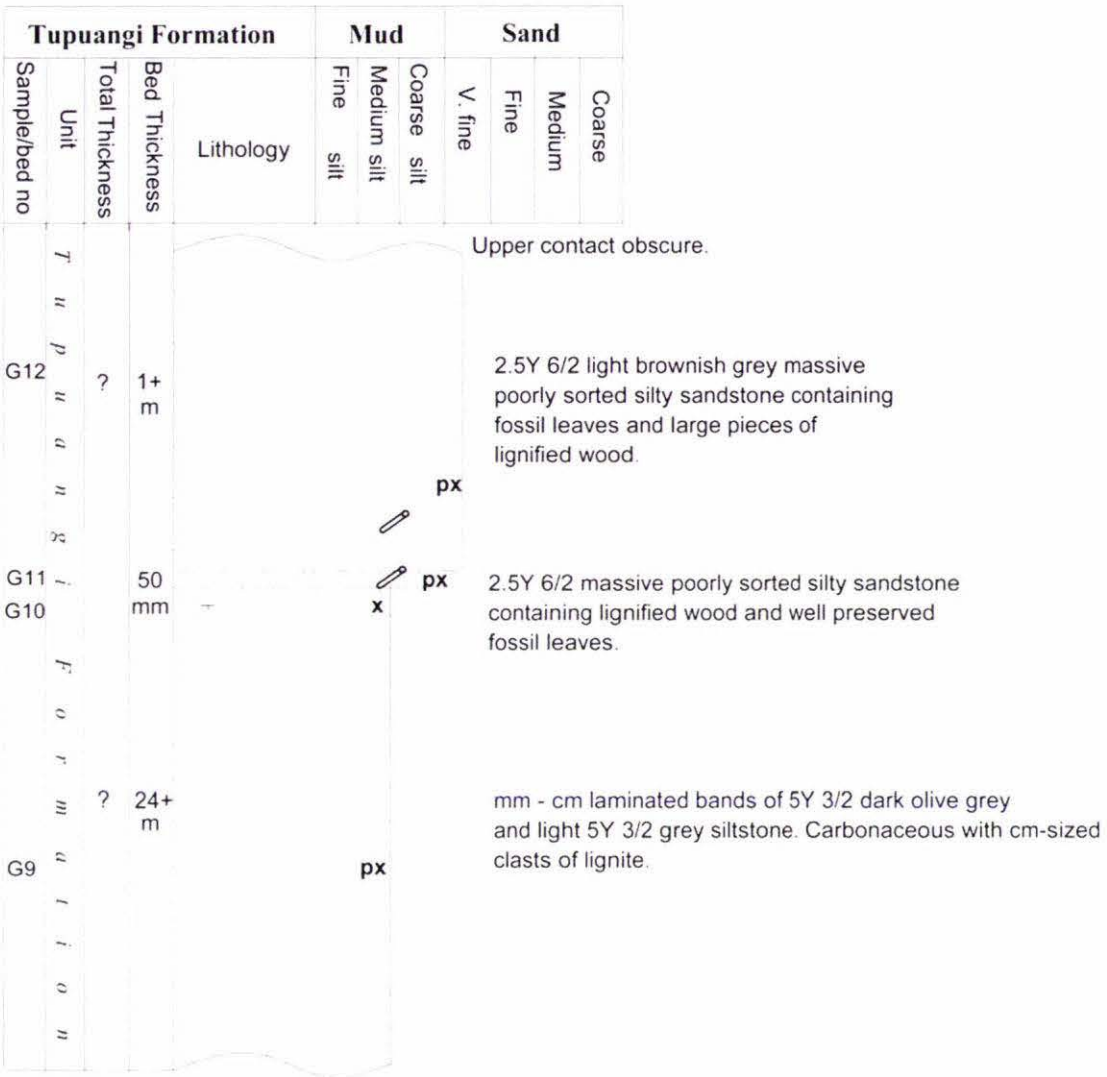

Key to symbols used in stratigraphic columns. (symbols from Andrews 1982).

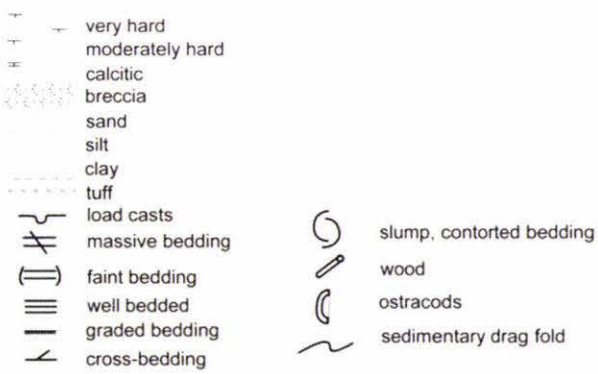

Figure 20. Stratigraphic column, Tupuangi Formation, Mangere Island. "x" = rock sample; "p" = pollen sample. (Grid ref: 667200 Topo. Map 260 Chatham Islands 2. All further grid refs. refer to this map.)

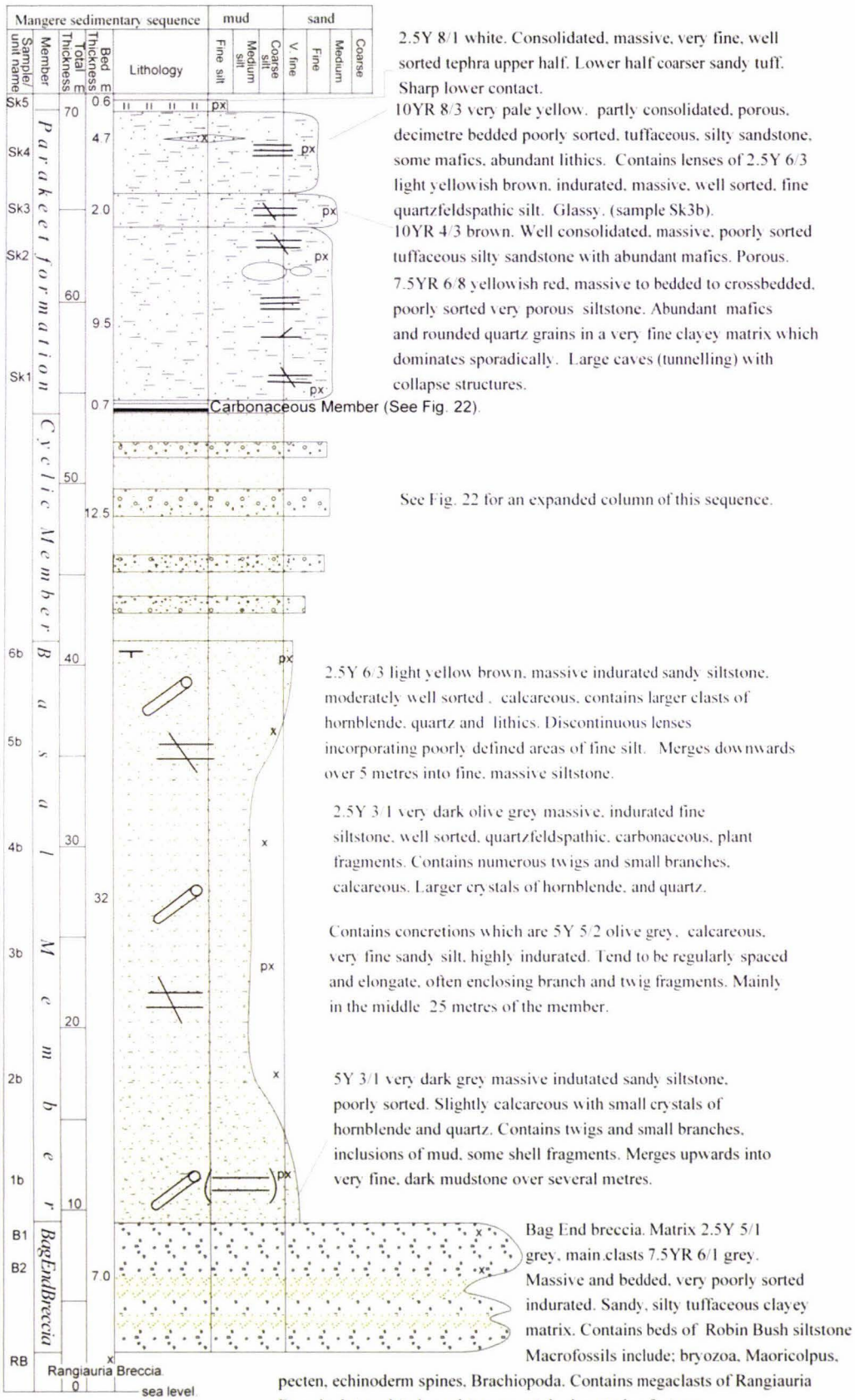

Figure 21. Stratigraphic Column, Mangere Formation, Mangere Island. "x = rock sample; "p" = pollen sample. (See key to symbols, p 53).

Cyclic member, Mangere Formation

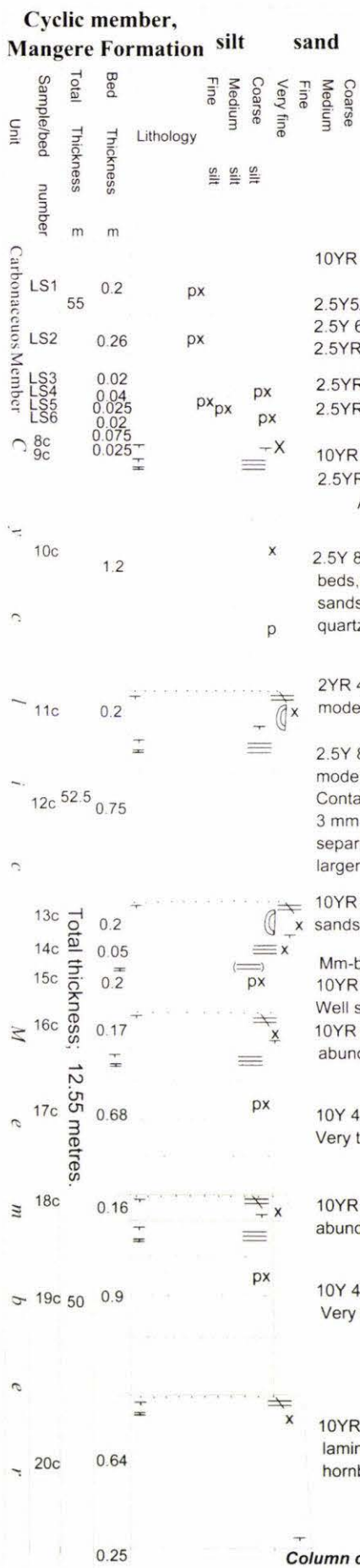

10YR 4/4 dark yellowish brown carbonaceous massive very fine siltstone. Poorly defined parting planes.

2.5Y5/1 black coarsely bedded to massive fine siltstone, carbonaceous.

2.5Y 6/3 light yellow brown silty sand. Finely bedded.

2.5YR 4/2 dark greyish brown silt. Carbonaceous, finely bedded with a 1.5mm very dark grey layer 8 mm from base.

2.5YR 4/2 silty sulphurous lignite weathers to a flaky edge.

2.5YR 5/3 light olive brown, well sorted mm-laminated siltstone with a 6 mm basal layer of poorly sorted, rusty sandstone.

10YR 4/3 brown massive sandy siltstone.

2.5YR 4/2 dark greyish brown indurated silty sandstone, poorly sorted. Abundant larger grains of hornblende, quartz, lithics and zeolites.

2.5Y 8/3 pale yellow. Series of dm-bedded calcareous, sandy siltstone beds,moderately well sorted separated by poorly sorted cm bedded sandstone units with abundant large crystals crystals of hornblende and quartz .

2YR 4/2 dark greyish brown. Indurated massive silty sandstone, moderately well sorted. Abundant larger grains of hornblende and quartz plus whole and fragmental shells of ostracods.

2.5Y 8/3 pale yellow. Well consolidated of mm- and dm-bedded, moderately well sorted, fine sandy siltstone with oxidised layers. Contains some mm thick laminated beds faced above and below by 3 mm gypsum crystals normal to the laminae.These siltstones are separated by cm thick, poorly sorted sandstone beds with abundant larger crystals of hornblende and quartz. Calcareous.

10YR 4/3 brown massive, indurated, poorly sorted, coarse silty sandstone. Larger crystals of hornblende and quartz with shell fragments of bryozoa, echinoderm and whole and fragmental ostracods.

Mm-bedded sharply defined, each bed strongly distinguished by colour.

10YR 5/2 greyish brown. Massive (vaguely bedded?) indurated siltstone. Well sorted with darker brown 1 mm layers. Calcareous.

10YR 4/3 brown massive silty sandstone, moderately well sorted with abundant larger crystals of hornblende and quartz.

10Y 4/1 dark grey . Well consolidated, cm-bedded, well sorted siltstone. Very thin fine sandstone layers at the base of the beds. Calcareous.

10YR 4/3 brown massive silty sandstone, moderately well sorted with abundant larger crystals of hornblende and quartz.

10Y 4/1dark grey . Well consolidated, cm bedded, well sorted siltstone. Very thin sandstone layers at base of beds. Calcareous,

10YR 4/2 dark greyish brown, massive, indurated silty sandstone with laminated silt inclusions. Poor sorting with abundant larger crystals of hornblende and quartz. Calcareous and normally graded.

Column continues on next page.

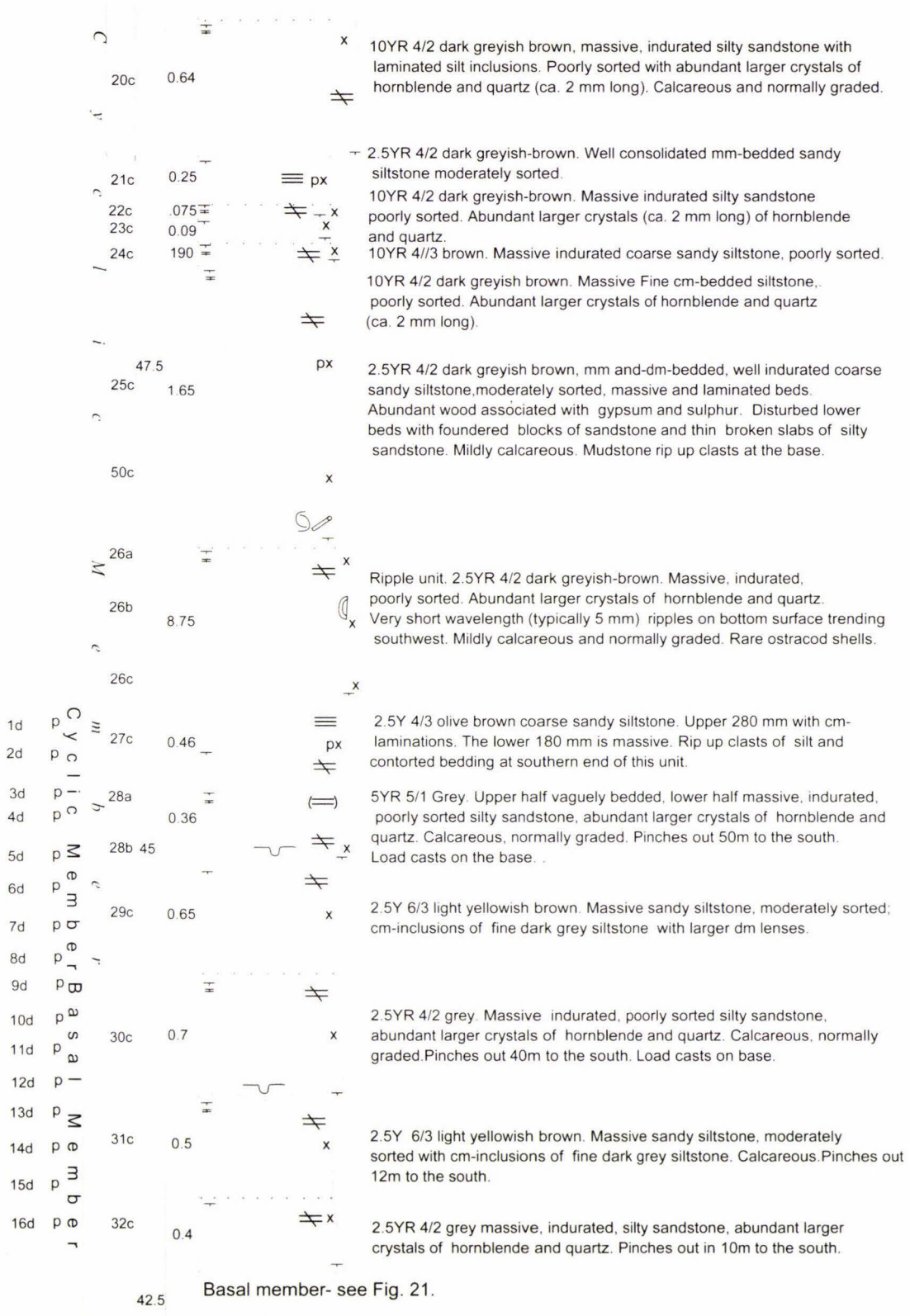

Figure 22. Stratigraphic column, Cyclic member, Mangere Formation.

An "x"=rock sample; "p"= pollen sample.
Column "A" parallel to the main column, represents the sequence at grid ref. 657193 where the units below 26c in the main column have pinched out. This is explained in figure 73. 1d to 16d are pollen samples. (See key to symbols, p 54)

3.3.0 Results of field and laboratory work.

Introduction.

In what follows, the Tupuangi Formation, Bag End Breccia, and each member of the Mangere and Parakeet Formations will be dealt with separately in terms of the results of field and laboratory work.

3.3.1 Tupuangi Formation (?).

This Formation was investigated to determine its relationship to Tupuangi Formation, Pitt Island.

The base of the outcrop of the Tupuangi Formation on Mangere Island (Fig. 23) is not visible. It appears at about 15 m above sea level, is at least 25 m in height and 75 m wide. It consists at the base of an unknown thickness of light grey (5Y 6/1) and dark olive grey (5Y 3/2) laminated siltstone that dips to the northwest at 12°. The siltstone is carbonaceous and contains mm-to cm-sized lignite clasts. This is followed by a 50 mm thick light brownish grey (2.5Y 6/2) silty sandstone bed containing well preserved fossil leaves. The top of the sequence consists of at least 10 m of massive light brownish grey (2.5Y 6/2) silty sandstone which also contains fossil leaves. A piece of flattened, lignified wood, 250mm x 160mm x 25mm, was sampled from it. The southeastern end of the outcrop is normally faulted. The downthrown side is not visible and is presumably below sea level.

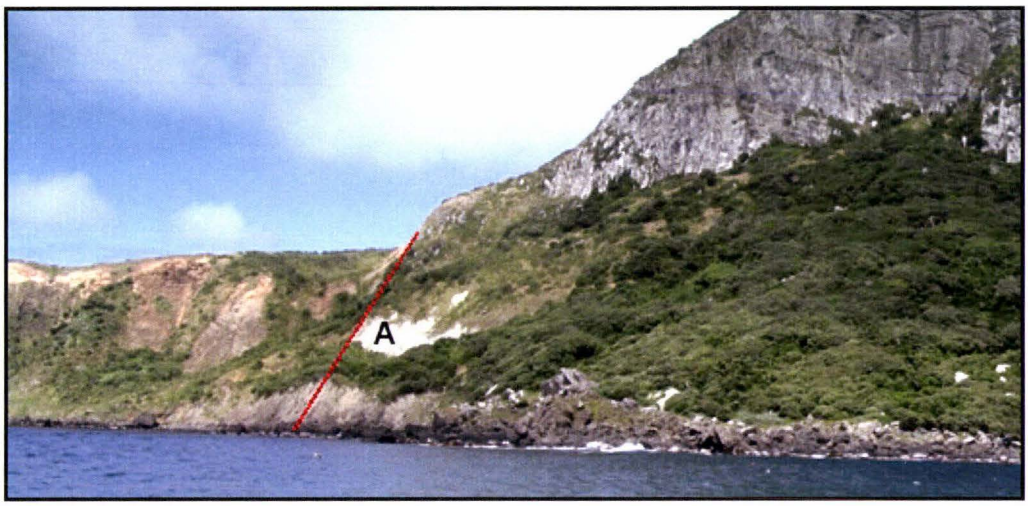

Figure 23. View of the southeast side of Mangere Island showing the Tupuangi Formation identified as the white patch (A) just to the left of centre (G.P.S. S 44 16.102′ W 176° 17 376′, grid ref. 667200). A normal fault (dashed red line) associated with a string of volcanic vents dislocates the southern end of the Formation and crosses the island (Fig. 14). The Mangere Formation is just out of the photo to the left (southwest).

3.3.2 Grain size analysis, Tupuangi Formation; Pitt and Mangere Islands.

A grain size analysis was carried out on these samples as an aid to their possible correlation.

	Mangere Island			Pitt Island		
Sample	T10	T11	T12	G1b	G2b	G3
Sand	28.15	66.4	88.9	26.5	80.2	82.8
Silt	17	29.8	3.8	10.9	8.2	5.6
Clay	54.8	3.8	7.3	62.6	11.6	6.5
Total	99.95	100	100	100	100	94.9

Table 1. Percentage distribution of sand, silt and clay fractions of Tupuangi Formation samples from Pitt and Mangere Islands. The Pitt Island samples were collected from Waihere Bay, Pitt Island by Dr C. Wallace.

3.3.3 XRD analysis, Tupuangi Formation; Pitt and Mangere Islands.

XRD analyses were conducted on samples from these islands as an aid to their possible correlation. The results are shown in Table 2.

	Mangere Island			Pitt Island		
Sample	T10	T11	T12	G1b	G2b	G3
Quartz	45	42	47	44	49	44
Feldspar	31	28	29	33	42	26
Mica	3.5	1	0.5	3	4	2
Ilmenite	0.8	0.4	1	1	0.5	0
Magnetite	3	1	2	1	2	2
Epidote	1	0.5	1.5	1	0.4	0.6
Zircon	0.6	0.8	0.5	0.6	0.2	0.7

Table 2. Relative percentage (error 10-15%) distribution of selected light and heavy minerals from XRD data for Tupuangi Formation, Pitt and Mangere Islands.

3.3.4 Fossils in Tupuangi Formation, Mangere Island.

Whole and fragmental leaves (unidentified) and flattened lignified wood were found in the two upper units (Fig. 20). The lower, massive siltstone, contained numerous small cm-sized carbon lenses. The outcrop was found to contain Cretaceous and earlier, but no later pollens.

The following is a list of the pollen assemblage found:

Podocarpidites

Microalatidites

Dacrydiumites

Microfoveolatosporus

Spheripollenites (sim.)

Triporoletes (sim.)

Perotriletes

Araucariacites

Classopollis

Coptospora ?

Cyathadites

Tetracolpites?

Annulispora (sim.)

Quadrasporites ?

Dictyosporites

Cicatricosisporites (sim.)
Foraminisporus
Gleicheniidites (sim.)
Lycopodiumsporites
Reticulatisporites ?
Periporopollenites

The pollens were identified by comparison from Mildenhall (1994). Much of the pollen was crushed or broken. The slides also contained abundant plant fragments, strongly lignified wood (or charcoal?) fragments, as well as abundant dinoflagellate spores and fragments.

3.3.0 Bag End Breccia (formerly Whenuataru Tuff).

Bag End breccia (Fig. 24) consists of a series of coarse indurated units with intercalated finer muddy sandstones. It occurs immediately under the Basal member, Mangere Formation, at the northeastern end of the outcrop and pinches out at grid ref. 657193 (Fig. 9). Its maximum thickness is 7.5 m. It contains fragmental macrofossils of bryozoa, echinoderm spines, brachiopods, *Maoricolpus* and *Sectipecten*. Some of the lower units display water-escape and bed-loading features, such as flame structures and load casts (Fig. 25). A unique feature of this breccia is the occurrence within it of megaclasts of Rangiauria Breccia, up to 6x4x4 metres in size, which are found on both sides of the island near the North and South Landings (Figs. 19 and 26). The breccia occurs as layers of various thicknesses of indurated breccia separated by fine mudstone units.

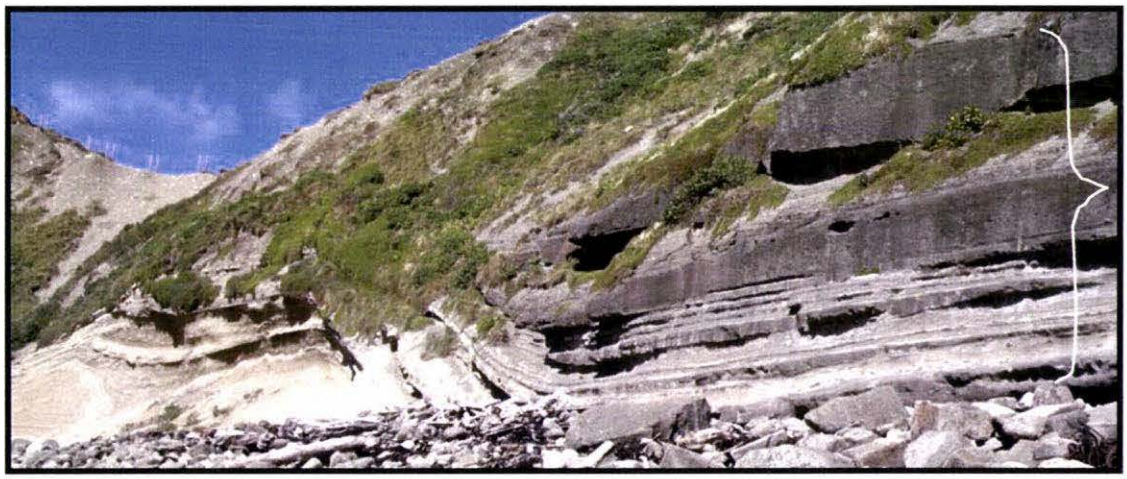

Figure 24. View showing the northeastern end of the Bag End breccia (bracketed to the southeast), North Landing. Note that it appears to be riding up over an outcrop of Robin Bush siltstone. Here the Breccia consists of beds of angular clasts in an indurated very coarse sandstone matrix separated by fine grained tuffaceous beds derived from the Robin Bush siltstone. The breccia is at its thickest to the right of the photograph and pinches out to the southwest. The saddle at the upper left is The Neck.

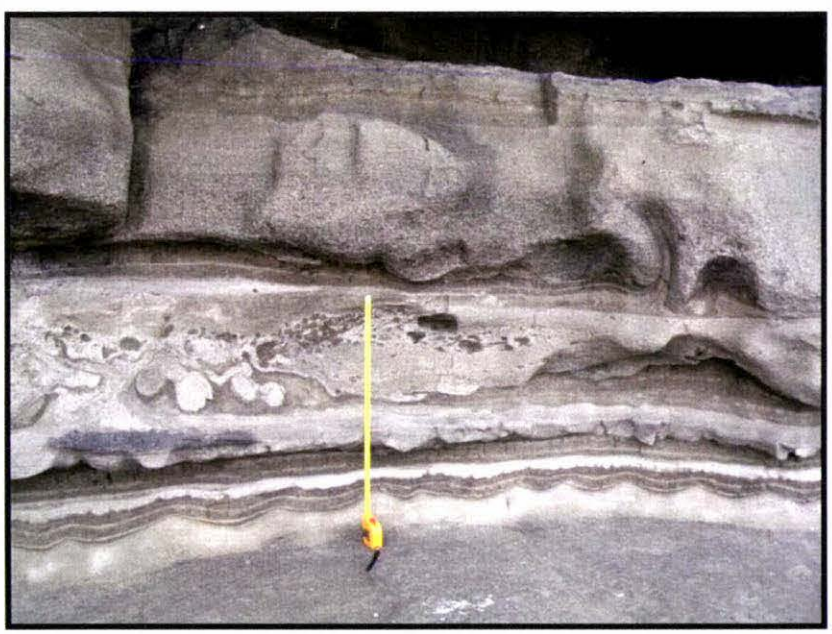

Figure 25. Detail of lower beds of Bag End breccia halfway along its outcrop at the South Landing. This shows, in the upper unit, some of the flame structures and load casts caused by sediment loading of water saturated mud layers by the overlying sand. At the left of the central mudstone unit are pillow type structures which probably resulted from the central unit being shocked when it was in a semi-consolidated state. The black clasts in the central sequence are probably foundered mudstone from the unit above. The lowest unit shows symmetrical ripples and is not thought to be part of the Bag End breccia but earlier marine sediments, (Robin Bush siltstone) overridden by the breccia. Length of tape is 750 mm.

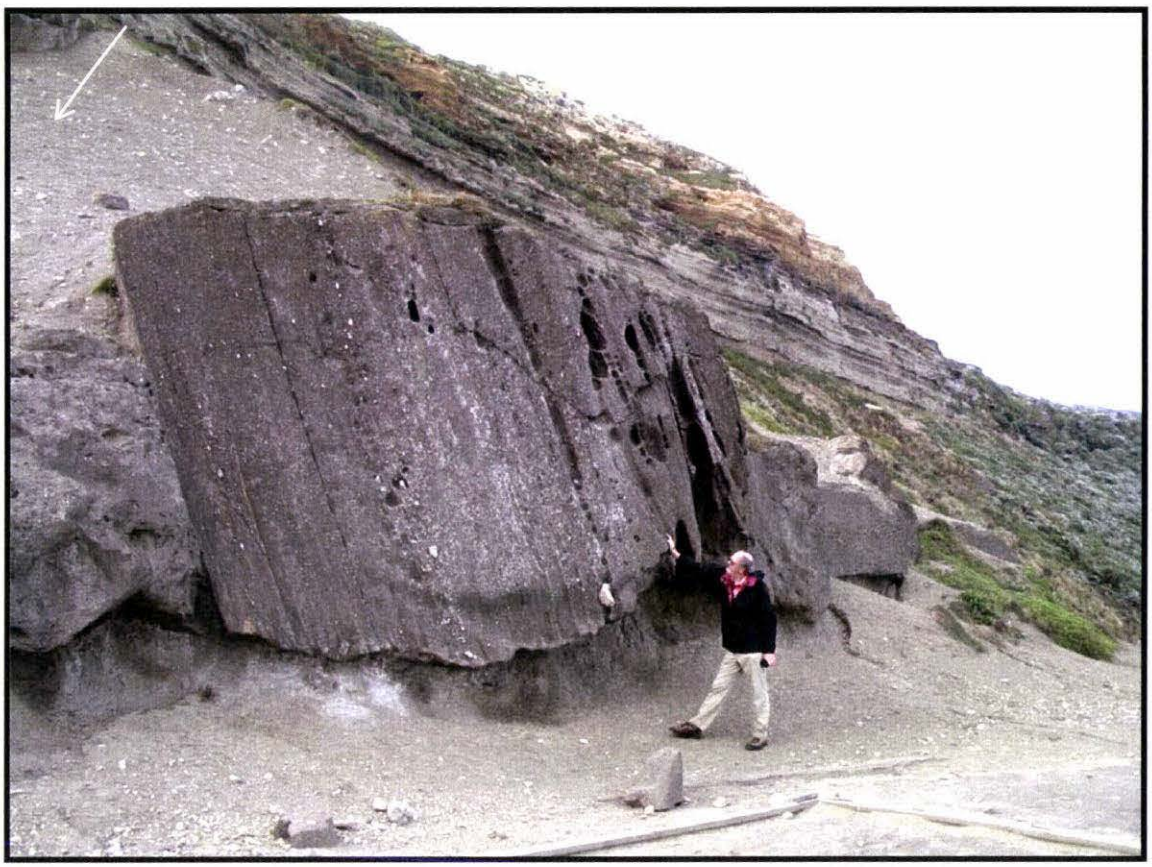

Figure 26. A megaclast of Rangiauria Breccia, with a maximum dimension of 6.6 m, incorporated into the upper part of Bag End Breccia (South Landing). The Breccia thins to the right and pinches out halfway along the visible face. The concretionary nature of the Basal Member, Mangere Formation, is arrowed at upper left. The foundation of a disused black robin aviary can be seen in the foreground.

3.4.1 Optical microscopy of Bag End Breccia.

A petrographic analysis was carried out as an aid to comparing this unit with the Whenuataru Tuff, on Pitt Island. The microscope slides show a very fine groundmass full of devitrified glass with subangular to subrounded lithics, of limestone and vesicular basalt. The basalt lithics contain numerous phenocrysts of hornblende, augite, magnetite/ilmenite, and plagioclase (Fig. 27).

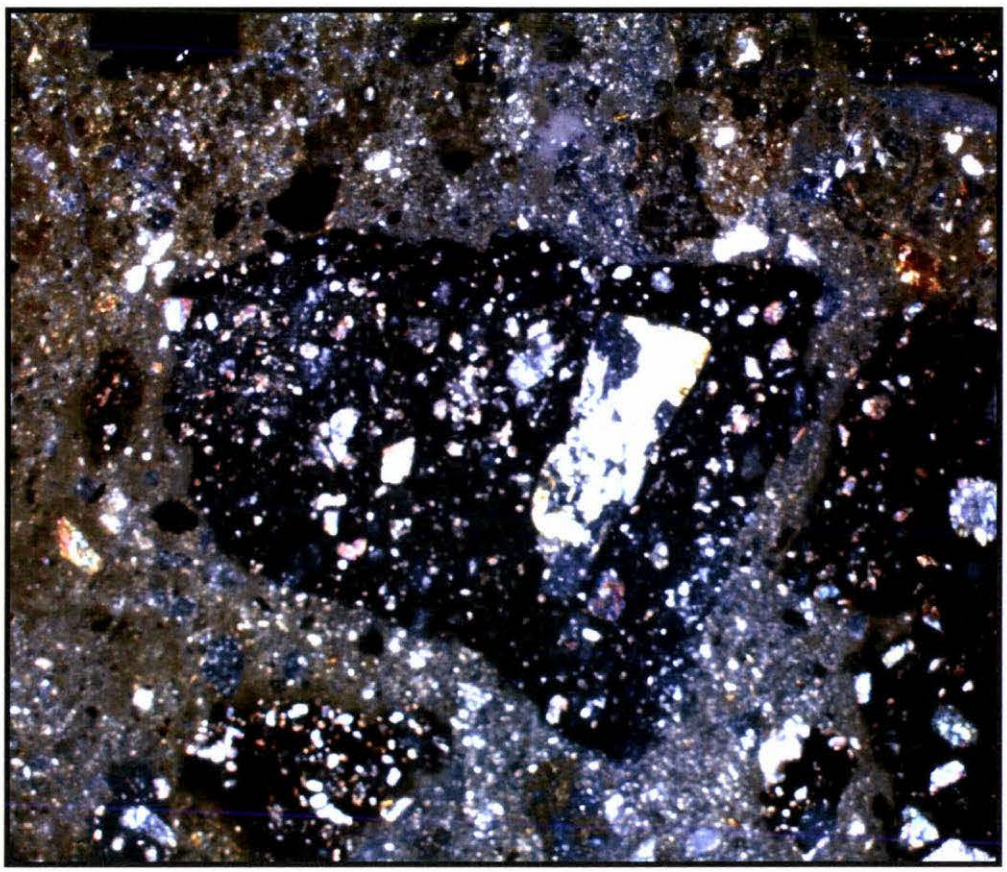

Figure 27. Photomicrograph of Bag End Breccia showing vesicular basalt lithics with phenocrysts of hornblende (*e.g.* the large arrowed phenocryst), augite, plagioclase and magnetite. The same crystals plus lithics, and inclusions of limestone xenoliths, occur in the very fine palagonitic matrix. Magnification 50x with crossed polars.

3.5.0 Mangere Formation.

3.5.1 Basal Member.

The type section for the Basal Member is based at grid ref. 658195 (to the left of the megaclast in Fig. 26). It is generally very fine grained and clayey except at the base where vague irregular bedding occurs. Here the siltstone contains lithics of vesicular basalt up to 10 mm diameter plus calcite, quartz, hornblende, and augite crystals. This merges at about 3-4 m above the base into a very fine mudstone almost all <32 μm grainsize. Several metres from the top there are increasing numbers and sizes of lithics, crystals, and woody material with irregular masses of fine claystone. Microscopic crystals of gypsum may sometimes be found associated with vesicles in

basalt near the upper boundary. The whole unit contains numerous generally irregular tubular concretions rich in calcite and usually with a wood nucleus. These tend to be regularly spaced at approximately 1 m intervals. The concretions seem to have formed around twigs and small fragments of wood. Most of the calcium in this member is in the concretions. Fossil wood (usually found associated with the concretions), in the form of twigs and small branches including rare small trunks is common, especially on the North Landing side. On the South Landing side, however, the wood and concretions are noticeably rarer. Most of the fossil wood appears to be concentrated on the northwest side of the member. In spite of the presence of wood, there is very little organic carbon in this member (Table 3).

Unlike the near vertical outcrop of the Cyclic Member, this unit forms a lower slope angle of *ca.* 40° and is largely covered with a very thin layer, or none at all of detritus (Fig. 28).

3.5.2 Loss on ignition, Basal Member. (see section 2.7.0)

This unit contains significant fossil wood suggesting, especially in the light of its very dark colour, that the unit itself might be carbonaceous. The results of loss on ignition of the silt fraction follow in Table 3.

Sample 1	0.49%
Sample 2	0.79%
Sample 3	0.52%
Sample 4	0.63%
Sample 5	0.60%

Average carbon = 0.6%.

Table 3. Loss on ignition (see Section 2.7.0), Basal Member. Sample 1 is from the base of the member. The Basal Member appears carbonaceous but any carbon is clearly concentrated in the wood fragments and concretions.

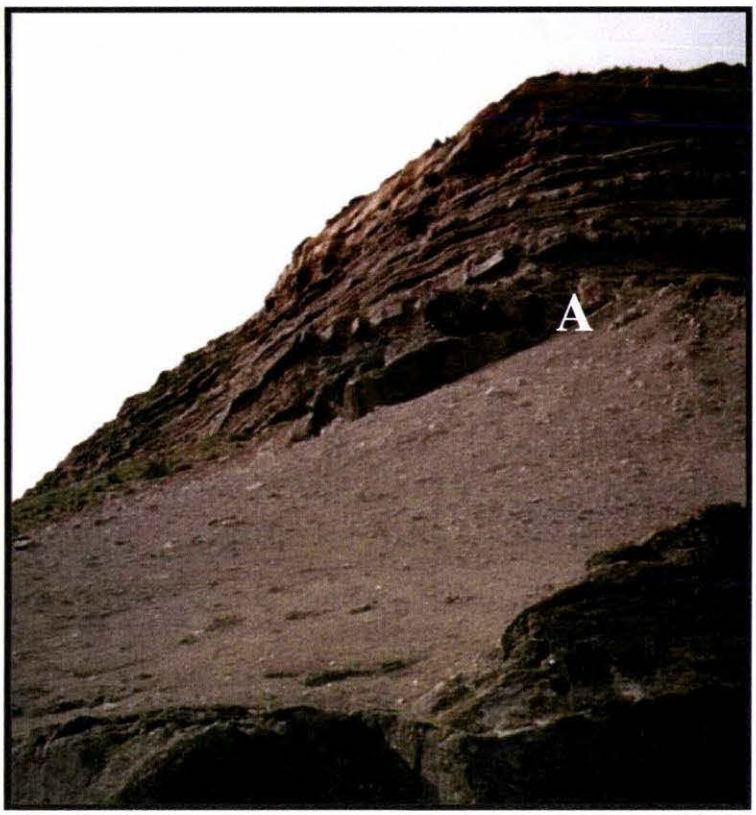

Figure 28. View of the Basal Member at grid ref. 668194. Note the numerous concretions and lack of detritus in this area. There is a marked change in slope between the Basal Member and the Cyclic Member at (A). The large rocks in the foreground are part of the Bag End Breccia.

3.5.3 Grain size analysis; Basal Member

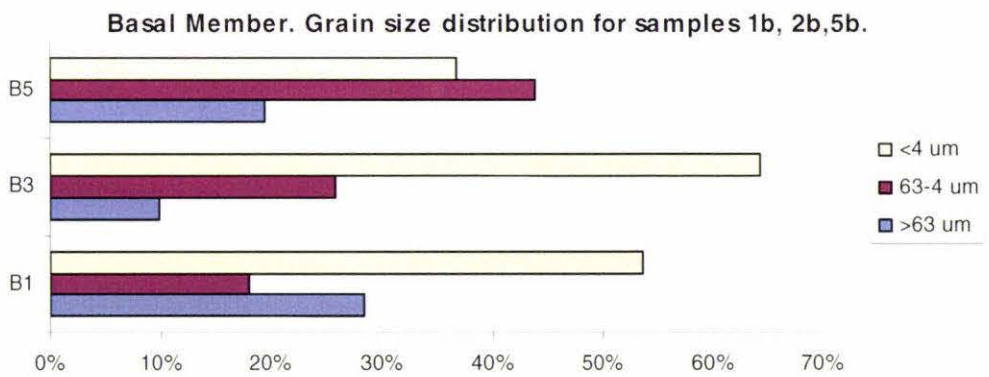

Figure 29. Percentage sand, silt and clay fractions for samples B1 (base), B3 (middle) and B5 (Top) of the Basal Member, Mangere Formation, showing the increased silt and mud fraction in the central (*ca.* 20 m) part of the member.

3.5.4 XRD analysis of rock samples; Basal Member.

The glass content was inferred as the complement of the sum of percentages for other minerals which were calculated directly from the XRD readout. This is supported by petrographic analysis, and a very strong reaction of all samples to the allophane field test. The kandite fraction was determined from DTA analysis of the silt and clay fractions. Volcanic glass is dominant in both the sand and silt fractions but is entirely missing from the clay fraction presumably because of alteration. Quartz and feldspar are quite low, but mica is prominent in the silt and clay fractions. Smectite and kandite dominate in the silt and clay fractions. A significant but undetermined amount of allophone not detected in the XRD analysis is present. Zeolites are represented in the silt and clay fractions also. The larger percentages were estimated to about 10-15% accuracy from the XRD readout. Smaller percentages of *ca.* 10% and less are not reliable but are a useful indicator.

	BASAL MEMBER: % mineral content.						
	SAND FRACTION.						
	Quartz	Feldspar	Mica	Chlorite	Hvy. Min.	Volc. Glass	$CaCO_3$
1b	7	10	0	3	16	63	1
2b	14	13	3	4	16	63	1
3b	12	13	0	3	16	55	1
4b	10	12	0	4	13	56	5
5b	30	17	3	3	13	34	0
6b	22	10	0	4	13	42	9
	SILT FRACTION.						
				Smectite	Zeolite		Kandite (DTA).
1b	12	15	15	34	1	20	4
2b	12	20	19	29	3	16	4
3b	6	10	17	41	2	21	3
4b	7	15	15	34	2	24	3
5b	6	10	14	46	1	20	3
6b	8	13	15	41	0	19	4
	CLAY FRACTION.						
1b	3	14	13	63	1	0	3
2b	4	13	10	63	1	0	4
3b	3	11	12	65	1	0	4
4b	4	18	9	64	1	0	4
5b	5	4	22	58	1	0	4
6b	4	13	18	61	0	0	4

Table 4. XRD results for rock samples from the Basal Member, Mangere Formation. Estimated margin of error is *ca.* 15%.

	HEAVY MINERAL FRACTION			
	H'blende	Augite	Ilmenite	Magnetite
G1	50	40	5	5
G1b	38	56	5	1
G2	67	25	5	3
G2b	49	42	7	2
G3	68	24	6	2
G3b	70	21	7	2
G4	60	30	7	3
G5	56	37	4	3

Table 5. XRD analysis of the heavy mineral fraction, Basal Member. (H'blende is Hornblende).

XRD analysis of heavy minerals separated from whole samples shows that hornblende is overwhelmingly dominant, with significant augite and lesser amounts of ilmenite and magnetite (Table 5).

3.5.5 Palynology; Basal Member.

Pollen is sparse in the Basal Member but plant fragments, many lignified, are relatively common, as are abundant whole, crushed, and broken dinoflagellates. There is significant charcoal (up to 50 μm in length) in the base of the Basal Member. This decreases in the middle 20 metres and increases again in the top 5 metres where maximum charcoal size increases to >50 μm. Much of the pollen is distorted, crushed or broken and is commonly unidentifiable. In addition to sampling the Basal Member (Fig. 21), 16 samples were taken at approximately 100 mm intervals from across the Basal/Cyclic Member boundary (Fig. 22) but adjusted slightly above the boundary to avoid the thin sandstone units. This boundary was sampled to see what environmental changes might have occurred with the change from massive mudstone deposition to alternating units of sandstone and mudstone, and also in the hope that some light might be thrown on whether this boundary is an unconformity. The following pollen (from very low counts per slide) have been identified:

1. Samples from 1.6 m above and below the Cyclic/Basal boundary.

(A):

(1) Those at approximately 100 mm intervals from above the Basal/Cyclic boundary:

trilete ferns

poaceae

asteraceae

Fuscospora

Myrsine

Coprosma

Podocarpus

Podocarpidites

Classopollis

Periporopollenites

dinoflagellates

Charcoal 0-50µm long

(2) Those at 100 mm intervals from below the boundary:

trilete ferns

poaceae

asteraceae

Phyllocladus

Fuscospora

Podocarpus

Myrsine

Coprosma

Cyathidites

Foriminisporis

Classopollis

an unknown well preserved, spherical, reticulate, dark brown pollen 25µm diameter

dinoflagellates

plus some charcoal <0-25µm long

(B).

Sample 1b (Fig. 20) taken from 500 mm above the base of the Member (Fig.20);

trilete ferns

asteraceae

Coprosma

Nothofagus

Podocarpus

Chenopodium

Triporoletes

Podocarpidites

Cicatricasporites

dinoflagellates

(C).

Sample 3b taken 15m above base of the member (Fig 21).

trilete ferns

asteraceae

Fuscospora

Chenopodium

Podocarpus

Classopolis

Pteris?

Tricolpites

Podocarpidites

dinoflagellates

3.5.6 Optical microscopy, Basal Member.

The microscope slides show that the central *ca.* 20 metres of this member have a very fine groundmass of silt to clay with very small, rare crystals of hornblende, augite and magnetite/ilmenite. Irregular clayey grey-brown coloured areas are common in the groundmass which appears to be altered volcanic glass. In the lower and top few metres of the member, the groundmass is slightly coarser (Fig.

30, left image) but grades into the very fine central portion of the member (Figs. 29 and 30 right image). Here the lithics and crystals of hornblende, augite, magnetite and ilmenite, though small (*ca* 0.3-0.4 mm), are sparsely but evenly distributed. A characteristic feature of the lower and upper portions of this member is scattered, often larger, clasts of limestone. Crystals and lithics are generally angular. Zeolites appear as small scattered spheres averaging *ca.* 0.1-0.2 mm in diameter which appear white under reflected light but remain in extinction under crossed nicols (Fig. 30). XRD analysis shows that the zeolite is analcime which is a cubic crystal and is therefore extinct under crossed nicols.

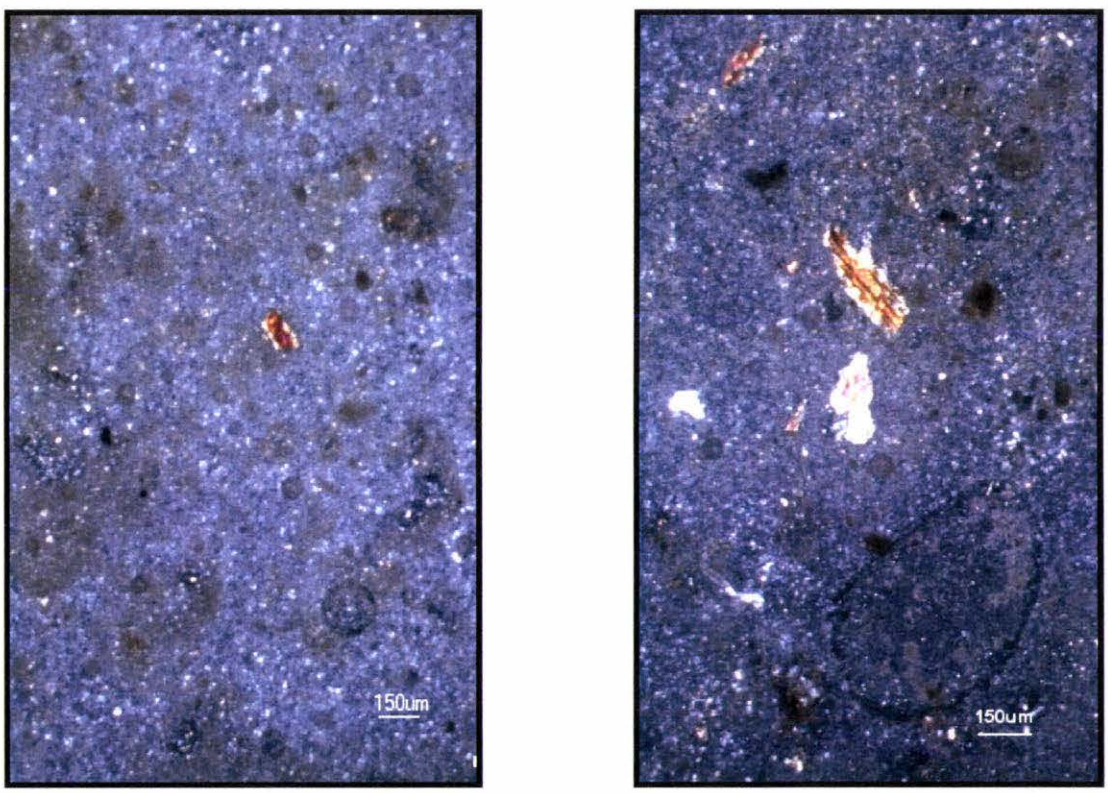

Figure 30. Photomicrographs of the Basal Member. The left-hand image was taken 1.5 m above the basal contact. Note the few, angular, crystals of hornblende and augite crystals set in a very fine matrix. The right-hand image was taken 15 m above the base. The number and size of larger clasts and crystals decreases dramatically in the central 20 m of the member.

3.5.7 Cyclic Member.

The stratigraphic column of the Cyclic Member (Fig 22, pp55&56 was taken at the extreme northeastern end of the formation. G.P.S. coordinates for the top are: S 44° 16.467′, W 176° 18.034′ and for the bottom of the member: S 44° 16.460′, W 176° 18.026′, (grid ref. 659195). The Cyclic Member consists of repeated units of horizontal, generally well consolidated, silty sandstone and sandy siltstones of varying thicknesses from millimetres to over 0.75 metres (in some cases with mudstone rip-up clasts in their bases) intercalated with siltstone units up to about one metre in thickness (Fig.31). The silt units of this member are all of essentially the same lithology as the Basal Member. The new factor is the appearance of intercalated beds of sandstone in the siltstones forming the Cyclic Member.

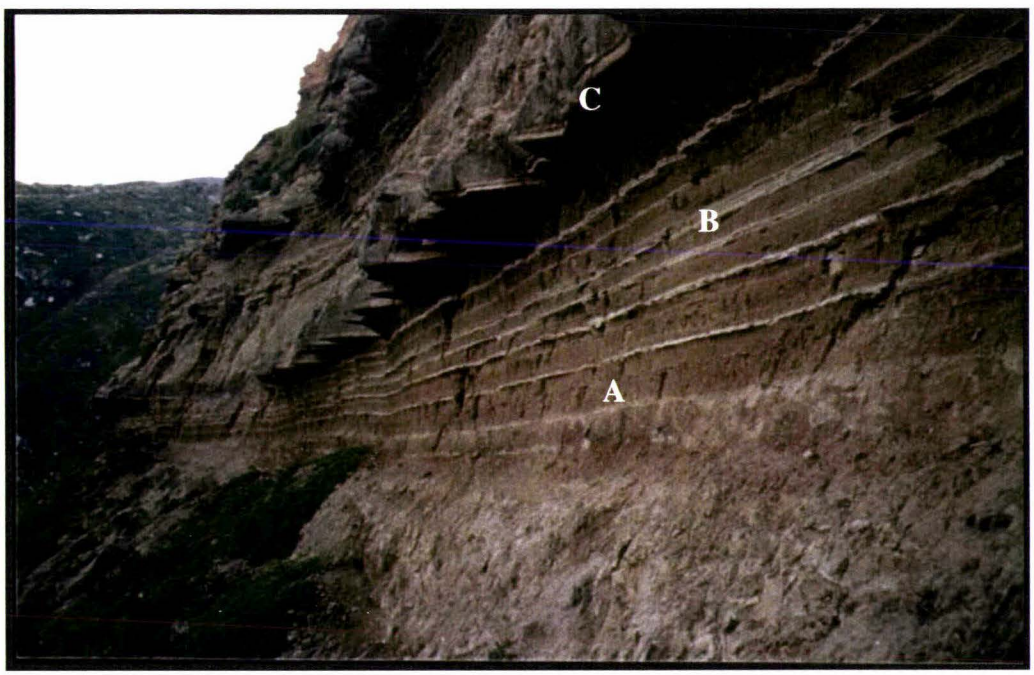

Figure 31. View of the Cyclic Member (North Landing side) looking towards the northeast from the centre of the face (grid ref. 657193) showing the junction between the Basal and Cyclic Members (A). The mudstone/thin sandstone sequence (B) above, is typical of the Cyclic Member. The lowest, thick, protruding sandstone unit shown above is bed 26c (C), informally named the ripple unit. The ripple unit here is 550 mm thick. Note the *ca.* 90° joint pattern, revealed by physical weathering that is characteristic of the sandstone units. To the left (just around the far corner in the photo) beds 27 to 32 merge into the lowest mudstone/thin sandstone unit. This area is characterised by foundered blocks, slabs and disturbed bedding (Figs 32 and 33).

Figure 32. A block fallen from the termination of unit 30. To the right of this the lowest unit of the Cyclic Member takes the regular form seen in the main face in Figure 31 (arrowed).

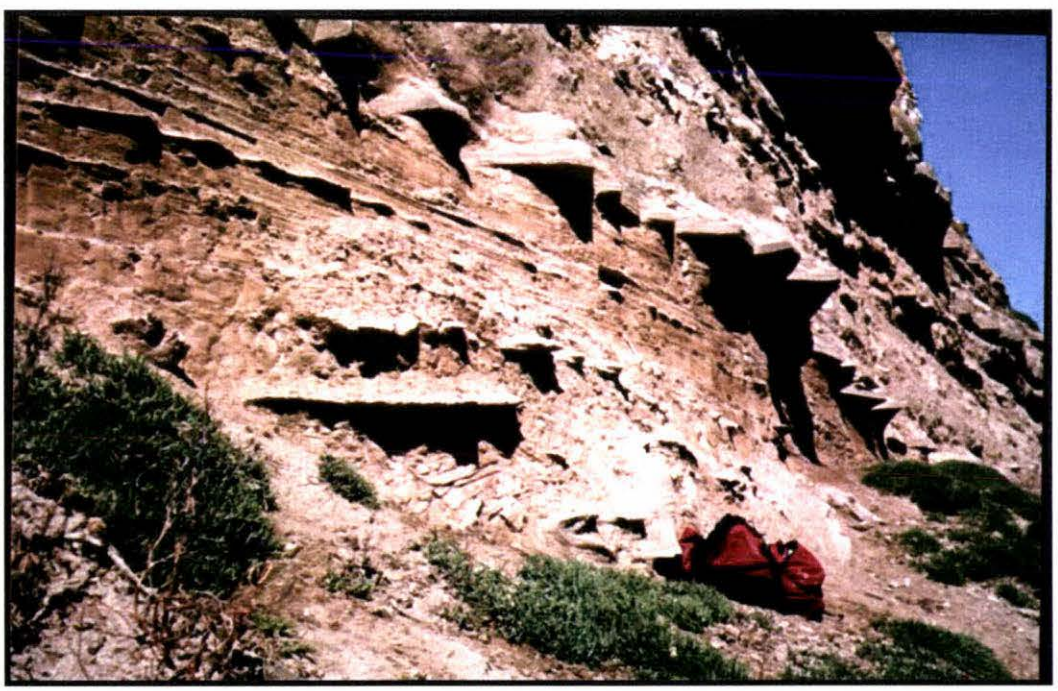

Figure 33. View showing disturbed bedding immediately above the Basal Member in the area to the northeast of the formation where units 27 to 32 are terminating. This is a result of slumping and at least two turbidites as shown in Fig. 36. The protruding, thick sandstone unit is the ripple unit. See Fig. 71 for an explanation of the disturbed bedding in this area.

Figure 34. View of the junction between the Basal and the Cyclic Members showing intraformational folding at grid ref. 657193 in the lowest bed of the Cyclic Member. This photograph was taken in the same vicinity (almost certainly in the same place) as the photograph in 1957 (Campbell *et al.* 1993 p. 152). Erosion (which appears to be rapid- the surface is barely chemically weathered) has destroyed the dramatic convolute bedding shown in that photograph.

Figure 35. Detail of the Cyclic Member above the South Landing showing a shallow, current channel fill (A) in the ripple unit and, to the left, the dislocated and overridden ripple layer (B) arrowed.

At the northeastern end of this unit on the North Landing side, measured apparent dips were; 2° at 250° and 1°at 200° (these angles proved too fine to process satisfactorily on a stereonet or by geometrical construction, but the true dip here is about 2.5° at 270°). At the southwestern end and at the Southern Landing the attitude is horizontal.

Characteristically the units are all poorly to moderately well sorted and consist of both quartzofeldspathic and volcaniclastic fractions. The largest grains are quartz, hornblende, zeolite and lithics. The sediments are all texturally and compositionally immature (Boggs, 2001, p143), in that the grains are all angular to subrounded and contain unstable grains such as lithics and feldspars. The matrix is clayey. Most of the units are continuous through the member but some show considerable disturbance with dislocated sandstone beds (Figs. 32-34) as is evidenced by foundered blocks and slabs of sandstone, as well as chaotically disturbed bedding in the units below 26c, (the ripple unit), *i.e.*, 28c, 30c, and 32c, at the northeastern end of the member (Figs. 32 to 34 also 71). These units terminate within 75 m. and pass into the lowest siltstone sequence. To the southwest, the two thicker sandstone units at the top of the member terminate within 25 m of the southwestern end of the Cyclic Member (Fig. 18) while the lowest bed of the sequence here shows intraformational folding at grid ref. 657193 (Fig. 34). Only the lower beds at the southeastern end, South Landing, are disturbed.

The sandstone units generally grade upwards and merge into the mudstones over millimetres to a few centimetres. Two of the lower sandstone units (28c and 30c) show load casts on their bases. Many of the sandstone units of the Cyclic Member have scattered soft aggregates of amorphous calcium carbonate which appears to be diagenetic.

Figure 36. View from the extreme northeastern end of the Formation, of the units below the ripple unit which here, is 850 mm thick and is just visible at the top of the photo (A). Load casts are present on the bases of units 28c and 30 (B & C). These units terminate *ca.*75 metres to the southwest. The lower sandstone unit (C) is 700 mm thick. Units B and C are turbidites.

Some sandstone units have very fine, almost symmetrical, ripples of short wavelength (<0.5 cm) and high amplitude (C 1.4 mm) on their bases. The ripples on 26c (the ripple layer) are oriented at 310° at the South Landing and at 305° at the North Landing The stoss side of the ripples faces 220° and this is the direction of their origin (allowance having been made for their position on the underside of a unit) (Fig. 37). A wavelength of < 0.5 cm with an amplitude of approximately 1.4 mm gives a ripple index of approximately 3.6. Higher units were not accessible to check this, but fallen blocks (of different thickness) show that some other units have

exactly the same ripple form (Fig. 37). As discussed in section 2.8.0 an experiment was performed to attempt to simulate these ripples in a large trough in windy conditions. The result of this is shown in Fig. 38. I observed wind driven wavelets on the shallow water of a tidal flat at Foxton. Unfortunately the substrate was too consolidated to form ripples but the ripples on the water surface matched those on the sandstones and Dr Wallace's result closely.

Figure 37. View of short wavelength, high amplitude, near symmetrical ripples found on the bases of some of the sandstone units in the Cyclic Member. 4 x full size.

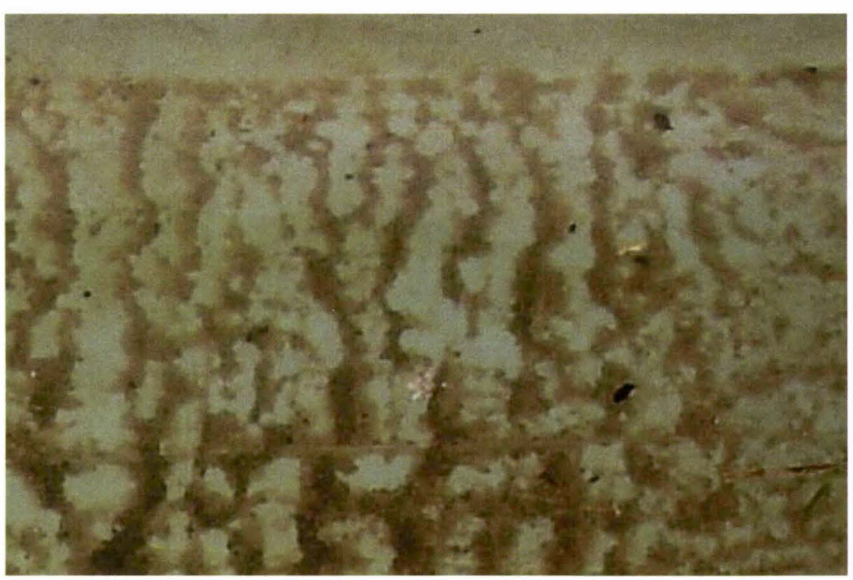

Figure 38. Image, to the same scale as Fig. 37, of ripples experimentally formed in trough using a similar grain size to Fig. 37 to simulate the very short wavelength ripples shown in fig. 37, above. Photo; R.C.Wallace.

The thicker sandstone units show variability in thickness, tending to become thinner towards the southeast. Some sandstone units have small mudstone rip-up clasts in their bases. No other sole marks or ichnofossils have been found either *in situ* or on fallen blocks.

The lowest siltstone unit has considerable growth of gypsum in joints as well as around fossil wood, where it typically forms radiating needles 1.5-2 cm long. In unit 12c, gypsum crystal needles 1 cm long can be found packed on each side of a 1 mm thick dark brown layer and normal to it (Figs. 39 and 40).

Figure 39. Fossil wood in the lowest unit of the Cyclic Member. The yellow colour to the right of the card is sulphur. The glassy sheen (arrowed) above the wood is gypsum.

Figure 40. Gypsum (arrowed) formed on the joint planes of the lowest unit of the Cyclic Member.

3.5.8 Stereographic analysis of joints, sandstone units, Cyclic Member.

Figure 41 shows the ellipsoid of stress for unit 26c. (This pattern of jointing is common in the sandstone units). The least principal stress, s3, is directed northeast-southwest at 10 deg to the surface. The principal stress, s1, is also horizontal and directed northwest-southeast. The intermediate stress, s2, is dipping 10 deg. southeast (Phillips, 1972).

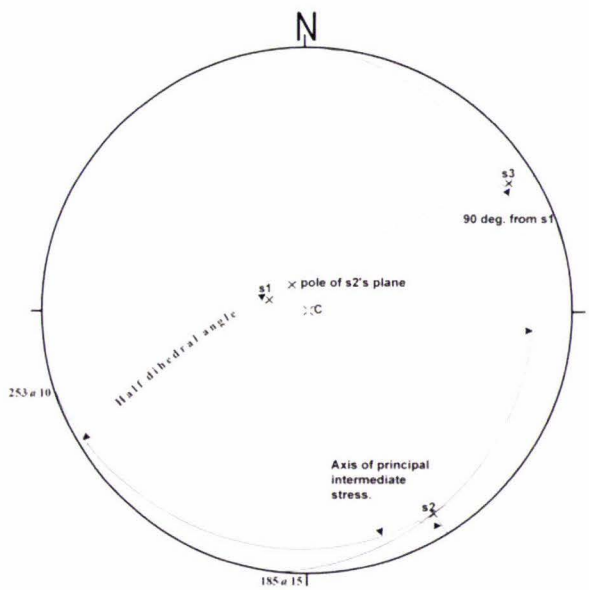

Figure 41. Stereographic analysis of joints in the ripple unit (26c), Cyclic Member.

3.5.9 Grain size analysis, Cyclic Member.

The following bar and cumulative frequency graphs are all bi- or polymodal with the result that statistics based on neither the graphical method of Folk and Ward (1975) nor the method of moments of Krumbein and Pettijohn (1938) give completely reliable results. However for each of the cumulative graphs below the method of graphical statistics of Folk and Ward (1975) have been calculated because,

even though the resulting value is somewhat skewed by slight bi or polymodality, the trend is clear.

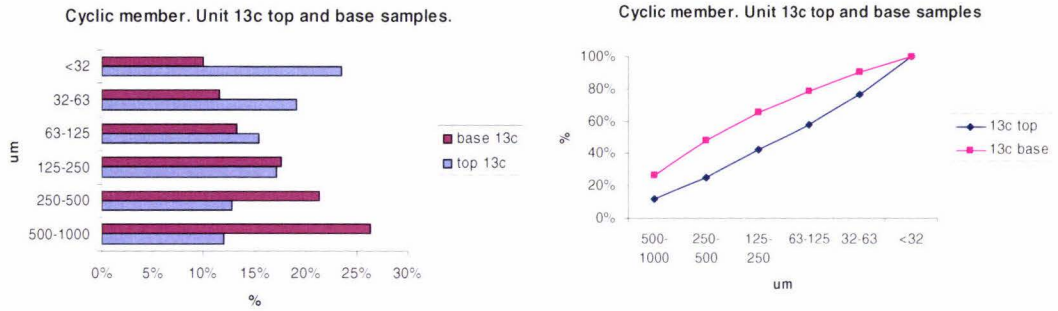

Figure 42. Bar and cumulative frequency graphs showing distribution of grain sizes for unit 13c, Cyclic Member.

	top	*Base*	
Graphic mean	2.6	*2.8*	
Inclusive graphic σ (φ)	1.5	*1.8*	poorly sorted
Inclusive graphic skewness	-0.51	-1.3	Negatively skewed

Table 6. Graphical statistics for Fig. 42.

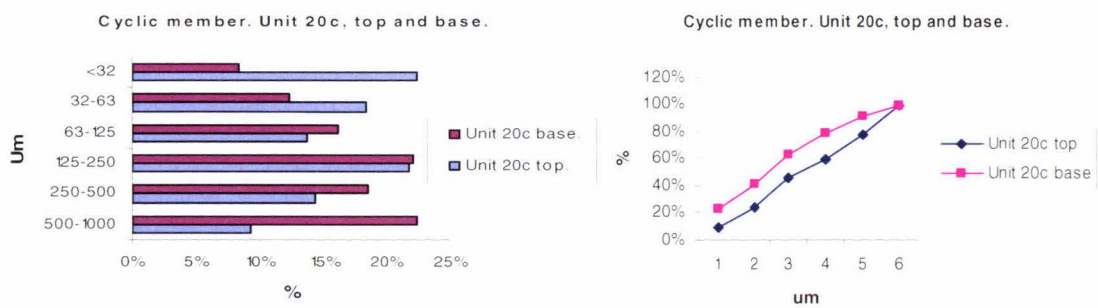

Figure 43. Bar and cumulative frequency graphs showing distribution of grain sizes for unit 20c, Cyclic Member.

	top	*Base*	
Graphic mean	2.8	*2.0*	
Inclusive graphic σ (φ)	1.7	*1.5*	Poorly sorted
Inclusive graphic skewness	0.07	0.1	Positively skewed

Table 7. Graphical statistics for Fig. 43.

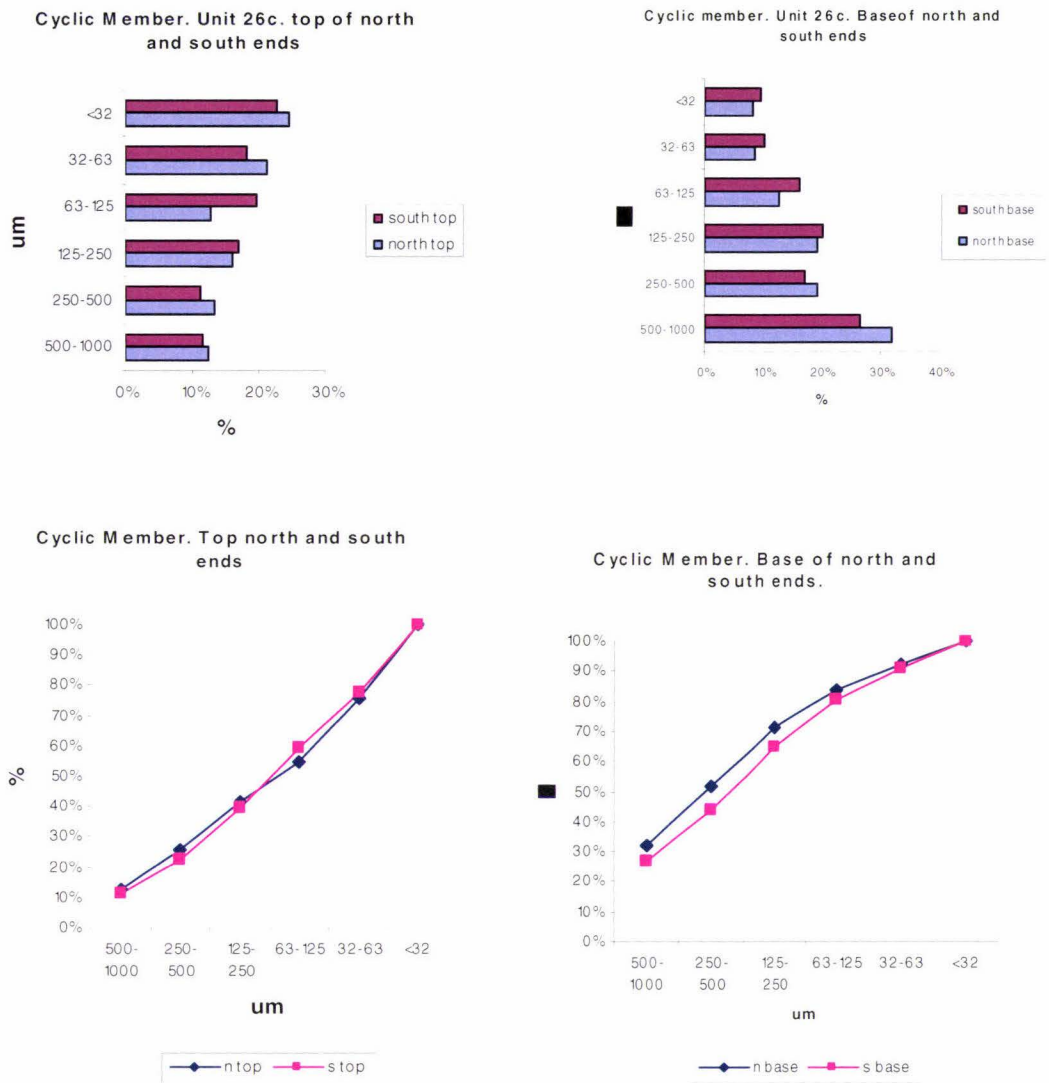

Figure 44. Bar and cumulative frequency graphs showing distribution of grain sizes for the top and base, north and south ends, of unit 26c, Cyclic Member.

	Top North end	Base North end	Top south end	Base south end	
Graphic mean	2.6	2.0	2.55	*1.9*	
Inclusive graphic σ (φ)	1.9	2.8	2.1	*2.4*	Very poorly sorted
Inclusive graphic skewness	0.036	-0.35	0.4	-0.06	Top-positive Base- negative

Table 8. Graphical statistics for Fig. 44.

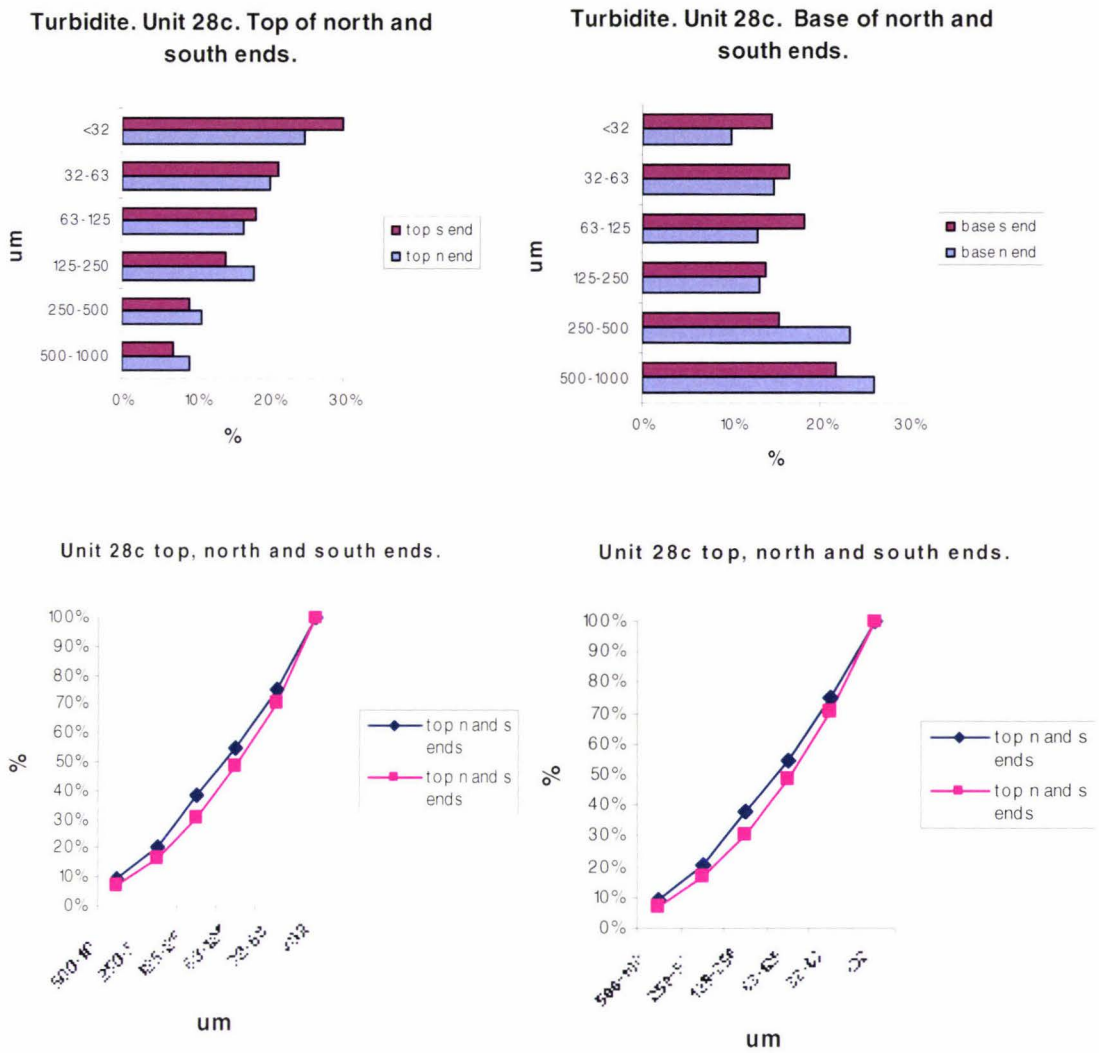

Figure 45. Bar and cumulative frequency graphs showing distribution of grain sizes for the top and base, north and south ends, of unit 28c, Cyclic Member.

	Top North end	Base North end	Top south end	Base south end	
Graphic mean	3.1	3.8	3.3	*3.7*	
Inclusive graphic σ (φ)	1.8	1.9	1.85	*1.84*	Poorly sorted
Inclusive graphic skewness	0.007	-0.2	0.23	-0.12	Top- positive Base- negative

Table 9. Graphical statistics for Fig. 45.

3.5.10 XRD results; Cyclic Member.

CYCLIC MEMBER

Sand fraction	Quartz	Feldspar	Chlorite	CaCO3	Gypsum	Amorphous or Volc. glass	Natro-alunite	%Heavy
11c	12	25	9	1	0	20	1	33
12c	9	5	0	0	50	4	0	32
13c	12	25	8	21	0	18	1	37
14c	30	20	3	1	0	41	0	5
15c	16	13	2	4	0	58	0	7
16c	25	30	9	1	0	19	1	17
17c	30	18	2	1	0	44	1	6
18c	12	22	8	2	0	28	2	34
19c	35	22	3	2	0	32	1	8
20c	25	16	4	2	0	32	2	23
21c	8	15	6	20	0	29	2	22
22c	30	16	0	1	0	49	1	5
23c	10	15	4	8	0	34	2	29
24c	25	17	3	2	0	47	1	6
25c	30	15	5	4	0	24	1	22
26c	0	4	0	2	90	3	0	3
27c	22	16	0	5	0	0	1	7
28c	3	0	0	1	95	1	0	1

Silt fraction.

				Mica	Zeolite		Smectite
11c	6	25	12	1	2	54	0
12c	17	17	12	1	2	46	10
13c	4	30	3	0	0	63	0
14c	20	15	0	3	5	52	5
15c	20	20	15	4	2	14	25
16c	8	20	20	2	0	47	3
17c	20	16	7	3	4	40	10
18c	5	18	3	1	0	73	0
19c	20	15	5	3	4	53	0
20c	8	20	4	1	0	67	0
21c	6	27	2	1	1	64	0
22c	16	12	6	3	3	50	10
23c	5	18	0	0	0	77	0
24c	17	13	5	3	2	50	10
25c	10	15	0	0	0	75	0
26c	20	15	6	2	3	54	0
27c	18	12	8	4	2	52	12
28c	18	11	5	3	3	55	5

Clay fraction.

			Mica	Kandite		Smectite
11c	3	14	3	4	66	10
12c	10	14	2	8	51	15
13c	3	15	4	0	73	15
14c	3	7	3	5	57	25
15c	5	17	4	5	29	40
16c	3	14	4	8	65	0
17c	5	8	4	10	33	40
18c	4	15	4	0	77	0
19c	6	8	4	8	44	30
20c	3	10	3	3	76	5
21c	2	15	3	2	73	5
22c	4	4	2	6	14	30
23c	3	13	3	0	78	3
24c	5	7	4	4	0	80
25c	3	10	2	0	80	5
26c	12	5	1	8	64	10
27c	7	8	5	5	15	60
28c	10	5	1	11		25

Table 10. XRD results for sand, silt and clay fractions, Cyclic Member.

Tables 10 and 11 show that the sequence is partly quartzofeldspathic and partly basalt-derived, as the heavy mineral fraction indicates. These results have been estimated from the graphical XRD readouts discussed in Chapter 2. They are less accurate for the lower percentages. Microscopic examination of thin sections show that the above values (Table 10) for $CaCO_3$ are underestimated as is mica in the silt fraction. Heavy minerals also occur abundantly in the silt fraction (as is evidenced by thin section analysis) but appear to be masked in the XRD readout mainly by the quartz and feldspar signals. Thus the percentages are calculated only on the minerals shown in the table (they were extracted and processed separately in the sand fraction). Volcanic glass and/or amorphous minerals are a major component of all fractions. Their percentage was determined as the complement of the sum of all other minerals. That this fraction is mainly volcanic glass (or altered volcanic glass) is supported by thin section analysis. Smectite and kandite (halloysite and kaolin) are the main clay minerals. In the sand fraction the results for units 12c, 26c and 28c appear anomalous as regards quartz, feldspar and gypsum. This is because these samples were extracted from gypsum-rich locations associated with fossil wood.

Cyclic Member				
Heavy mineral fraction				
Sample	H'blende	Augite	Ilmenite	Magnetite
11c	34	53	7	6
12c	73	15	8	4
13c	47	42	6	5
14c	65	26	9	0
15c	87	3	10	0
16c	85	3	10	2
17c	83	4	10	2
18c	50	42	6	2
19c	80	7	10	3
20c	64	28	8	0
21c	32	60	5	3
22c	78	10	8	4
23c	40	52	6	2
24c	62	28	8	2
25c	40	53	7	0
26c	53	40	5	2
27c	63	28	9	0
28c	72	20	6	2

Table 11. XRD results, heavy minerals: Cyclic Member.

XRD analysis of heavy minerals separated from whole samples shows that hornblende is overwhelmingly dominant with significant augite and lesser amounts of ilmenite and magnetite. This is very similar to the Basal Member.

3.5.11 Microprobing of hornblendes in the Cyclic Member and Rangiauria Breccia.

It was suspected that there might be two populations of hornblendes in the Mangere and Parakeet Formations based on the likelihood that hornblendes came from both the Rangiauria Breccia and Red Bluff Tuff of Pitt Island. Seven samples of seven hornblendes from each of the Rangiauria Breccia, unit 30c of the Cyclic Member, Mangere Formation, and the Skua Member, Parakeet Formation (from Sk1 and 2), were microprobed as an aid to determining their provenance (Appendix 3). The data (Fig. 46) show the comparison of Mg and Fe *vs.* alkalis for hornblendes.

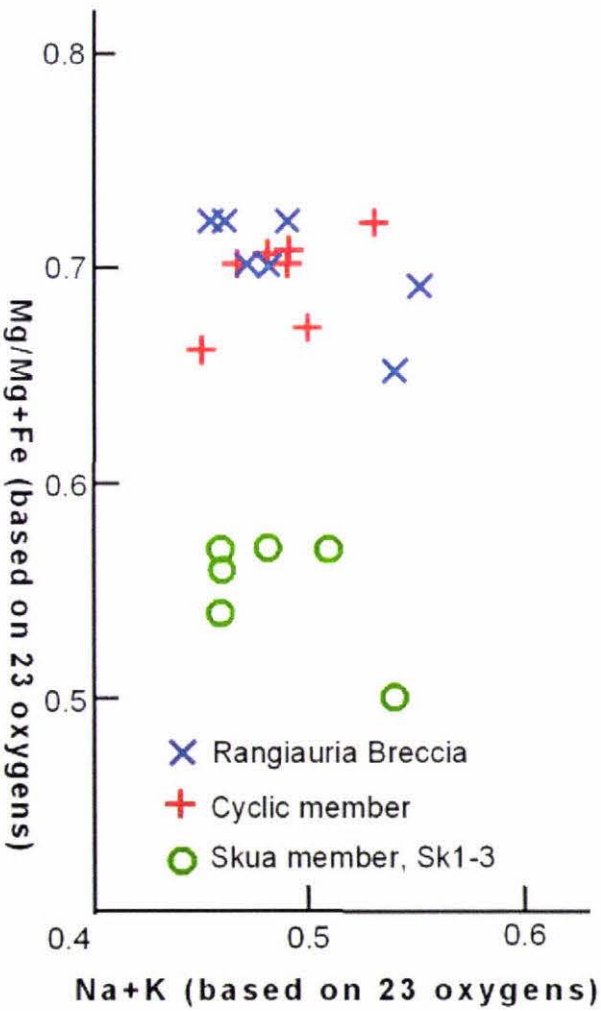

Figure 46. Graph of Mg/Mg+Fe ratio against Na+K for hornblendes showing the similarity between hornblendes in the Cyclic Member and Rangiauria Breccia.(See p 98 for a discussion of hornblendes of the Rangiauria Breccia vs those of the Parakeet Formation.

3.4.12 Fossils.

As stated in Chapter 2, no siliceous or calcareous microfossils (i.e. foraminifera, coccoliths, diatoms or radiolarian) were found despite six separate samples being examined. Bryozoa, ostracods, an echinoderm spine, a mollusc (very thin, fragile, brittle shells of *Cirsotrema*?) and polychaete tube fragments were found mainly in unit 13c, with similar but rarer examples in units 12c, 15c, 21c and 27c. The ostracods were kindly identified by Bruce Hayward (Geomarine Research, pers. com.) as *Xestoleberis* sp and *Leptocythere* cf. *lacustris* He also identified a mollusc as *Arthritica ?bifurcata*.

3.4.13 Palynology: Cyclic Member.

The pollen shown in the accompanying pollen diagram (Fig. 47) were extracted from the mudstone units of the Cyclic Member. In addition to the Pliocene pollen listed in this diagram, a considerable number of Cretaceous and Jurassic pollens were found. No count was made of these as they are all interpreted to have been recycled from the Tupuangi Formation (Mildenhall 1994, p. 21; Campbell *et al* 1993, p. 149). A list of the Cretaceous and Jurassic pollens identified using Mildenhall (1994) follows:

plentiful whole and fragmented dinoflagellates with some acritarchs.

Classopollis

Perisporopollenites

Microcacridites

Cacadopites (sim)

Lycopodiumsporites

Foraminisporus

Triporoletes (sim)

Phimopollenites

Tricotomosulcites

Schizosporus (sim)

Peripollenites (sim)

Macrofoveolatosporus

Dactyopolis

Asteropollis

Araucariacites (comp)

Cicatricasporites

Podocarpidites

Podidites??

Gleicenidites

Histiopterix?

The diagram shows that, throughout the period of deposition of the Cyclic member no large trees grew in its vicinity. However small trees and shrubs, notably *Myrsine, Coprosma,* and asteraceae, were common throughout this period, especially in the upper half of the sequence. The greatest variability of species was largely in the lower part of the sequence from 17c–27c where herbs and ferns predominated. Grasses were well represented everywhere except perhaps for 25c when ferns were dominant.

Fuscospora pollen (listed under "exotics" in the pollen diagrams referring to their origin from mainland New Zealand) was not found in the lower part of the sequence but increased in numbers from 17c to 11c where a major influx of *Fuscospora* pollen occurred. Podocarp pollen is more evident in the middle portion of the sequence.

Charcoal is characteristic of the units 21c to 12c with an additional isolated appearance close to the base of the sequence (sample 27c). Except for units 21c and 15c the charcoal is mainly less than 50μm long.

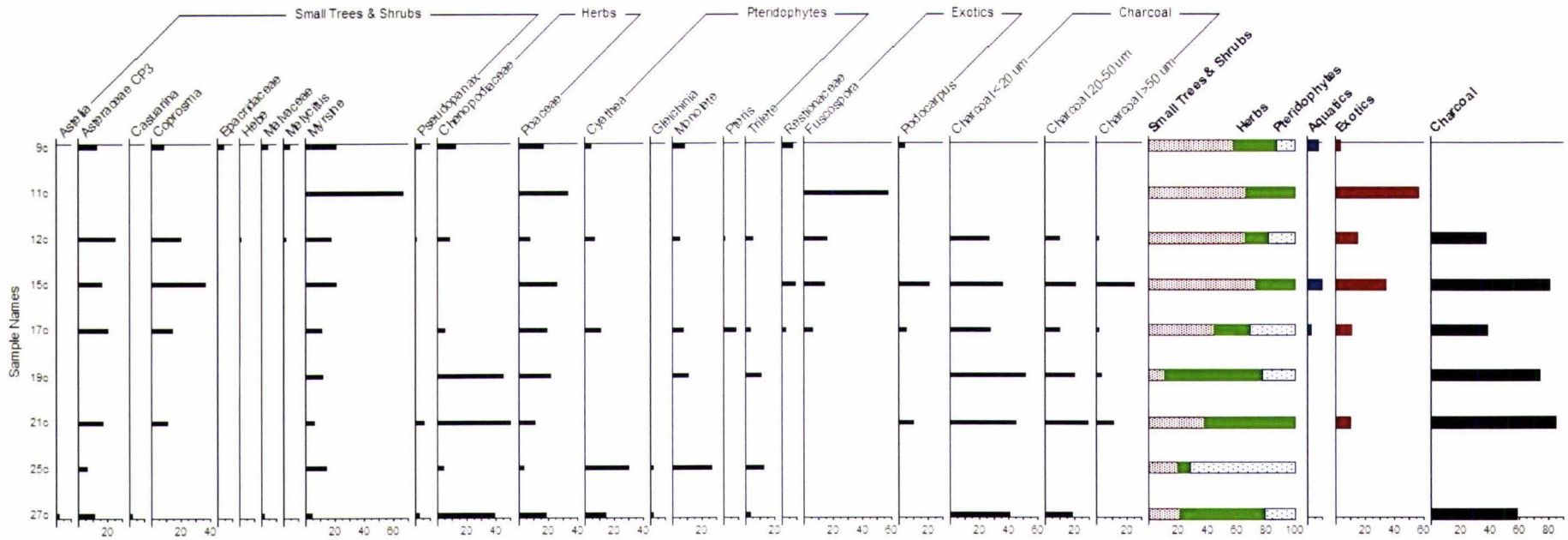

Figure 47. Relative pollen diagram of the Cyclic member.

Note: "Exotics" here means "not found on Chatham Islands from at least the late Pliocene to present".

3.6.0 Parakeet Formation.

3.6.1 Carbonaceous Member.

The Carbonaceous Member is seen on the cliff face (Fig. 18) as a black narrow band, between the Cyclic and Skua Members. It is only accessible *in situ* at the southern end of the formation on the cliff edge where it intersects the surface and is actively weathering and eroding. An intact fallen block at grid ref. 657194 gives the thickness of this member as 565mm (Fig. 48). (An *in situ*. type section was not possible in this case because of difficulty of access). This fallen block consists of the six beds shown on the stratigraphic column of Fig. 22. The Carbonaceous Member pinches out approximately 200 m from the southeastern end of the member. The Carbonaceous Member marks a distinct break from the environmental conditions that prevailed when the Cyclic Member was deposited. Samples of rock were collected *in situ* from the southern end of the outcrop, and from the fallen block, for petrographic and pollen analysis. These samples were subject to loss on ignition to determine the percentage of carbon. The results are shown in Table 12.

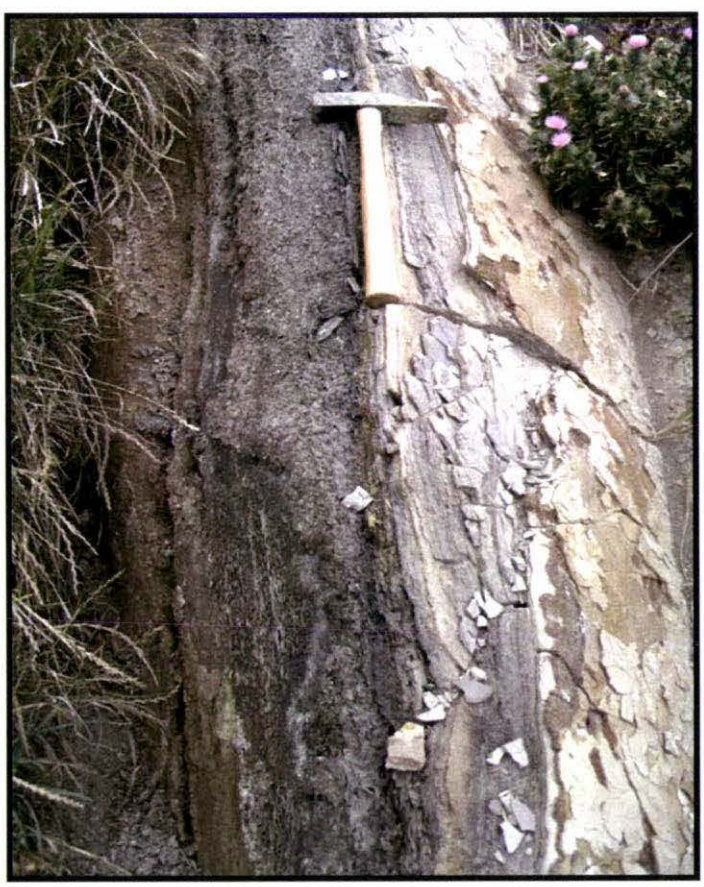

Figure 48. The hammer is lying on the base of the fallen block of the Carbonaceous Member which comprises six separate beds.

3.6.2 Loss on ignition: Carbonaceous Member.

Sample 1	14.0%
Sample 2	12.5%
Sample 3	20.0%
Sample 4	9.4%
Sample 5	11.7%
Sample 6	22.7%
Sample 7	18.1%
Sample 8	16.3%

Average organic matter content= 14.4%.

Table 12. Loss on ignition interpreted as organic matter content of the Carbonaceous Member samples- samples 1and 2 are *in situ* and 3- 8 are from the fallen block.

3.6v.3 Palynology, Carbonaceous Member.

The pollen diagram for the Carbonaceous Member (Fig. 49) is in two parts: samples Lks 1 and 2 and samples Lk 1 to 6. Lks 1 and 2 were sampled *in situ* from a partially eroded sequence of the Carbonaceous Member outcropping on the skyline ridge of Mangere Formation at its southern end. Samples Lk 1- Lk 6 are from a fallen block of the Carbonaceous Member found lying on the Basal Member (Fig. 48). Both sets of samples show the same thing - a preponderance of pteridophytes with *Cyathea* and monolete ferns dominant except for unit Lk 6, at the base of the member, where grasses become more abundant. Among small trees and shrubs a wider array of species is represented than in either the Cyclic or Skua Members. A wide range of aquatics and exotics is present throughout the sequence. Although charcoal is significant in the upper part of the sequence, no particles greater than 50μm long were found. As with the preceding members a similar range of Cretaceous and pre-Cretaceous palynomorphs (recycled from the Tupuangi Formation (Mildenhall 1994)), in varying states of preservation, were found together with abundant organic debris., The calcareous algae, *Botryococcus,* was found in abundance in this unit and probably accounts for its organic content.

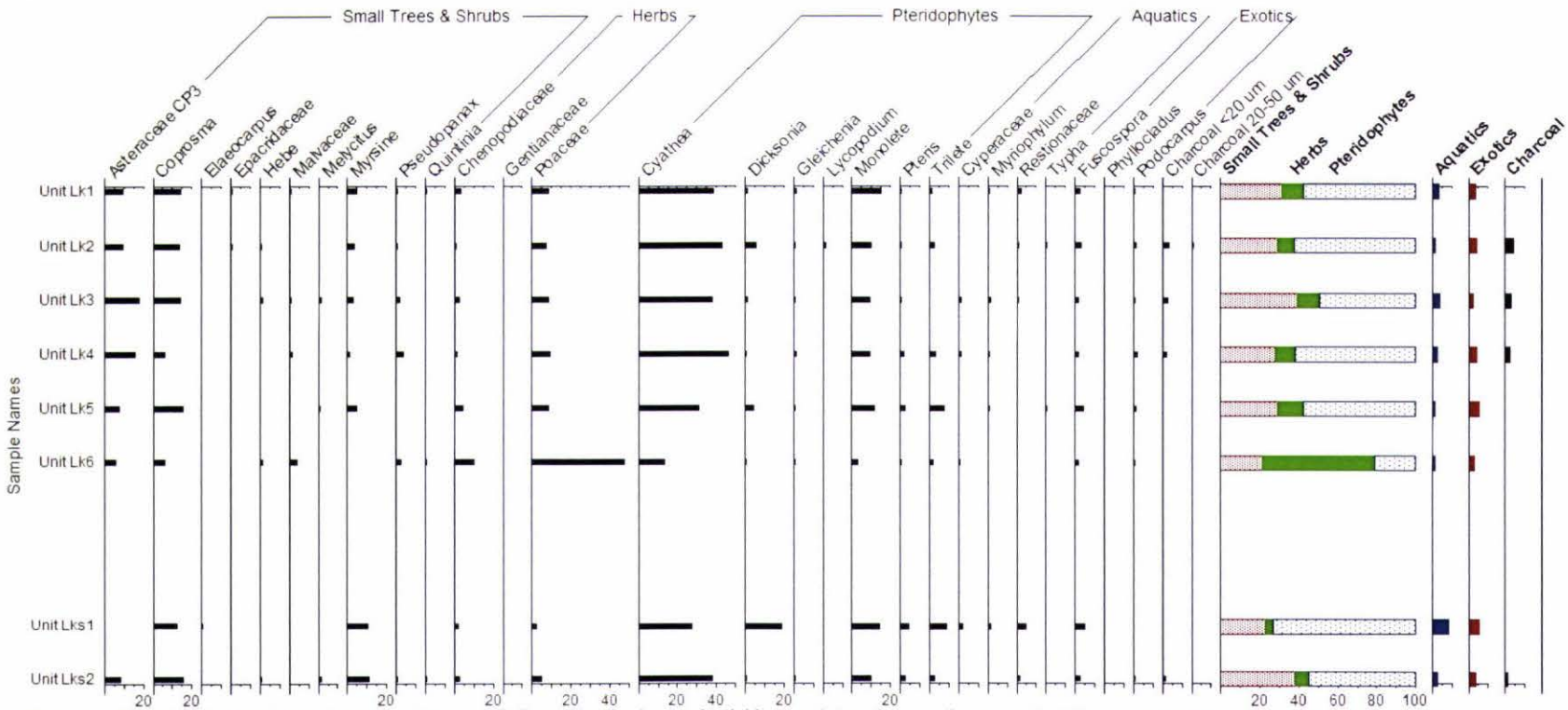

Figure 49. Relative pollen diagram from a fallen block deposit (LK), and *in situ* sediments (LKS), of the Carbonaceous member.

3.6.4 Fossils.

No fossils other than palynomorphs were found in this sequence.

3.6.5 Skua Member.

The Skua Member, because of its steepness, is accessible only from some places along its top edge and it was from here that samples were collected. Apart from this, use was made of telephotography (Fig. 50 and 51) to see the structures in the member.

This member is underlain by the Carbonaceous Member except at the northern end of the formation where it rests directly on the Cyclic Member. The basal unit of the Skua Member is a distinctive, highly oxidised, glassy, clay-rich, yellow-red sandy siltstone (Sk1/2), with conspicuous, probably water-formed, tunnels (Figs. 50 and 51). Bedding in this unit varies from massive horizontal, to laminar, to cross-bedding (Fig. 50). Above the yellow-red silty sandstone is a glassy brown siltstone (Sk3) followed by a glassy very pale yellow-white siltstone (Sk4) containing lenses of very fine silt. The member is capped by a layer of almost pure volcanic glass (Sk5) which is covered separately in Section 3.5.8.

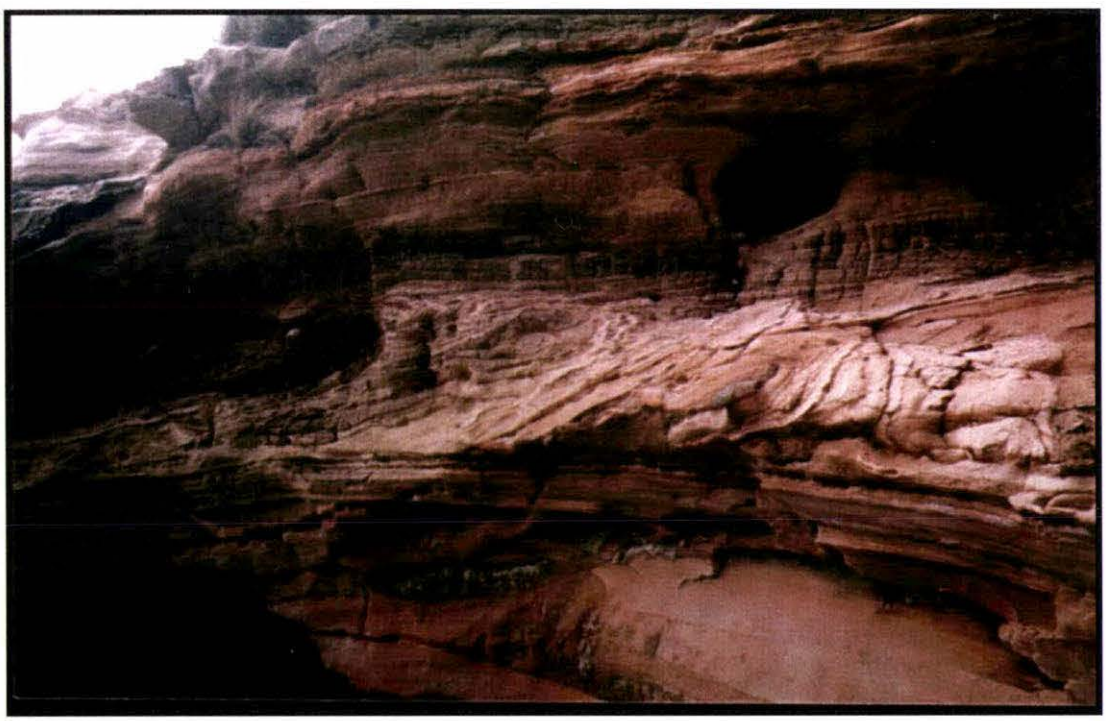

Figure 50. Detail of the Skua Member showing massive, laminated, cross-bedded, and tunnelled units within the yellow-red siltstone. At the extreme upper left of the photo is the white tuffaceous unit, Sk3. Telephoto x10.

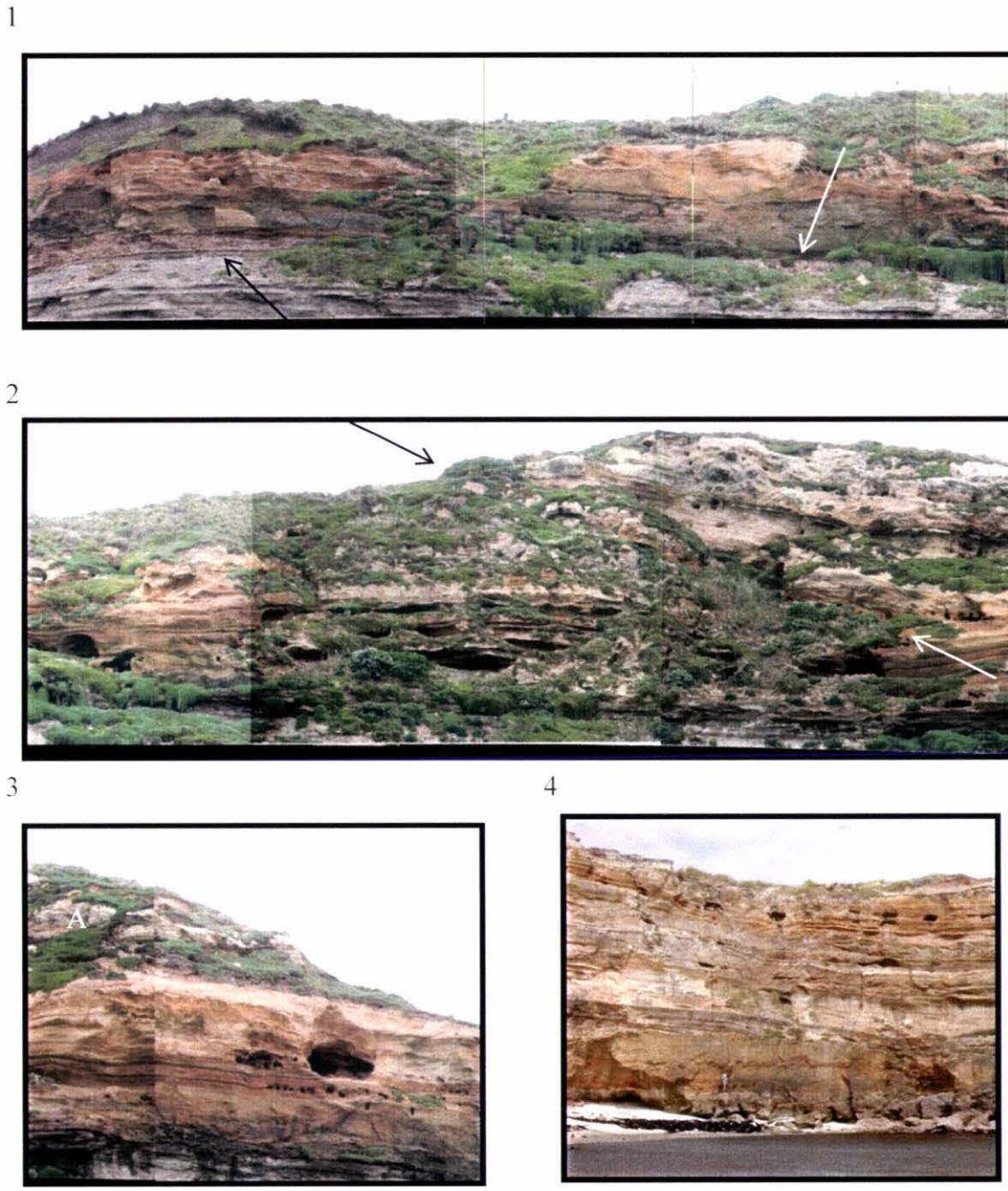

Figure 51. Panoramic view of the Skua Member.

On the left of image 1 the Carbonaceous Member (arrowed) between the Cyclic and Skua Members is clearly seen. On the right the arrow shows no intervening Carbonaceous Member. Water tunnelling in the red unit, here is incipient and poorly developed, presumably because the sediments are more compacted than further on the right. The Carbonaceous Member is clearly seen at the base of the red-yellow sandstone in images 2 and 3. In the field from binocular observations the

strata look to be dislocated and collapsed in the centre-right part of image 2. There could be an unconformity here (arrows) representing wind erosion and advancing dunes. Above the yellow-red siltstone (Sk1/2) in image 2 are the light brown and pale yellow-white glassy, sandy siltstone units, Sk3 and 4 (Fig. 21). (Photo; Mark Bellingham Telephoto x 10). Photo #4 was taken by K. Holt just north of Red Bluff, Chatham Island (grid ref 465615). Note the similar lithology to Photos 1 to 3.

3.6.6 Fossils.

No micro- or macrofossils apart from palynomorphs were found in this sequence.

3.6.7 Grain size analysis, Skua Member.

Grain size analysis of unit Sk3 and 4 of the Skua Member produced the following results:

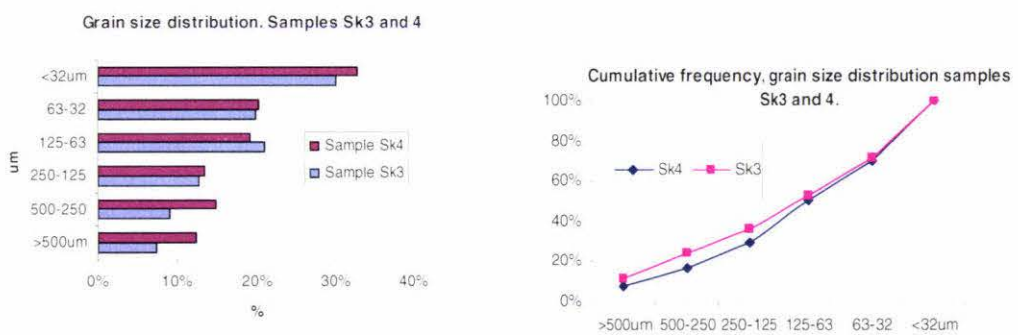

Figure 52. Grain size comparison of Skua Member units Sk3 (yellow brown silty sandstone) and Sk4 (pale yellow sandstone).

	Sk3	Sk4	
Graphic mean	2.1	2.3	
Inclusive graphic σ (φ)	2.1	2.3	Poorly sorted
Inclusive graphic skewness	0. 34	0.6	Positively skewed

Table 13. Graphical statistics for Fig. 52.

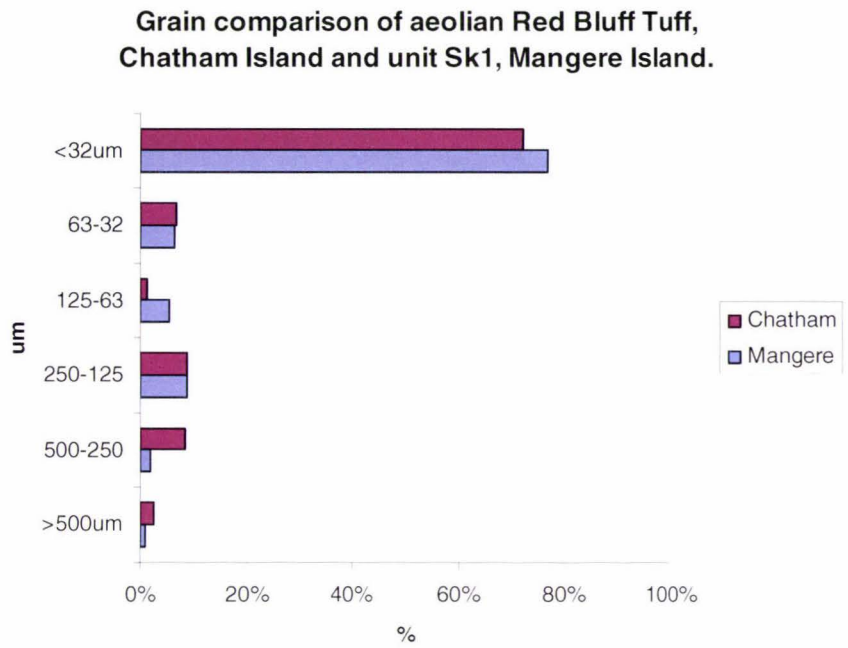

Figure 53. Graph comparing the grain distribution of the aeolian Red Bluff Tuff at grid ref.478534, Owenga Road, Chatham Island (sample from K. Holt. Pers. Comm.) and Sk 1, yellow-red siltstone, Mangere Formation, showing that these sediments have essentially the same grain size distribution.

3.6.8 Tephra; Parakeet Formation.

The Parakeet Formation is capped by an almost pure glass tephra (Sk5) (Fig. 21) with glass shards at the base up to *ca.* 0.5mm average diameter (Fig. 54). The chemical data for the tephra are given in Appendix 2. A ternary diagram (Fig. 55) compares this tephra with tephras from the central North Island volcanic zone, mainland New Zealand. The data for these tephras were taken from Shane *et al.* (1996), Froggatt, (1983), and Shane and Froggatt, (1994). The plot for the tephra data clearly falls into three distinct groups or populations. Unfortunately it is difficult to know whether this is real or an artefact as the glass is somewhat altered and was difficult to microprobe. The silica content of the tephra is 77%.

The evidence from the ternary diagram and the quartz content, shows that the glass is rhyolitic and is likely to have come from the central North Island volcanic zone of mainland New Zealand.

There was no sign of the sodium chloride reported in this unit by Campbell *et al.* (1993, p 149 and 150).

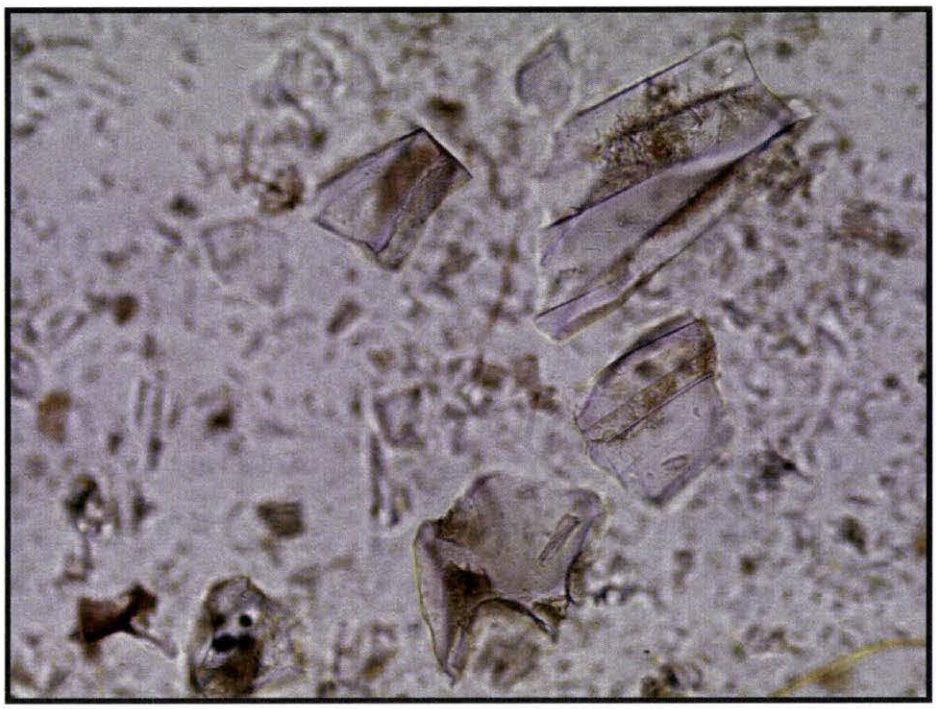

Figure 54. Microphotograph of glass shards from the coarser sandstone tuff at the base of unit Sk5. The shards range from <32μm to > 0.45mm.

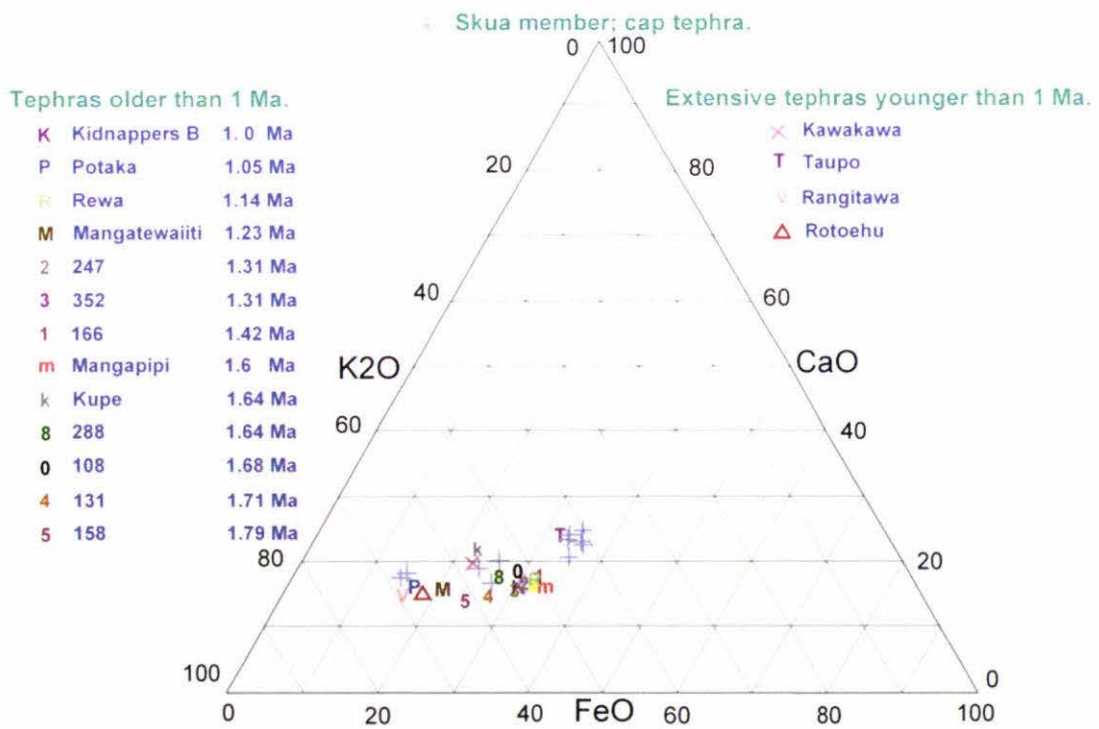

Figure 55. Ternary diagram showing Skua Member tephra (unit Sk5) for comparison with tephras of the Taupo Volcanic Zone, North Island, New Zealand. The glass compositions were averaged from Shane *et al.* (1996) and Froggatt (1983) to avoid overcrowding of data on the figure.

3.6.9 Palynology, Skua Member.

The sequence shown in (Fig. 56) starts immediately above the Carbonaceous Member with a sample from the base of the yellow-red sandstone and another from its top (samples Sk1 and 2). The upper sample comes from the middle of the light yellowish brown siltstone unit (Sk3) above the yellow-red unit (Sk1 and 2). Samples from above this were processed but no pollen was found in them.

The pollen diagram shows that the base of the Skua Member is essentially the same as the top of the Carbonaceous Member, with grass becoming the main vegetation at the top of the sequence. Among small trees and shrubs, asteraceae, *Coprosma*, and *Myrsine* are represented to the virtual exclusion of other species, but *Coprosma* and *Myrsine* disappear in sample Sk3 where herbs and ferns become dominant. Grasses become dominant by the end of this sequence. The aquatic restionaceae, appears at the base of this sequence. There is a relatively strong *Fuscospora* signal in mid-sequence and a strong charcoal signal at the base and middle of the sequence with a significant amount of charcoal greater than 50µm in length.

SKUA MEMBER

Mangere Formation Chatham Island Group

Relative Pollen Diagram

Analyst G. Davies

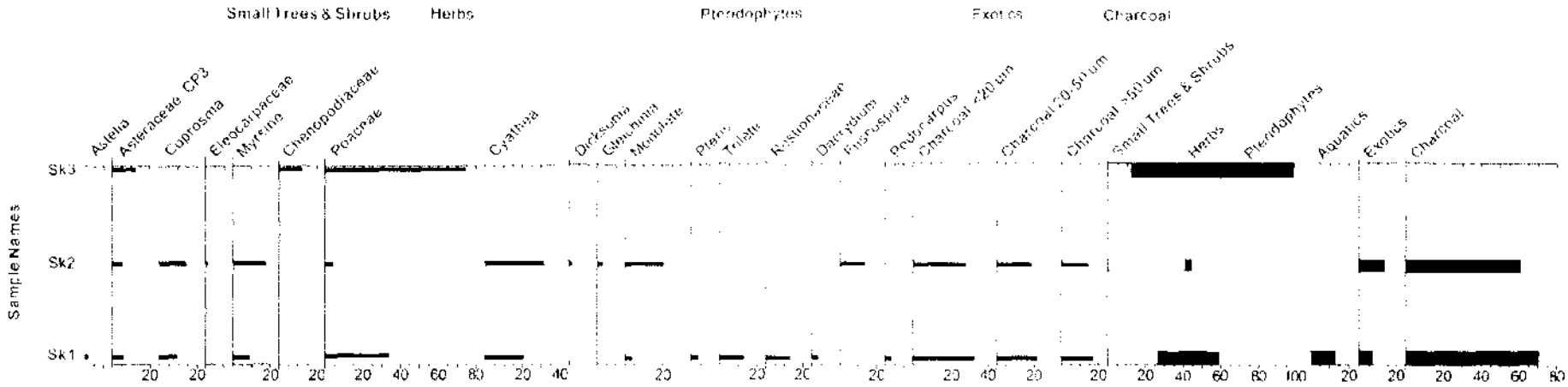

Figure 56. Relative pollen diagram of the Skua member

3.6.10 Microprobing of hornblendes: Rangiauria Breccia and Skua member.

In association with the Cyclic Member (Fig. 46) (reproduced below as Fig. 57), hornblende samples from the Skua Member (Sk1/Sk2) were microprobed (Fig. 57) to determine whether they came from the Rangiauria Breccia. A comparison shows that this was not the case. Figure 46 shows a close correspondence between the hornblendes of the Rangiauria Breccia and Cyclic Member whereas Figure 57 shows a distinct lack of correspondence.

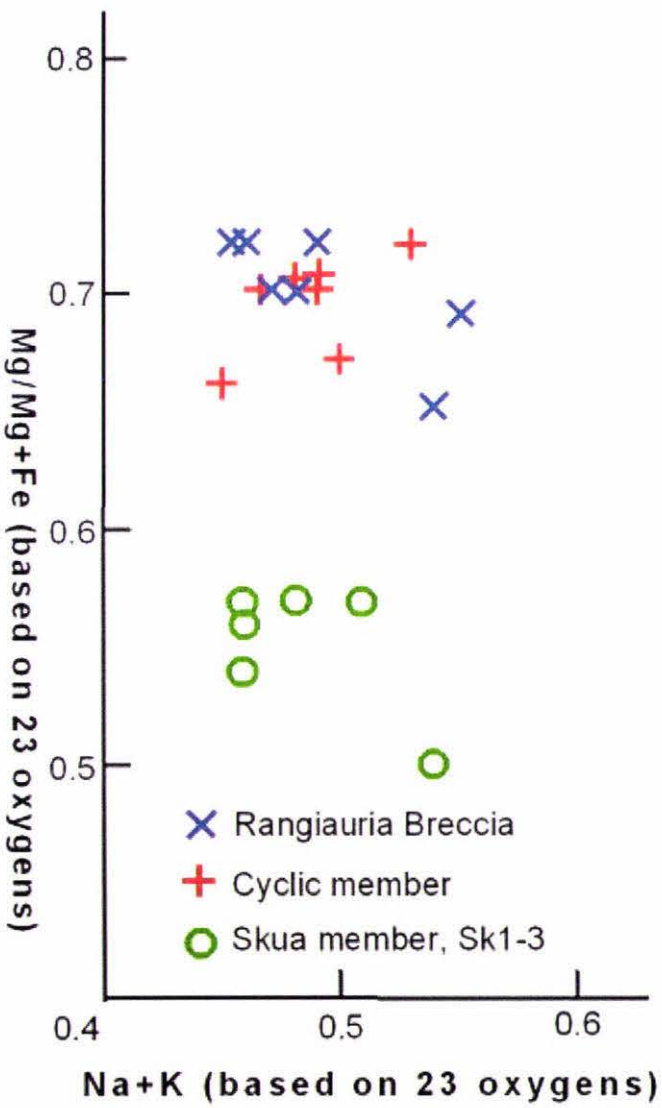

Figure 57. Graph of Fe and Mg against Na+K for hornblende samples from Sk 1/2, the Parakeet Formation. See Appendix 3 for the raw data.

3. 6.11 XRD analysis, Skua Member.

Unit Sk 5 is entirely silt/clay and is composed largely of volcanic glass (table 14). Volcanic glass is the dominant mineral followed by quartz and feldspar except for the clay fraction where kandite is abundant., Allophane is prominent in the clay fraction. Traces of gibbsite occur in all fractions (Table 14).

Skua Member

Sand fraction.	Hvy. Min	Vol.glass	Quartz	Feldspar	Kandite	Gibbsite	Zeolite
Sk1	3	53	10	6	26	2	0
Sk2	4	40	29	20	12	0	0
Sk3	0	61	21	18	0	0	0
Sk4	0	53	20	21	3	1	2
Sk5	0	>90	trace	trace	4	0	1
Silt Fraction.	Smectite						
Sk1	3	58	19	9	9	2	0
Sk2	9	39	15	19	12	3	3
Sk3	4	35	20	20	21	0	0
Sk4	0	44	22	24	8	0	2
Sk5	0	>90	trace	trace	0	0	0
Clay fraction.							Allophane
Sk1	5	42	13	3	23	2	12
Sk2	10	42	12	7	21	2	6
Sk3	8	44	4	18	19	4	3
Sk4	5	45	18	13	16	0	3
Sk5	0	>90	trace	trace	3	0	2

Table 14. Results of XRD analysis of samples from the Skua Member.

Heavy mineral fraction.	%hvy min.	Hornblende	Augite	Ilmenite	Limonite	Magnetite
Sk1	3.6	76	18	2	4	0
Sk2	9	79	11		6	4
Sk3	4.2	81	15	2		2
Sk4	6	74	20	3	1	2
Sk5	<3	trace	trace	0	0	0

Table 15. Results of XRD analysis of samples of the sands from the heavy mineral fraction, Skua Member.

Sample Sk1 is at the base of the member. As with the rest of the formation, hornblende dominates the heavy mineral fraction of the sands (Table 15), with

significant augite and lesser amounts of ilmenite and magnetite. Iron oxyhydroxides derived from the magnetite give the base unit of this member its strong yellow/red colour.

3.6.12 Microscopic and XRD comparison of a sample of aeolian Red Bluff Tuff from Owenga Rd., Chatham Island and sample Sk1, Skua Member, Parakeet Formation.

The mineralogical and lithological similarity of these units is shown in Figures. 58 to 60.The Owenga Road sample is of wind-blown Red Bluff Tuff (K. Holt, pers. Comm. 2005).

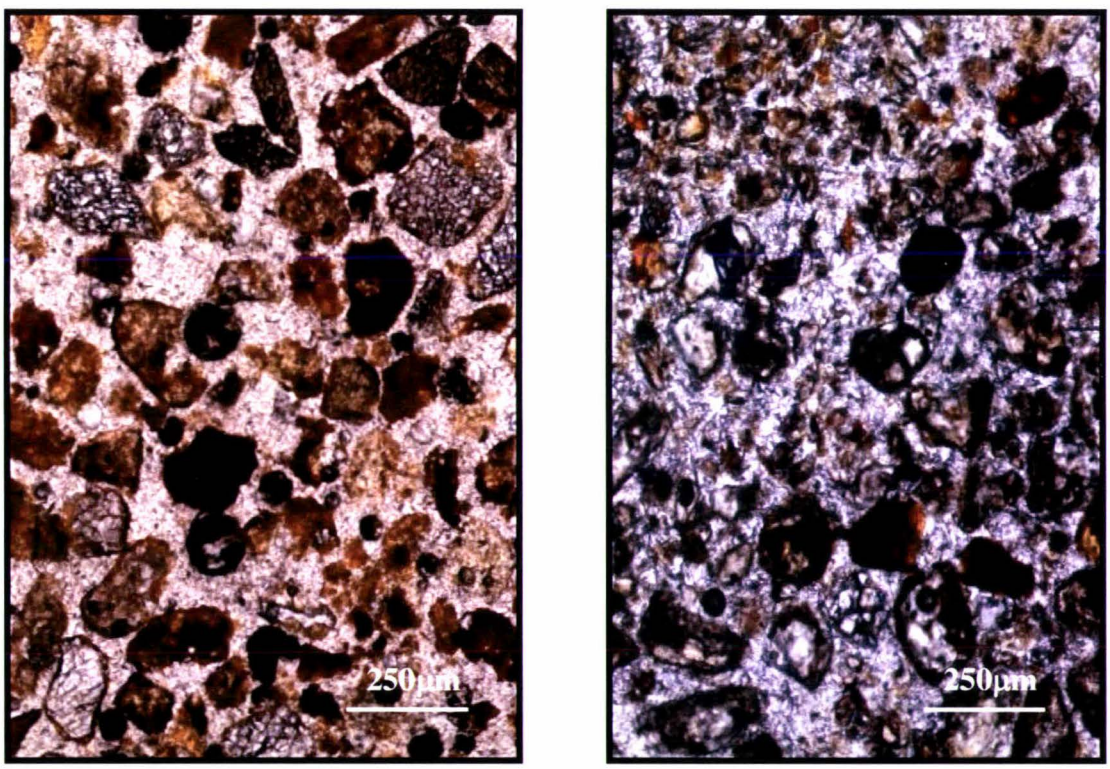

Figure 58. The photomicrograph on the left is of the yellow-red Skua Member, Sk1, Parakeet Formation. That on the right is from an outcrop of wind-blown material from Red Bluff Tuff at grid ref. 478534 on the Owenga Road. Note the rounding of the grains, their similar size, the coating of iron oxide on most of the clasts, as well as the similar altered glassy matrix. The different colours of the slides are a result of their having slightly different thicknesses.

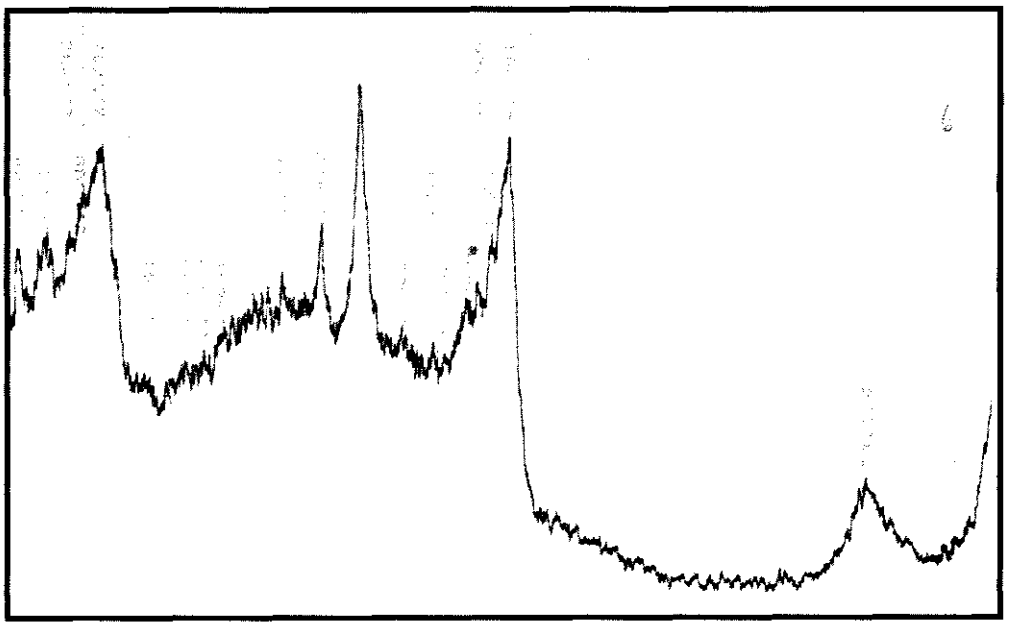

Figure 59. XRD trace, yellow-red siltstone (samples Sk1 & 2) Skua Member, Mangere Formation. The large area to the left under the graph is amorphous material, largely altered glass.

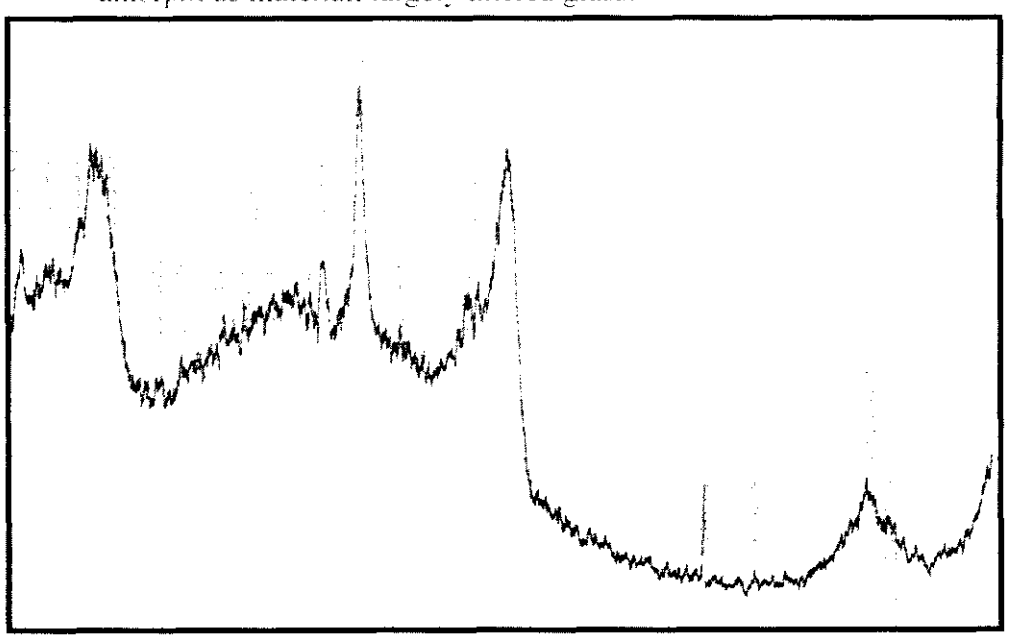

Figure 60. XRD trace of wind blown material from Red Bluff Tuff at grid ref. 478534, Owenga Road, Chatham Island (sample supplied by K.Holt).

Figures 58, 59, and 60 show that the wind-blown material at Owenga Road and the Skua Member yellow-red siltstone sediments (Sk1/2) have essentially the same mineralogy and give essentially the same XRD trace (except that Fig. 60 has additional spikes at 7.0772 and 8.3270 Å). A comparison of the first three photographs of Figure 51 with the fourth emphasises this similarity.

Chapter 4.

Discussion.

4.0.0 Tupuangi Formation.

A newly located sedimentary outcrop at the southwestern end (G.P.S., S °44 16.102′ W 176° 17 376′, grid ref. 667200) of Black Robin Bush, consisting of siltstone and silty sandstone has been recently exposed by shallow landsliding in the area. This outcrop is lithologically indistinguishable in the field from units of the Upper Cretaceous (Urutawan to Teratan) Tupuangi Formation on Pitt Island. Tupuangi Formation is the only quartzofeldspathic sedimentary formation in the Pitt/ Mangere Island area. Both the Tupuangi Formation on Pitt Island and at the new locality on Mangere Island have similar granulometry containing abundant epidote, zircon, and stressed quartz, as well as similar amounts of heavy minerals (Tables 1 and 2). All this is indicative of a common origin from Chatham Schist. Also these sediments contain only Cretaceous and earlier pollen (section 3.2.5) which suggests direct correlation to the Tupuangi Formation of Pitt Island (Campbell, *et al.*, 1993 p 43). Further both units have plentiful wood and carbonized plant fragments.

The sedimentary outcrop on Mangere Island at grid ref. 667200 is therefore interpreted as a remnant of the Tupuangi Formation which once stretched from Pitt Island. Campbell *et al.* (1993, p 43, Mildenhall and Wilson 1976 p. 122 and 126,) suggested that the local Tupuangi sediments were deposited in a delta under non-marine and estuarine conditions. Evidence for this is the paleoslope direction, channel directions, cross-bedding, conglomerate beds, flaser and linsen structures, burrowed horizons, coaly, carbonaceous and lignite horizons (Campbell, *et al* 1993 p 42). This delta may have extended beyond Mangere Island. It is also reasonable to suppose that the younger strata of Red Bluff Tuff, Kahuitara Tuff, Southern Volcanics and the Onoua and Matanganui Limestones of Pitt Island also extended out towards, or covered Mangere Island and that, in addition to the local Rangiauria Breccia, they may have contributed to the sediments of the Mangere Formation.

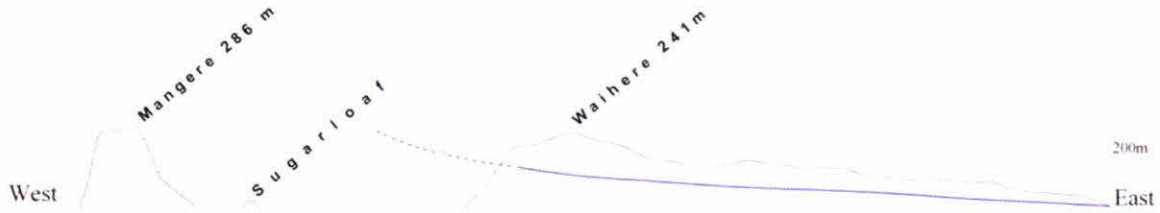

Figure 61. Cross-section of Pitt and Mangere Islands from the mouth of Second Water Creek in the east to Mangere Island in the west (Vertical exaggeration = 2). The blue line is the present bed of Second Water Creek and the dotted line its probable extension. This section shows the high sea cliff of western Pitt Island demonstrating that Tupuangi Formation, forming this western cliff, as well the overlying strata, extended well beyond the present coast of Pitt Island.

4.0.1 Relationship between Pitt and Mangere Islands.

Extensive Late Miocene (late Tongaporutuan to early Kapitean) volcanism (Campbell *et al.* 1993) appears to have resulted in thermal doming of the study area, as the opposing dips of Tupuangi Formation on Pitt and Mangere Islands show. Faulting, and to some extent volcanism, would have provided planes of weakness in the Tupuangi sediments and their overlying strata, thus accelerating coastal erosion of these poorly consolidated sediments by the frequent heavy seas arising from prevailing storms from the southwest to northwest. Extensive erosion is indicated by steep, high sea cliffs on the western and southern sides of Mangere, Pitt, South East, and Chatham Islands; not to mention the very extensive wave cut platform on the western side of Mangere Island (which is also, partly explained, by having been cut into the poorly consolidated sediments of the lower peninsula). That there has been sufficient erosion to eliminate all of the Tupuangi Formation in this area except the single exposure on Mangere and the locations on Pitt Island, is supported by Knox *et al's.* (1957) bathymetric map (Fig. 61) of the sea floor between Mangere and Pitt Islands. This shows deep, broad scouring of the sea floor, uncharacteristic of anywhere else around these islands. An alternative to the above is that there was always a sea channel partly or wholly open between Pitt and Mangere Island. This option is not favoured as the Mangere Formation is full of quartzofeldspathic sediment and reworked pollen derived from the Pitt Island area. If there was a sea

channel between Pitt and Mangere Islands the Mangere Formation would have been much richer in local Mangere Island sediments.

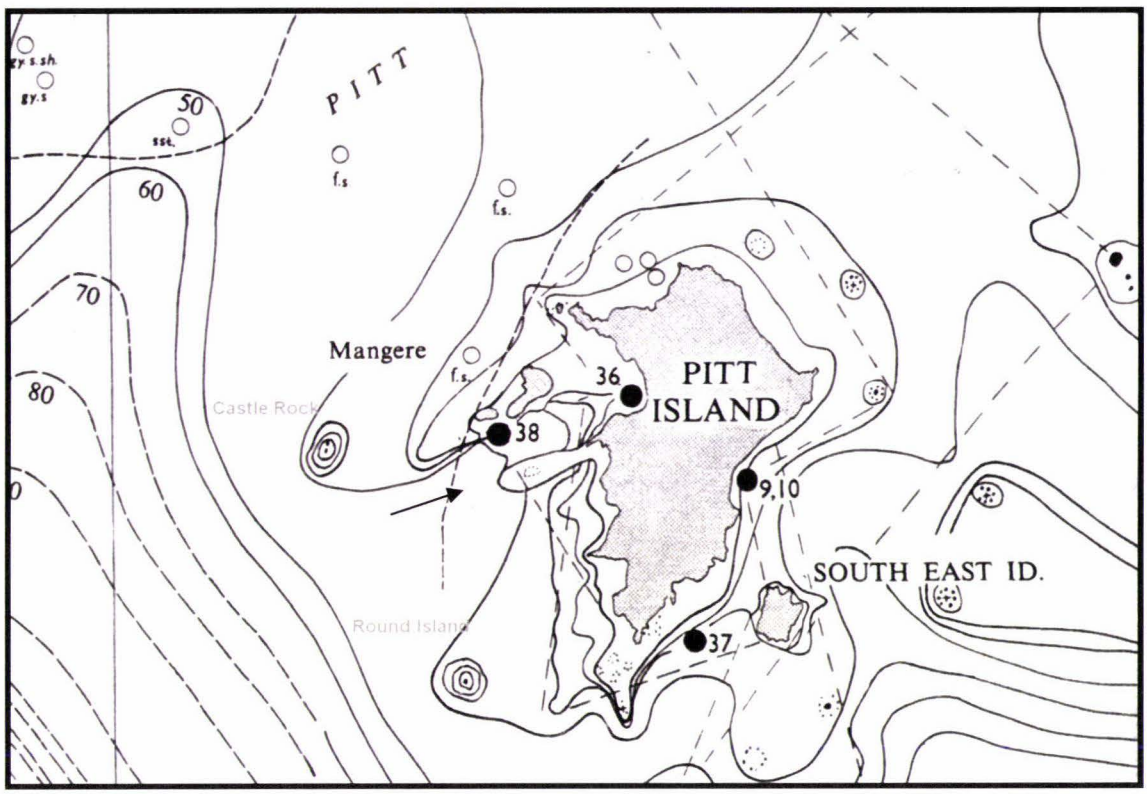

Figure 62. Bathymetric map of the sea floor around Pitt and Mangere Islands from Knox *et al.* (1957). Note the intense scouring of the sea floor between Pitt and Mangere Islands. This is a result of common southwesterly to northwesterly storms attacking the poorly consolidated Tupuangi sediments which had been weakened by faulting and volcanism. The joined 10, 20 and 30 metre contours along the southeast coast of Mangere Island indicate an undersea scarp at least 20 m high which may represent a scoured volcanic flank along the southern coast of the island or, more likely, in view of the fault pattern of northern Pitt Island(Fig. 65), a fault scarp in Pitt Strait between Mangere and Pitt Islands. A feature of this map is the 4 km long feature interpreted here as a debris avalanche of Rangiauria sediments from Waihere Head (arrowed) which post-dates the scouring and probably occurred as a result of the sediments being undercut by marine erosion. Another interpretation might be that it is a linear volcanic feature. Castle Rock and Round Island are incorrectly labelled by Knox, *et al.* They should be The Castle and Round Rock respectively.

Dr Clel. Wallace (pers com.) pointed out that both Pitt and South East Islands slope eastward to sea level with the drainage totally in that direction (Figure 63).

This suggests the possibility that these surfaces lead up to the rim of a volcano (a remnant of which presumably would be Sugar Loaf and the northern part of Mangere Island itself).

This map also shows an example of a probable volcanic debris-avalanche or linear volcanic deposit extending 4km southwest across the sea floor from Waihere Head. This may represent an example of lower peninsula facies, of the Rangiauria Breccia and the relative ease with which it is eroded.

Figure 63. Topographic map of Pitt Island showing that the drainage pattern rises exclusively near the western coastal cliffs and slopes to the east. Clearly the streams have been beheaded by coastal erosion.

This idea can be extended to take in The Castle and Sail Rock to the west of Mangere Island as well as Round Rock, implying the possibility of a caldera (or calderas). Note the broad flat reentrant between The Castle and Round Rock (Fig. 62) within which an extensive Mangere Formation could have been deposited, later to be eroded so that now only the remnant on Mangere Island remains. However the idea of a caldera is unlikely as there is no evidence of ring faults in the area. On the other hand this may be seen as an extensive volcanic field with multiple cones (some of which may now be eroded below sea level) with low lying areas between them

into which sediments were deposited. This raises the possibility that there may have been several "Mangere Formations" with only a remnant of one remaining.

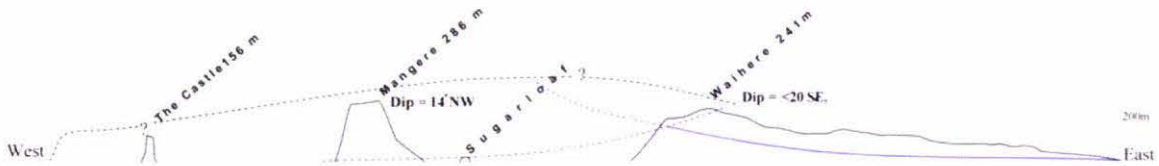

Figure 64. Model of Pitt/Mangere Island after Rangiauria volcanism. With the onset of volcanism the area was below sea level. At some time, presumably during Rangiauria volcanism in the Kapitean or early Opoition, the local area emerged as a result of sea level fall in the late Mangapanian (Haq,1987) and possibly also thermal doming as is evidenced by the opposing dips of Tupuangi Formation on Mangere and Pitt Islands. The doming was accompanied by crustal extension and faulting (Fig. 65). The dashed stream flowing towards the west is an inferred Mangere Stream introduced in Figure 67.

4.0.2 Local regional faulting.

Faulting is evident both on northern Pitt Island (Figure 65), which shows well developed horst and graben structures, and on Mangere Island where high angle clastic dikes are common in the south-western cliffs of the lower peninsula. On Mangere Island there is a normal fault (here named the Tupuangi Fault) which cuts Tupuangi Formation and is associated with the string of vents shown in Figure 66. Watters (1978) shows a fault converging on the western end of this fault and another fault between Mangere and Little Mangere Islands. As mentioned above there is also probably a fault in the strait parallel to the eastern side of Mangere Island. The trend of the Mangere Island faults (except for the fault between Mangere and Little Mangere Islands) is generally similar to those of northwest Pitt Island and is indicative of the regional tensional stress pattern (principal stress directed northwest-southeast, Fig. 41) resulting from thermal doming, that has given rise to the horst and graben structures of the area (Figure 65). A possible scenario, therefore, is that the lower peninsula is a graben structure which might partly account for its lower altitude than north Mangere and Little Mangere Islands. Within this graben there is the possibility of a nested graben in which the Mangere Formation accumulated.

Such a nested graben would be controlled by faults through The Neck and the saddle below which the Department of Conservation hut stands (Fig. 5).

That faulting over Mangere-northwest Pitt Island was contemporaneous with Rangiauria volcanism is clear from Maps 3 and 4 of Campbell *et al.* (1993) (Figure 65), which show faults truncating all units below the Whenuataru Tuff. However the evidence for such faulting on Mangere Island (except the linear vent/Tupuangi Fault) is not strong and more investigation of the lower peninsula as a possible graben structure is needed. It is possible that a graben here could be the result of magma chamber emptying, in which case its bounding faults (Fig. 66) would be independent of regional fault patterns.

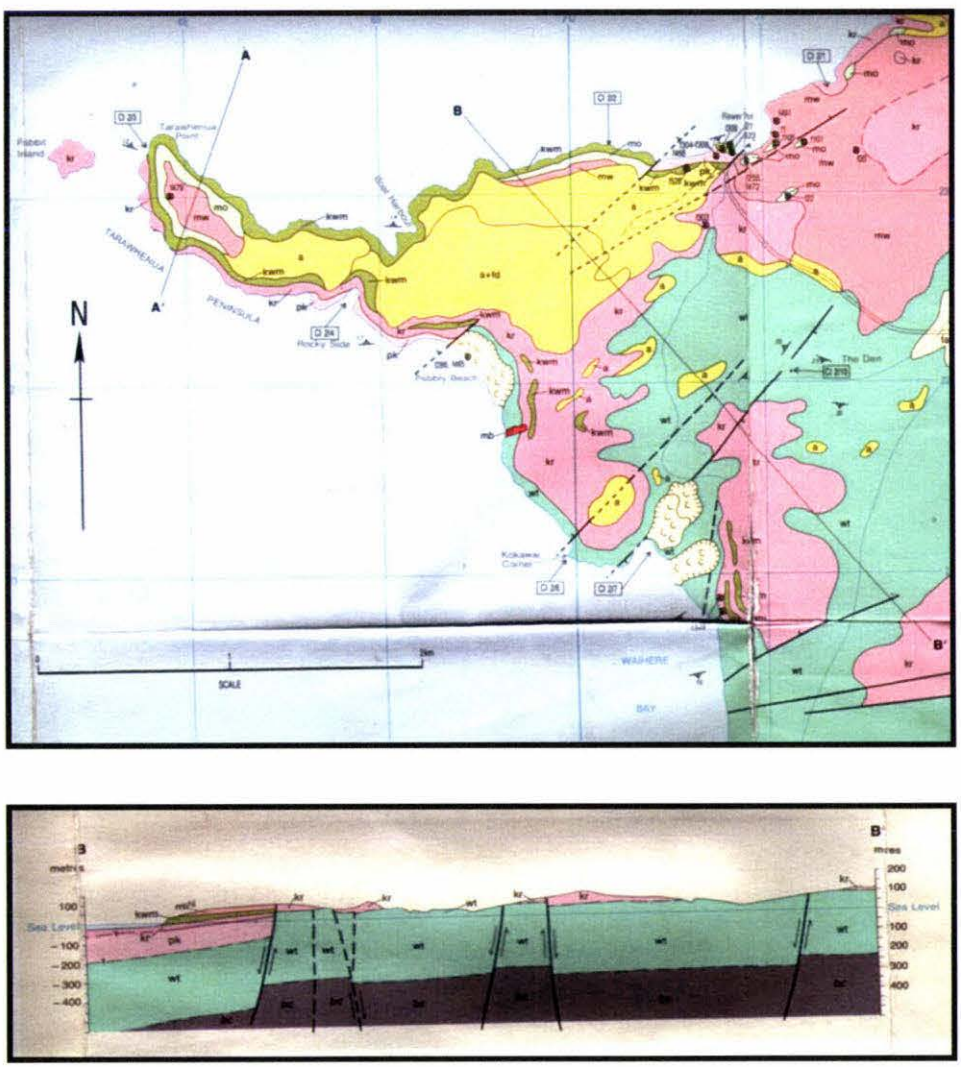

Figure 65. Map and cross-section of northwestern Pitt Island. (see cross sections, maps 3 and 4, Campbell *et al,*.1993).

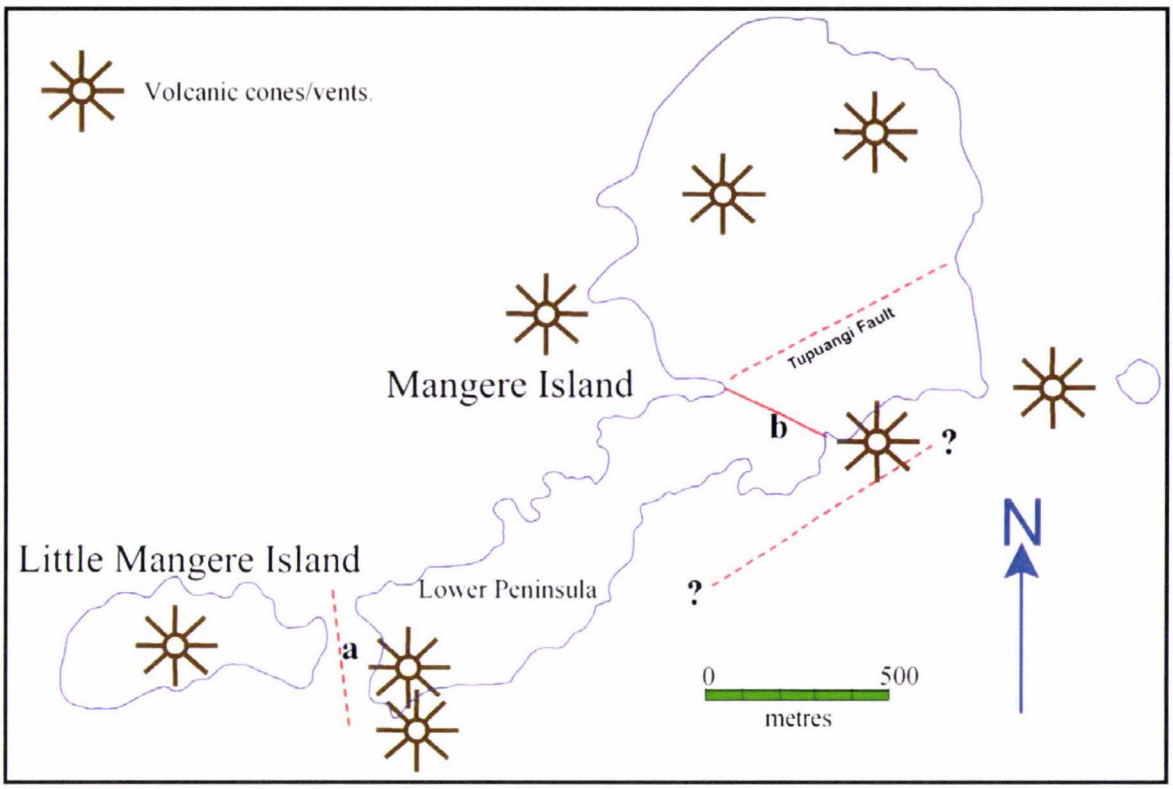

Fig. 66. Map of Mangere and Little Mangere Islands showing location of faults. Faults labelled "a" and "b", which may define the lower peninsula as a graben (see text above) are from Watters (1978).

In addition to the possibility of a graben or caldera complex which could be invoked to explain the origin of the Mangere Formation there is the likelihood that there was an arm of the sea, or an estuary, between the "twin peaks" of the northern Mangere massif and the peaks at the southern end of the lower peninsula. The Mangere Formation sediments appear to have been deposited into this marine basin or estuary whether or not it was structural.

With thermal doming, associated with Rangiauria volcanism, came at least partial emergence of the Mangere volcanoes. At the time the Mangere Formation was deposited (Mangapanian), global sea level is thought to have been about 50 m above present. However in the late Mangapanian, sea level began to fall (Haq, in Campbell *et al.* 1993 p. 178) which would have resulted in further emergence of the area and the acquisition of a vegetation cover. This is the situation when the Mangere Formation sediments began to accumulate as depicted in Figure 67.

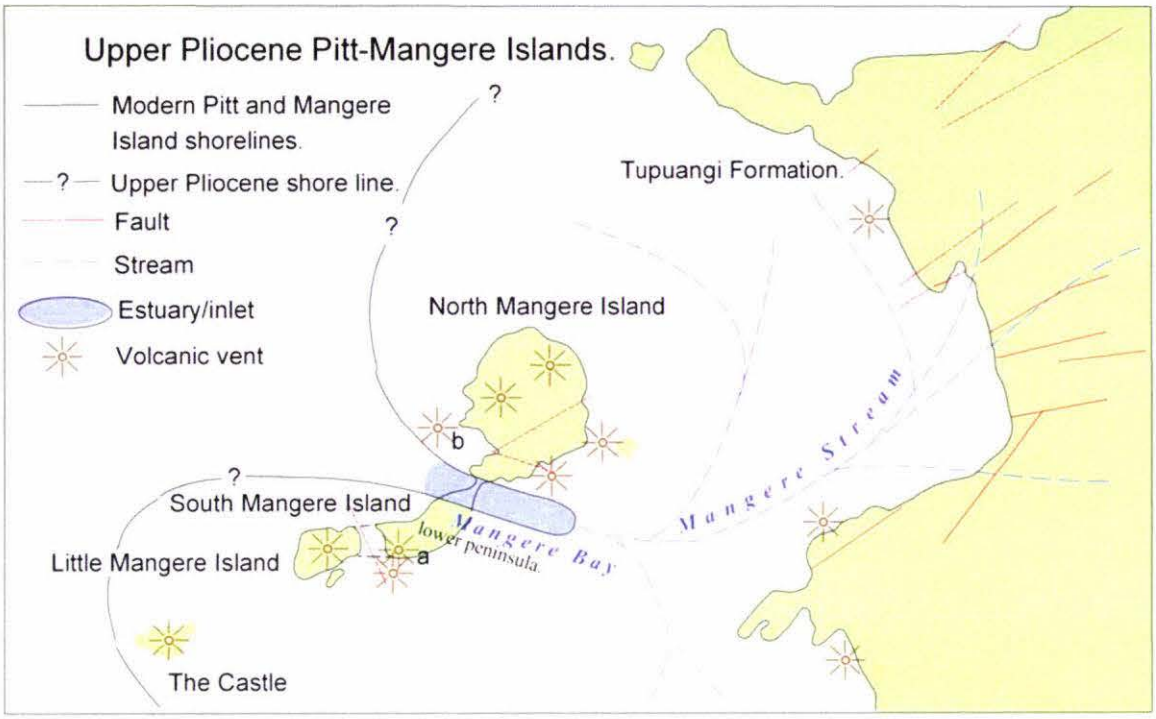

Figure 67. Model depicting the inferred situation after the end of Rangiauria volcanism. Mangere "Island" is a complex of volcanic centres ("Twin Peaks") clustered at each end of the present island. Pitt and Mangere Islands are joined by the Tupuangi Formation which extends an unknown distance to the west and south. There is another major volcanic centre outside the diagram to the south at Rangiauria Head, Pitt Island. (The letters "a" and "b" are referred to on p 111).

4.1.0 Bag End Breccia.

The Bag End Breccia (named from an informal site in Black Robin Bush) is here defined as the unit formerly defined as Whenuataru Tuff immediately underlying the Mangere Formation by Campbell *et al.*(1993). Its type section is at the old black robin aviary, grid ref. 657195

Campbell *et al.* (1993 p. 136) state that Whenuataru Tuff is found on Mangere Island under the colluvial skirt along the north-eastern cliff/shoreline (at Black Robin Bush), and also immediately beneath the Mangere Formation. Whenuataru Tuff is a "...brown-grey to red-brown, massive to well bedded volcaniclastic sand, silt and palagonite tuff (crystal, lithic) of limburgitic basalt composition." Two samples that they described, and identified as palagonite tuff consist of "...large numbers of fragments of dark brown, originally glassy, volcanic

rock up to 1mm across, and numerous shell fragments up to about 5mm accompanied by scattered foraminiferal tests. In the volcanic rock fragments the original glass was probably altered rapidly by contact with sea water; much of the original texture has been obscured by the alteration, although occasional fragments show well preserved vesicular texture. In addition to the rock fragments, relatively few crystal fragments of augite, brown hornblende and rarely feldspar are present in the tuff" (Watters, in Campbell 1993 p. 137). Further, the Whenuataru Tuff contains volcanic bombs and is partly matrix- and partly clast-supported.

It is considered that the "Whenuataru Tuff" on Mangere Island (renamed Bag End Breccia in this study) underlying the Mangere Formation is lithologicaly different from the Whenuataru Tuff of Pitt Island because the unit beneath the Mangere Formation is lithologically and genetically quite different from the descriptions given above, and from the type section on Pitt Island. It is a matrix-supported indurated breccia, containing megaclasts and not nearly as rich in shell fragments as Whenuataru Tuff on Pitt Island. Unlike the Whenuataru Tuff, it contains no volcanic bombs. It is also coarser than Whenuataru Tuff and contains numerous pebble sized, mainly vesicular basaltic clasts of characteristic blue-grey colour, unlike Whenuataru Tuff, and its matrix is very fine and light grey coloured (Figure 68). The very fine Bag End Breccia unit was deposited after Rangiauria volcanism and the deposition of Whenuataru Tuff had ceased as its deposition required low energy conditions. The similarity of its fossil shells to the Whenuataru Tuff fossil shells show that its deposition followed closely on the deposition of the Whenuataru Tuff.

The Bag End Breccia is, therefore, a discrete sedimentary deposit distinct from the Whenuataru Tuff and the Rangiauria Breccia, It is therefore named in this study as the Bag End Breccia from an informal site in Black Robin Bush).

Figure 68. Comparison of Whenuataru Tuff (left) and Bag End Breccia (Right). Whenuataru Tuff is clearly finer grained with generally smaller clasts and a stronger light yellow colour compared with the sample of Bag End Breccia. Whenuataru Tuff has a much greater amount of palagonite and broken fossil shells than the Bag End Breccia which has larger subangular to subrounded vesicular basalt clasts in a very fine grey matrix. The white clast in the Bag End Breccia is quartz. (3× full size).

Bag End Breccia, therefore, is not a tuff but a breccia interpreted to result from volcanic cone collapses and consequent volcanic debris avalanches. This situation is analogous to that described by Ballance *et al* (1991, 2004 p.578) for the Parnell Grits where collapse of the Auckland western volcanic cones resulted in subaerial debris avalanches entering the sea. Similarly Bag End Breccia originated as collapses of volcanic cones ("a" and "b" Fig. 66) from both the northeastern massif and Little Mangere Island. There appear to have been several collapses with some time between them, to allow for some consolidation of the previous flow deposit. The collapses entered the sea at a point near the mouth of an interpreted inlet or estuary, here named Mangere Bay. They flowed a further several hundred metres under the sea and were finally stopped by the massifs of northern Mangere Island or Little Mangere Island ("a" and "b" Fig. 67). Thus, unlike the Whenuataru Tuff, the relatively sparse fossil fragments in it were picked up adventitiously as the flows

crossed the sea floor. The avalanches flowed to the western side of the present Mangere Formation so that only a thin skirt of material which had spread out sideways from the main flow as a result of its coming into contact with the massive north and south Mangere volcanoes now underlies the Mangere Formation. Within this thin skirt of material is preserved a megaclast at the South Landing (Figure 19) and two megaclasts are preserved at the disused aviary near The Neck, North Landing (Figure 26). These megaclasts were deposited near the edge of the main flow. The megaclasts were able to be transported because of high internal pore water pressure, as a result of liquefaction, creating increased matrix strength. The high pore pressure, despite incorporation of some water into the front of the flow, would have been maintained under water for the short distance of flow. By the standard of Ballance and Gregory (1991 p. 198) these were relatively weak flows, with little erosive power, which flowed only a short distance and did not disturb a set of symmetric sea floor ripples underlying a thin cover of sediment over which it had passed (Figure 25). Because of the short flow distance, the main bulk of the flow which was seaward of the Mangere Formation (and now eroded away) soon came to a halt against the northern and southern massifs while the finer, wet matrix material and some large clasts continued to flow away from the sides as an underwater analogue of Palmer *et al's.* (1991) unconfined axial B facies (their axial C facies would not have had time to develop). The B facies of Palmer *et al.* (1991) is equivalent to the type C facies of Glicken (1991 pp.101-103). After it had entered the water and come to rest with the axial A facies further to the west, lateral momentum of the megaclasts ceased and they sank towards the base of the flow (Ballance and Gregory 1991 p. 198, Ballance *et al.* 2004 p.78). The Bag End Breccia, therefore, represents the uneroded undersea remnant of axial B facies (Palmer *et al.*, 1991) of volcanic debris avalanches that plunged into the ocean from the northern and southern massifs.

There is direct local evidence for this type of collapse (Figures 69 and 70) at grid ref. 669198 (Figure 69). At this site the debris avalanche would have flowed out towards the east, onto the Tupuangi Formation, perhaps providing a barrier to the north for Lake Mangere to form (Figure 71). Such flows, originating from the northern end of the island, and travelling over a greater length of sea floor, would

have incorporated a considerable amount of sea life and may have been incorporated in the contemporary Whenuataru Tuff (V.E Neall, pers. com).

Figure 69. View of a sea-cliffed volcanic remnant at grid reference 669198. Mangere Island Black Robin Bush is at the extreme right of the photograph. Note the bedded sequence of lavas to the left of the outcrop showing that there was once a volcanic cone nearby. A detail of this photo showing a volcanic debris avalanche appears below (Fig 70). (photo. V. E. Neall).

Figure 70. Detail of Figure 69 showing variously oriented megaclasts formed as a result of a volcanic debris avalanche. The megaclasts are similar to, and may be part of, Bag End Breccia.

4.2.0 Origin of Lake Mangere.

It is here postulated that the debris avalanches represented by Bag End Breccia blocked an arm of the sea between the "Twin Peaks" of northeast and southwest Mangere Island. The last avalanche, originating from the southwest, finally cut off Mangere Bay and gave rise to a fresh water lake. It was in the resulting freshwater lake that the Basal Member of the Mangere Formation was deposited.

Flame structures in this avalanche all point to the north-east (Figure 24). Flame structures are essentially load casts (Boggs 2001 pp. 89,106; Pettijohn and Potter 1964 Plate 53b; Collinson and Thompson p.146, figure 9.2) though Boggs (p. 106) suggests that, on occasion, some horizontal movement may occur to point the flame in the forward direction. In the case of Bag End Breccia the structures are all pointing in the same direction suggesting that the breccia moved from southwest to northeast. This is not definitive as flame structures are known to point also in the direction opposite to movement (op. cit.) but the right to left movement here is supported as shown in Figure 26 which shows the megaclast compressing the much finer material on the left but less so on the right. This shows that, as the main mass of the debris avalanche came to a halt, the greater momentum of the megaclast caused it to continue to move a little to the left, compressing the much finer material in front of it with less compression behind it. Further support for this direction of movement is afforded by the flow pinching out towards the southeast, and its thickening towards the north, as well as its riding up the strata at its northern end (Fig. 24). A paleogeographical reconstruction is shown in Figure 71.

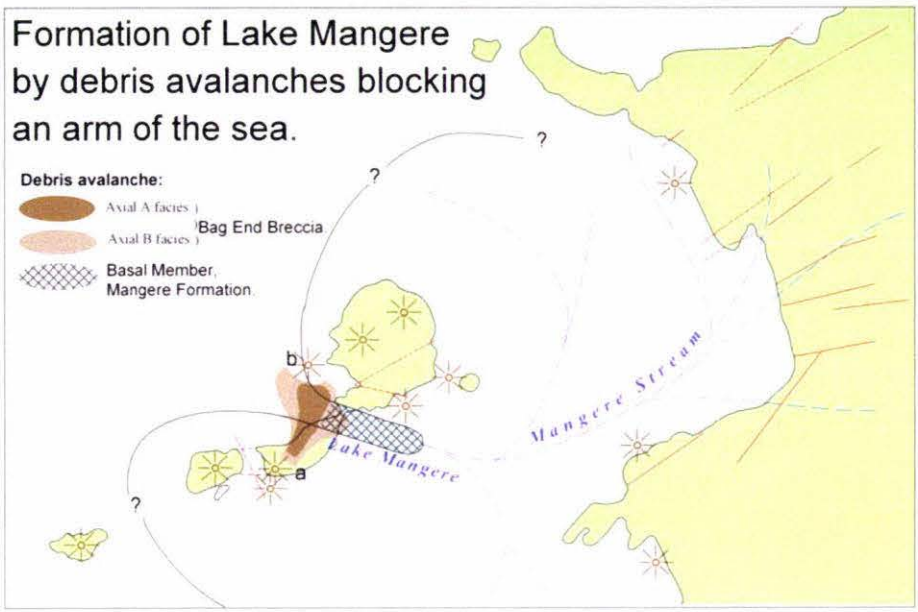

Figure 71. Model for the origin of Lake Mangere. Volcanism has died out. The flank of volcano "a" collapses and flows across Mangere inlet coming to rest against volcano "b", cutting off the inlet and forming the Bag End Breccia. Quiescent, low energy conditions ensue. Lake Mangere is formed and fills with sediment from the surrounding volcanoes and from erosion of the Tupuangi Formation and younger sediments derived from Mangere Stream.

4.3.0 Mangere Formation.

Mangere Formation was laid down as a series of horizontal strata in a cut-off arm of the sea between two volcanic centres. It consists of the post eruptive Basal and Cyclic Members (Fig. 17). The type section is in two parts because of the difficulty of access to the Cyclic Member. The Basal half of the type section, near the disused aviary, is shown by an "x" in Figure 17, Grid ref. 658195. The Cyclic half, just above The Neck, is marked by a "y" in Figure. 17 and has a grid ref. of 659195.

4.3.1 Basal Member.

The Basal Member, deposited post-eruptively, is 30 m thick and consists of massive very fine sand to pure siltstone (Figures 27, 28, and 29) with a high glass/palagonite content and some alteration to allophane. This sediment is derived mainly from the local Robin Bush siltstone and Landing Point sandstone in a low energy situation. As the XRD results show (Tables 4 and 5), the quartzofeldspathic

fraction is low compared with the glass/ clay fraction. Sufficient time had elapsed since the cessation of volcanism for the slopes around the lake to become clothed with vegetation which, together with a presumably equable climate, resulted in low erosion rates and the deposition of fine sediment. Some fine-grained quartzofeldspathic sediments with Cretaceous and earlier pollen also entered the lake from the Tupuangi Formation, together with minerals from the Chatham Schist. The basal 3 to 4 m is mixed with small clasts and sand from the Bag End Breccia. This gives way in the central *ca.* 22 m to a very fine mudstone almost all of which is less than <32 μm grain size. This in turn gives way to the slightly coarser material at the top of the unit reflecting the onset of the sea breaching the "dam" formed of Bag End Breccia. (section 4.3.1). Diagenetic changes have concentrated most of the calcium in this member in the concretions (Fig. 28). Much of the finer material is volcanic glass altered to palagonite or clay as Table 4 shows. In spite of the presence of wood, there is very little carbon in this member (Table 3) which suggests that the lake was oligotrophic. This is supported by the lack of macro- or microfossils other than wood and pollen. Most of the fossil wood appears to be concentrated on the northwest side of the member towards the lake outlet where currents would tend to carry it. Clasts visible under the microscope are all angular (Fig.29) and are compositionally and texturally immature showing that they have been transported only a short distance.

4.3.2 Palynology.

The pollen found in this unit (Section 3.3.7) is mainly recycled Cretaceous material from the Tupuangi Formation. Pollen of Pliocene age is sparse and often difficult or impossible to identify because it is typically more damaged than the Cretaceous palynomorphs. There is no obvious explanation for this as the Cretaceous pollen would almost certainly have been transported a greater distance and therefore subject to greater abrasion. A possible explanation might be that whereas the conditions in the Tupuangi Formation were conducive to pollen preservation, the Pliocene pollen was first deposited in the volcanic Robin Bush siltstone where conditions may have been alkaline and was then transported from there to the lake (as pointed out above, much of the sediment for the Basal Member came from the Robin Bush siltstone). In any case, this situation seems anomalous and needs further investigation. Pliocene pollen that was identified, shows that there

was at this time a coastal association of shrubs, herbs, grasses and ferns. This is characteristic of the whole sequence. From this it also seems clear, based on the pollen suite (Section 3.3.7), that the transition from the Basal Member to the Cyclic Member did not involve a significant climate change. This supports a marine breaching of the Bag End Breccia "dam" as the explanation for the changing environment into the Cyclic Member.

4.3.3 Cyclic Member.

4.3.4 Introduction.

As discussed in Chapter 2, the presence of marine ostracods, bivalves, bryozoa, sulphur, and gypsum in the Cyclic Member point to the probability that the Bag End Breccia barrier was breached by the sea. This could have been partly by marine erosion of the Bag End Breccia but also possibly as a result of a rising sea level in the Waipipian/Mangapanian as the Haq *et al.* (1987) sea level curve suggests (Campbell *et al.* 1993 p.178). This allowed the influx of salt water and wave activity which destabilised the vegetated slopes bordering the lake (Fig.72).

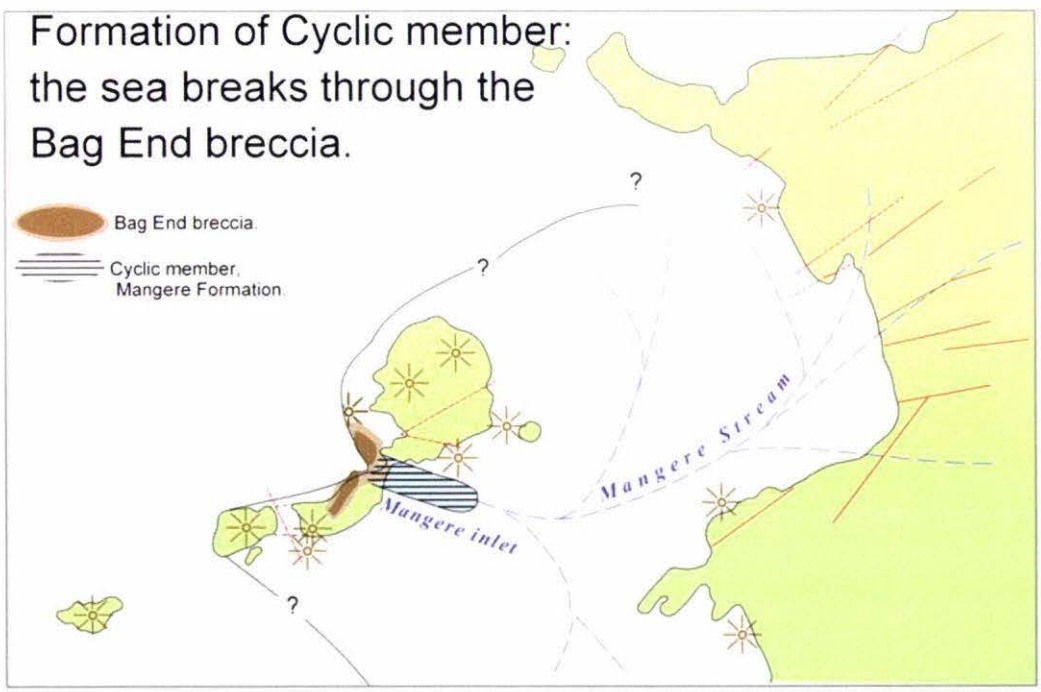

Figure 72. Paleogeographic reconstruction of the situation when the sea breached the barrier of the Bag End Breccia resulting in the deposition of the Cyclic Member.

As a result of this, coarser sediments were available to form the sandstone units of the Cyclic Member. The beginning of destabilisation is evident in the coarsening upper few metres of the Basal Member. Destabilisation is supported by the large number of sizeable wood pieces in the lowest units of the member derived from the slopes surrounding the lake (Fig. 39). Sulphur and gypsum, also associated with the wood, strengthen the case for marine influence.

It is considered that the alternation of mudstone and sandstone units (especially for the thicker sandstone units) in the Cyclic Member may be a result of the coincidence of periodic violent storms and high tides releasing large quantities of sand and silt from the surrounding slopes into the lake, all texturally and compositionally immature. This sand was derived locally from the Landing Point sandstone, Robin Bush siltstone and, slightly further afield, by way of the Mangere Stream, from the surrounding Tupuangi Formation with its overlying strata. The presence of large volcanic and quartzofeldspathic fractions plus mica and rare zircons and epidotes in these sediments confirms this derivation (Table 10).

Many of the parallel-bedded sandstone units that comprise the formation, though mostly normally graded, show little difference in grain size from base to top as well as little or no erosive evidence on the underlying units when they were emplaced. This is explained as a mainly continuous storm-driven loose slurry of sand from the surrounding slopes which largely settled on the lake bed without marked grain size separation or erosion of the lake bed (Figs. 42 to 45). These figures also show that there was no significant lateral change in grain size along several of the sandstone units (Figs. 43 and 45). Several of the thicker sandstone units, however, have rip-up clasts in their bases which indicates that they were density flows. All of the sandstone units are positively skewed , mainly because of the high influx of Robin Bush siltstone (Tables 6 to 9). Units 26c and 28c show negatively skewed bases but this is a result of (poorly developed) normal grading; the bases and tops were sampled in these units to detect changes in grain size along the length of the outcrop (2.1.2).

At the northeastern end of the Mangere Formation, disturbed bedding (Figs. 32- 33) is common in the lower units of the Cyclic Member as a result of turbidity currents, slips, slumps, and slides from the adjacent slopes into wet sediments. The

parallel bedded units here terminate against more chaotically bedded units (Fig. 33). A model to explain this is given in Figure 73.

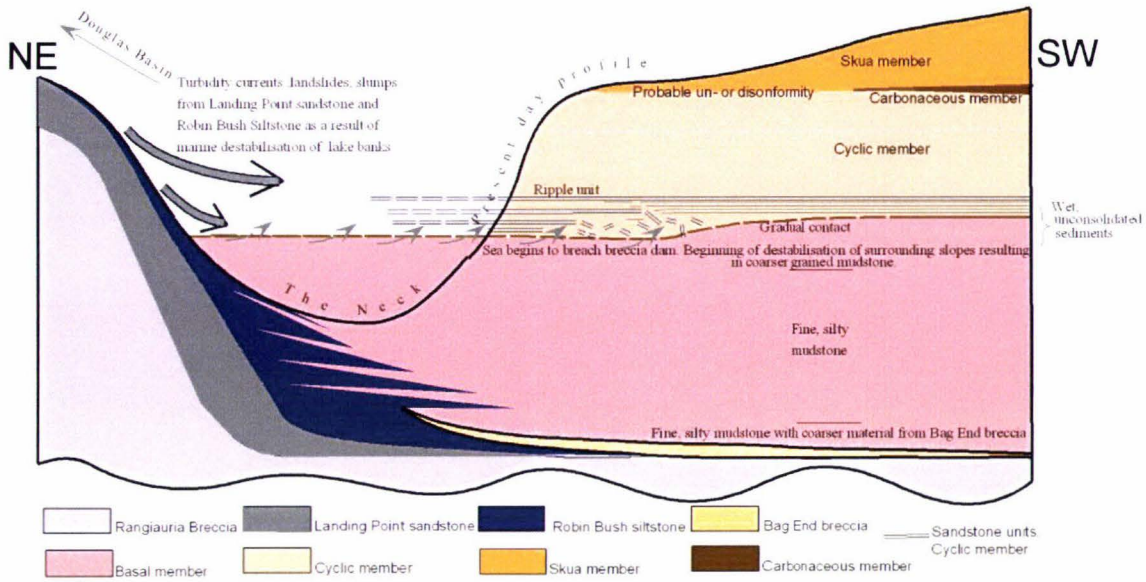

Figure 73. Model (not to scale) to explain the disturbed bedding at the northwestern end of the Cyclic Member, Mangere Formation. Marine breaching of the debris avalanche dam and consequent marine incursion during periodic storms resulted in turbidity currents, slumps, and slides of Landing Point sandstone flowing onto the wet, partly consolidated mudstones derived from Robin Bush siltstone and the Tupuangi and younger strata, which had been deposited in quiescent periods. As a result blocks of sandstone either broke off and sank or disintegrated into smaller blocks (Figs. 32 and 33). At the northeastern end of the formation the contact between the Basal and Cyclic members is gradual as a result of mixing. Near the southwest end of the Formation, the lowest sandstone unit has been distorted to a convolute bed, presumably by the momentum of an incoming density/turbidity current from the southwest (Fig. 34). Dense *Hebe* covering at the southwestern end made it impossible to determine whether extensive disturbed bedding occurred here also. However on the South Landing side, the ripple unit has been dislocated and overridden rather than foundering (Fig. 35).

Many of the sandstone units have ripple casts of very short wavelength (*ca.* 0.5 mm) on their bases. These ripples are all oriented in the same direction by wind from the southwest quadrant (Figs. 37 and 38). The ripples are close to symmetrical probably because, in an enclosed lake, a fairly steady wind would set up a standing wave pattern on the lake which would be reflected at its bed. It seems likely therefore

that the lake was fairly shallow (ripple size would increase with depth) at this time, especially as it had already been filled to *ca.* 32 m (see pp 75 and 76). This suggests that the rising sea level (or subsidence) that resulted in the breaching of the Bag End Breccia dam continued during the deposition of the Cyclic Member resulting in a shallow lake in which the ripples found on several beds of the sequence could form.

This unit then records a series of quiescent periods during which sediments similar to those of the Basal Member were deposited, interspersed with higher energy periods when storms deposited thicknesses of sandstone ranging from millimetres to around 80 centimetres. The main source of the sandstones is from the Mangere volcanoes themselves with input from the Tupuangi and later formations. The mudstones, like the Basal Member sediments (but slightly coarser), originate both from the Tupuangi and later formations and also locally from the Robin Bush siltstone. Input from Pitt Island provides the quartzofeldspathic fraction of these sediments. The thickness of the sandstone units decreases upwards as the slopes around the lake again stabilise and become vegetated. This suggests that the Cyclic Member was deposited in a relatively short time. By the end of Cyclic Member time Lake Mangere was filled with sediment to a depth of around 45 m and would have been relatively shallow.

A feature of the sandstone units of the Mangere Formation is a distinct jointing pattern at ca.90° (see 3.4.8). This gives a principal stress pattern of northwest-southeast as a result of doming. This doming postdates the Cyclic Member and may correlate with tectonic uplifts in the Castlecliffian (Fig.79).

4.3.5 Post-Cretaceous pollen.

The Cyclic Member does not appear to be a very good environment for preserving pollen and is similar in this respect to the Basal Member (see section 4.2.1). It seems probable, also, that fast sedimentation may have resulted in the preservation of fewer species because a wider range of species was expected. A characteristic of the pollen diagram (Fig. 47) is the unlikely sudden transitions in species, but this is probably an artefact of the sampling interval which varied considerably depending on the thickness of the sandstone units separating the sampled mudstone units.

The small trees and shrubs as well as the herbs put the area in a coastal setting. In unit 27c the suggestion is that the climate was drier and cooler (lack of ferns, dominance of herbs). The charcoal present here is mainly < 20 μm in size with none > 50 μm. The presence of the 20-50 μm fraction suggests fire in the local region rather than wind blown material from New Zealand probably from fires on Chatham Island. This gave way to a wetter regime at 25c. The climate appears to have become drier and cooler again between 21c and 10c as is shown by the reduction in ferns as well as increasing amounts of charcoal. Fires at 21 and 15c, producing charcoal fragments > 50 μm appear to have been in the immediate vicinity. Conditions become somewhat wetter and warmer again at 9c. Sample 10c appears anomalous as the presence of no species other than *Myrsine* and Poaceae pollen is very unlikely. The influx of *Fuscospora* pollen at this time is indicative of windy, dry conditions

4.4.0 The Parakeet Formation.

In view of the fact that the units above the Cyclic Member were deposited under quite different conditions from the Mangere Formation *i.e.* mainly by aeolian action after a probable hiatus involving terrestrial erosion and a short-lived shallow lake, these units have been separated into the newly named Parakeet Formation. The type locality for this formation is along the southern cliff edge of the Mangere Formation as it was originally defined by Campbell *et al.* (1993). This is shown by the letter **z** in Figure 17, grid refs. 656193 to 658194 and comprises the Carbonaceous and Skua Members, plus the tephra capping of the sequence.

4.4.1 The Carbonaceous Member.

At this stage there had been either a lowering of sea level or a gentle uplift of Mangere (and Pitt?) Island or both as the next unit of sediments, the Carbonaceous Member, is associated with a fresh water lake having an abundance of *Botryococcus* (Figure 74). The abundance of organic carbon (Table 12) is indicative of its prolific production by *Botryococcus* colonies (Jian Qin, 2005).

Campbell *et al.* (1993 p 176 to 178) give evidence from the superposition of Titirangi Sand on Motorata Limestone just north of Ko Oreaeo Point, Chatham

Island for a sea level drop of around 80 m at about this time (though, according to Campbell, some of the apparent drop could be a result of regional uplift contingent on plate compression as a result of the Kaikoura Orogeny). The uplift at Mangere Island at this time may well correlate with this event because the Titirangi Sand is early Nukumaruan/Late Pliocene age which would put the termination of the Cyclic Member as late Pliocene. This also fits with the sea level curve of Haq *et al.* (1987) (quoted in Campbell *et al.* 1993 p 178). After this, sea level again rose, (Haq *et al.* 1987) with possible marine erosion of the Cyclic Member. There is possible support for marine erosion and an unconformity here in that the contiguous lower peninsula is relatively flat topped (Figure 2) and not very different in height from the Mangere Formation; the difference in height could easily be accounted for by the greater erodability of the Cyclic Member. Further, photographs show a slight change in slope in the marine cut cliffs of the Island at about the same height as the lower peninsula. Support for this might also come from an investigation of the thin sedimentary sequence at the extreme southwestern end of the lower peninsula (see Figure 5). Thus the Cyclic Member, now well above sea level, may have been subject to some erosion before the advent of a fresh-water lake with a consequent unconformity. It was not possible to examine the contact between the Cyclic Member and overlying lake sediments closely enough to ascertain this, though binocular study gave the impression that the lake sediments were unconformable with the Cyclic Member sediments and that there had been some erosion of the Cyclic Member. Whether there was a hiatus here or not, a lake formed on the Cyclic Member surface and pollen samples suggest a generally swampy area with a shallow lake. This lake was geologically ephemeral as less than 600 mm of lake sediment was deposited.

The lack of suitable time constraint and the possibility of an unconformity means that some or all of the Parakeet Formation could have been deposited at any time from Upper Pliocene to late Pleistocene. Mildenhall puts an upper limit of Mangapanian on the Mangere Formation (Campbell *et al.*1993, p 150) on the evidence of *Rhoipites alveolus* (Mildenhall 1994). However, it is not clear from the Geological Survey Fossil Records exactly where in the sequence *R. alveolus* was found. It was not above the Cyclic Member as all the N Z Geological Survey fossil record forms appear to have come from below the Carbonaceous Member. In any case, if *R. alveolus* was to be found in the Parakeet Formation it would most likely be

found in the lake bed which had not been previously sampled. But the presence of just one or two pollen grains may not prove significant as pollen recycling is ubiquitous in the formation. If only one or two *R. alveolus* grains were found in the lake bed they could possibly have washed in from older, higher standing, surrounding sediments or been blown in with the onset of wind blown Red Bluff Tuff (see 4.5.0).

Clearly there is a major interpretation change here from the previous studies. As will be shown in the following discussion the Parakeet Formation units were deposited quite differently and, originally, over a larger area than the Mangere Formation. In view of this the Carbonaceous and Skua members plus the capping tephra are collectively referred to the Parakeet Formation.

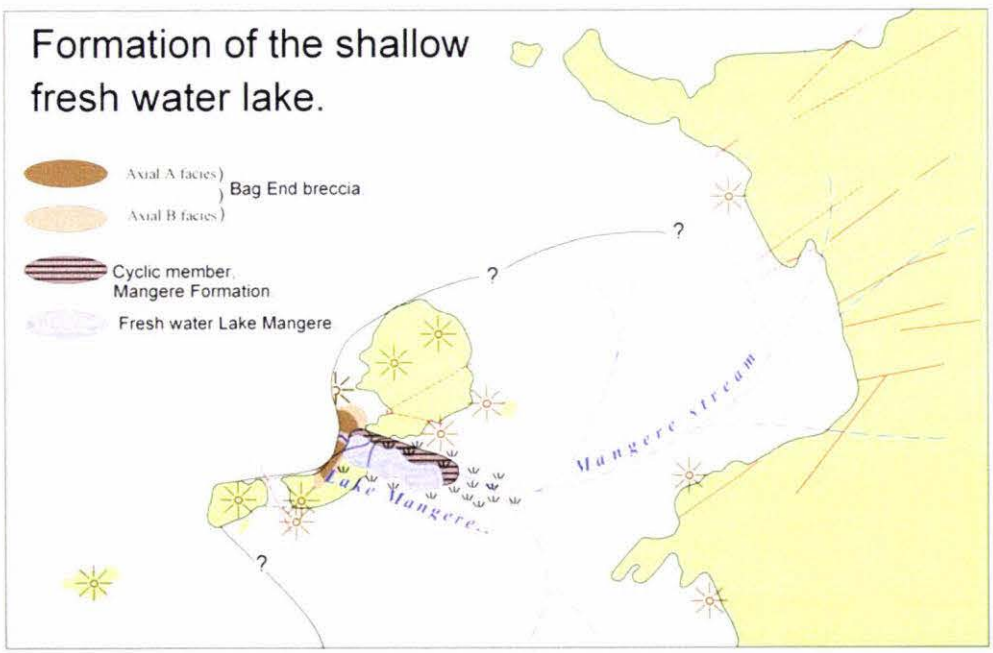

Figure 74. Model for the the formation of a fresh-water lake on the Cyclic member sediments, surrounded by marshy land, as is evidenced by the pollen diagram.

4.4.2. Palynology.

The pollen diagram for the Carbonaceous member (Figure 47) is in two parts. Samples Lks 1 and 2 are *in situ* and are taken from the cliff edge at the southwestern end of the member. Samples Lk1 to 6 are from a fallen block from close to the deepest part of the lake. As far as can be ascertained, pollen samples Lks1 and 2

correlate with samples Lk4 and 5. Overall the pollen diagram shows that the climate was moist and warm at this time as is evidenced by the dominance of pteridophytes. Since grass is everywhere significant it appears that the area was somewhat open with plentiful small trees and shrubs but, as is characteristic of the whole sequence, no larger trees. This is not surprising as there appears to have been few large trees except the recently arrived *Dracopyllum arboreum* on the Chatham Islands at any time since at least the upper Pliocene. The total lack of *D. arboreum* in any of the pollen samples is a puzzle since it is now ubiquitous on Pitt Island less than 4 km away today. This probably means that it was a late arrival on the Chatham Islands. Probably seeds were transported to the Chatham Islands from the sub- Antarctic islands and/or mainland New Zealand by ocean-going birds sometime in the Pleistocene. (There are some sediments that are probably Pleistocene at the extreme southwestern end of the lower peninsula which could be sampled for pollen to possibly clarify this question). As pointed out above, the Carbonaceous and Skua Members could be Pleistocene. Sample Lk6, dominated by grass is unexplained though revegetation after erosion is a possible explanation. Aquatic pollens suggest that the lake edges were swampy. The climate appears to have been windy as is evidenced by the exotics *i.e.* wind-blown pollen from mainland New Zealand. The shrubs and small trees present are characteristic of a coastal area. The lack of charcoal larger than 20 μm is indicative of wind blown charcoal from Australia or mainland New Zealand or peat fires from Chatham Island.

4.4.3 The Skua Member, Provenance and paleoenvironment.

Up to this time coastal erosion of the largely weakly consolidated Tupuangi Formation sediments had been proceeding apace and the original coastline was rapidly retreating; the retreat being delayed only by the volcanic massif of the Mangere volcanoes. It is postulated that, at this stage, a deposit of Red Bluff Tuff was being actively eroded or uncovered by the sea (Fig. 75) and was supplying material to be transported by the prevailing south-to-northwesterly winds to the area of the Mangere Formation. This aeolian material overwhelmed the shallow lake and its surrounds with dunes. That the material of samples Sk1 and 2 was wind blown is clear from the photomicrographs of Figure 57 which show rounded grains, the larger fraction of which is well sorted. The smaller fraction is almost entirely altered

volcanic glass also derived from Red Bluff Tuff. Further evidence that this is aeolian-derived Red Bluff Tuff comes from a site on the Owenga Road, Chatham Island known to be of wind blown Red Bluff Tuff (K.Holt, pers. com.). Samples from this and the Skua Member were made into thin sections (Figures 57 to 59). These show that the lowest unit of the Skua Member is derived from Red Bluff Tuff. Further, comparison of photographs 1 to 3 of Figure 50 with photograph number 4 taken by K. Holt at grid reference 465615 just north of Red Bluff, Chatham Island shows a strikingly similar lithology even to the water tunnelling in these permeable sediments. Such dunes have also been observed above the sea cliffs of northwestern Pitt Island (Dr Clel. Wallace, Pers. Com.)

X-ray traces of these samples have almost exactly the same form (Figs. 59 and 60), raising the question of the relationship between them. It is possibile that these units have a similar origin and that samples Sk1 and 2 are reworked from Red Bluff Tuff. Further it seems likely that the two units Sk3 and Sk4, much paler in colour but lithologically similar to Sk1and Sk2, are also composed of unweathered wind-blown Red Bluff Tuff.

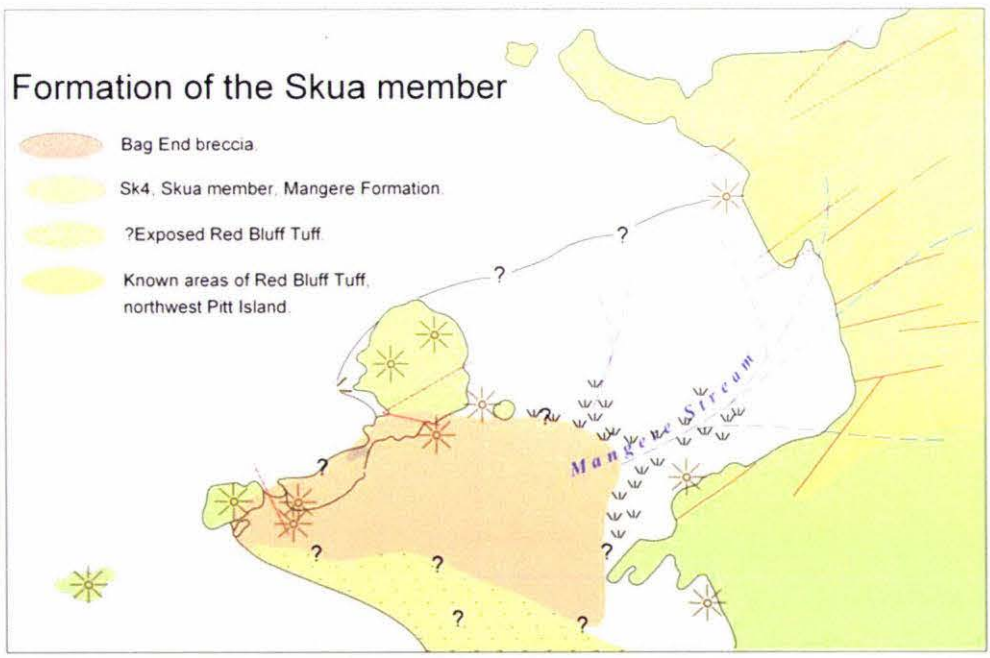

Figure 75. Deposition of the yellow-red sandstone unit (Sk1 and 2). Marine erosion uncovered a deposit of Red Bluff Tuff. Wind blown material from this exposure overwhelmed the lake and was deposited over a relatively wide area as is shown by the thickness of the deposit

4.4.4 Palynology (Figure 56)

Pollen sampling was widely spaced between the lower two units of the Skua Member. Sample Sk1 comes from immediately above the Carbonaceous Member which was being overwhelmed by wind blown Red Bluff Tuff and is essentially the same as that of Lk1 (fig.49). The high charcoal levels suggest that local fires occurred at this time possibly as a result of drier conditions. It is probable that much of the pollen for Sk2 came from vegetation growing in moist areas between dunes and from the periphery of the dune field. Except for grasses, the species show little variation between samples. Sample Sk3 is from the grey-white sandstone immediately above the yellow- red Sk1/2 unit. At this time, possibly as a result of fire as well as a drier climate, grass was dominant. No pollen was found above this level in the sequence.

4.4.5 Deposition of the tephra unit (Figure 75)

A very pure altered rhyolitic tephra caps the Mangere Formation. This appears to be the only outcrop of its kind and approximate age in the Chatham Islands (no other local sources have been reported to date). The only volcanism of comparable age are the unnamed Pliocene Volcanics of South East Island, Star Keys, and the Pyramid Phonolite, all of which are basic in composition (Campbell *et.al*, 1993 pp. 150 and 151) The nearest rhyolitic volcanism of approximately similar age is the North Island of New Zealand and it is inferred that New Zealand is the source of the Mangere tephra as New Zealand tephra are known to have reached the Chatham Islands (Campbell *et al.*, 1993 p. 162). Attempts to relate this tephra to the Taupo Volcanic Zone, New Zealand by microprobing was made difficult because of its state of alteration. Figure 55, which compares this tephra with older tephras from the Taupo Volcanic Zone, shows that the tephra contains three populations. Clearly the tephra bears a strong similarity to the Taupo Volcanic Zone tephras shown on the diagram (Figure 53) but at the present time any specific correlation remains problematic.

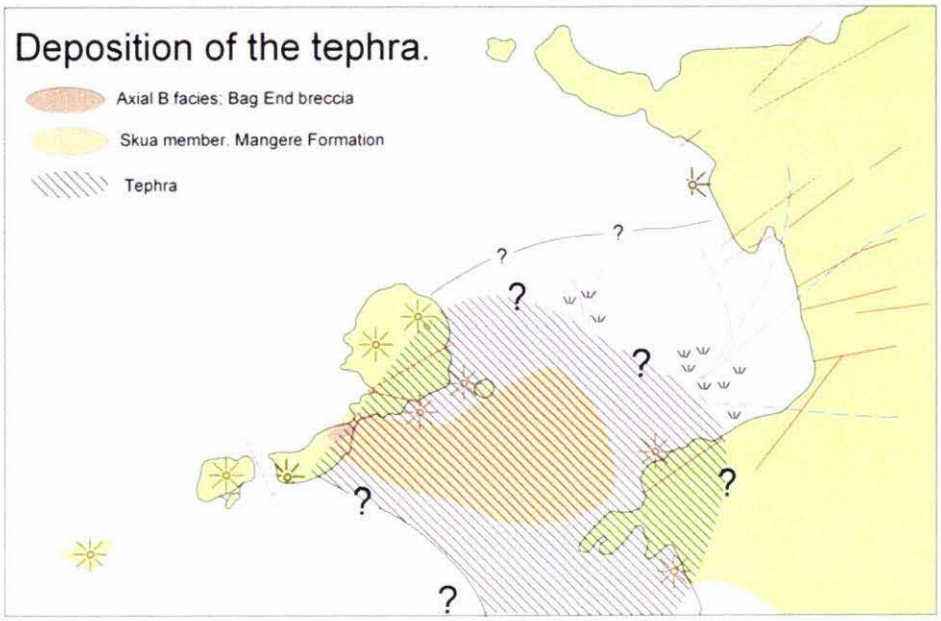

Figure 76. Model for the deposition of the tephra unit.

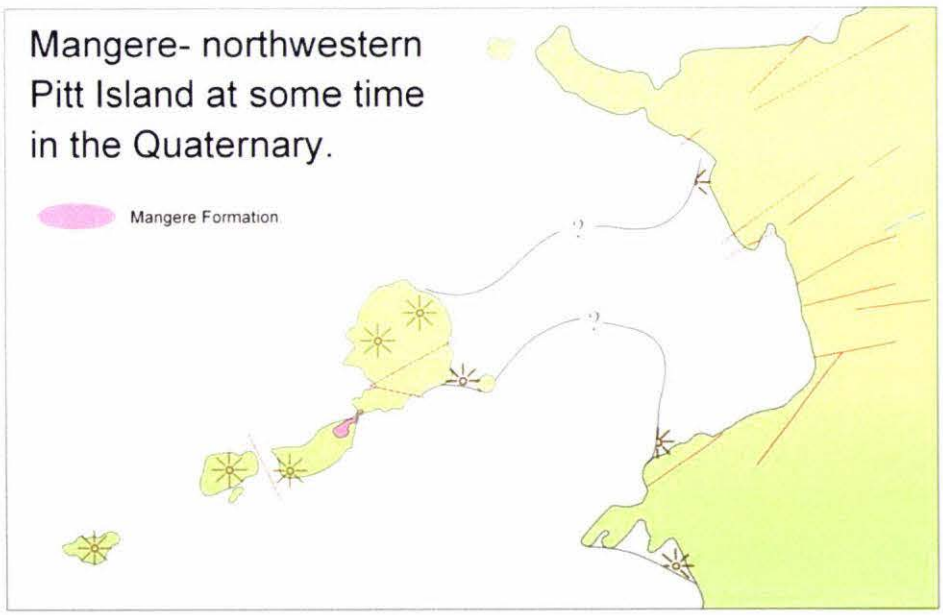

Figure 77. Model of Pitt and Mangere Islands by the mid-Quaternary. Mangere Formation has been reduced to a rapidly eroding remnant. That present day erosion also is rapid is suggested in Figure 34 and by the lack of chemical weathering of the rocks of the Formation.

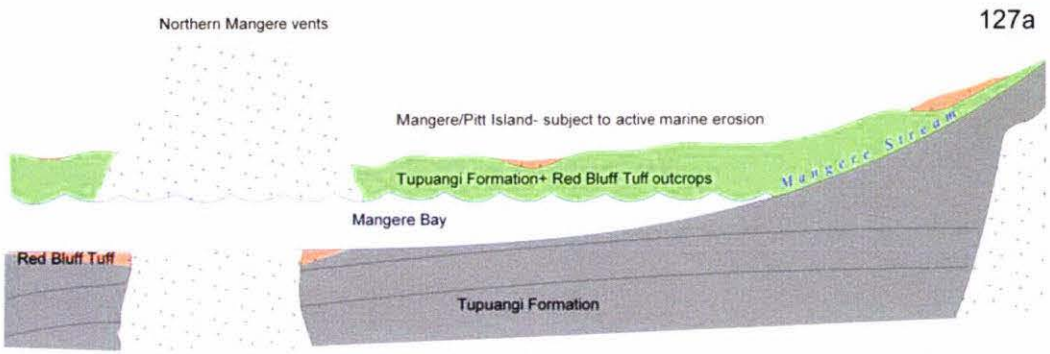

1. Mangere volcanoes have emerged from the sea. Mangere Bay lies between the northern and southern volcanoes. Kapitean? Some thermal doming.

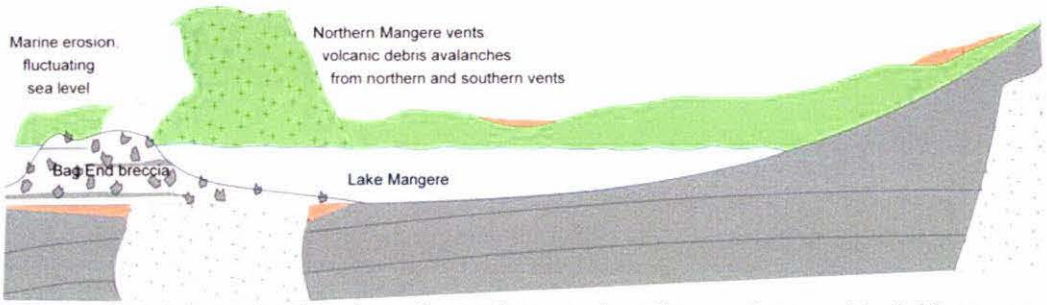

2 Volcanic debris avalanches from the northern and southern volcanoes block Mangere Bay to form Lake Mangere. Opoitian?

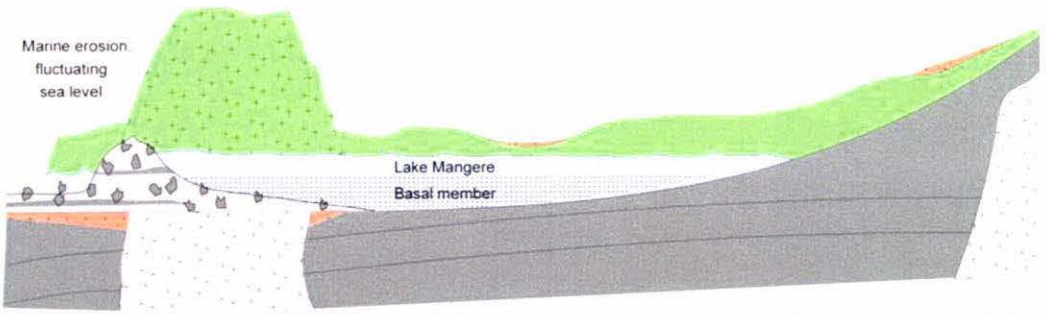

3. The volcanoes and Pitt/Mangere Island are vegetation-covered. Low energy conditions prevail. The fine-grained Basal member is deposited in Lake Mangere. Waipipian?

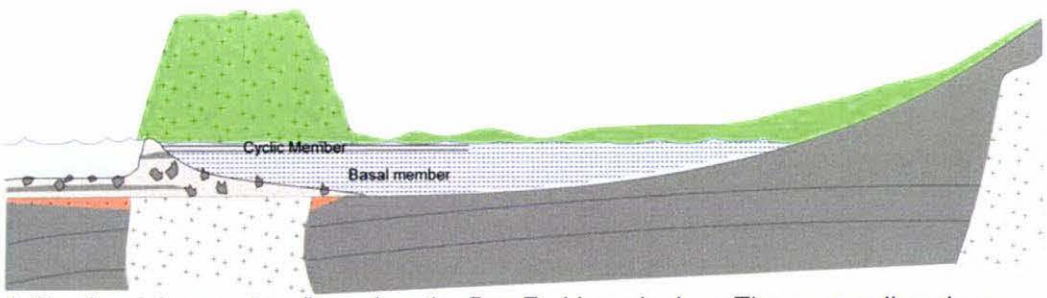

4. Sea level rise overtops/breaches the Bag End breccia dam. The surrounding slopes are destabilised and the Cyclic member sandstone units are deposited during storm events. Mangapanian?

Figure 78a. Diagrammatic summary of the history of the Mangere sedimentary sequence.

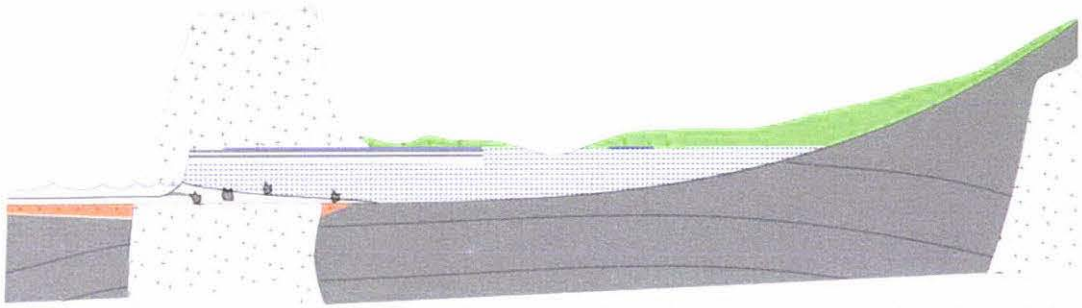

5.Uplift (further thermal doming?) and/or sea level fall. Subaerial erosion of Cyclic member. A shallow fresh water lake forms on top. Carbonaceous member is deposited. Marine erosion in Mangere Strait is attacking the Tupuangi and Mangere Formations.

Mangapanian-Nukumaruan?

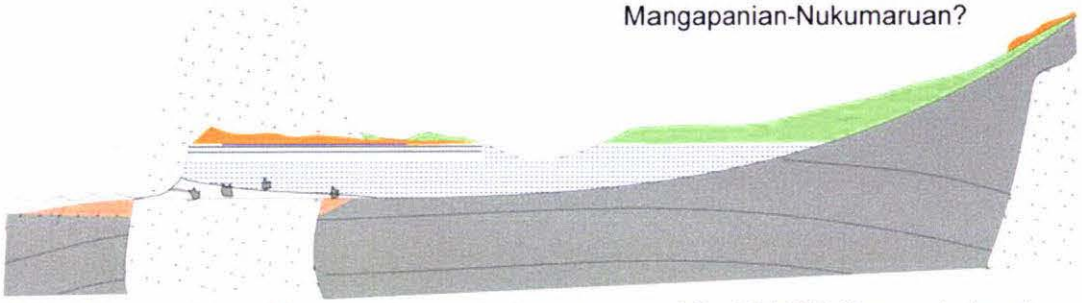

6 Wind blown material from marine eroded or uncovered Red Bluff Tuff overwhelms the lake. Deposition of the Skua member. Nukumaruan-Castlecliffian?

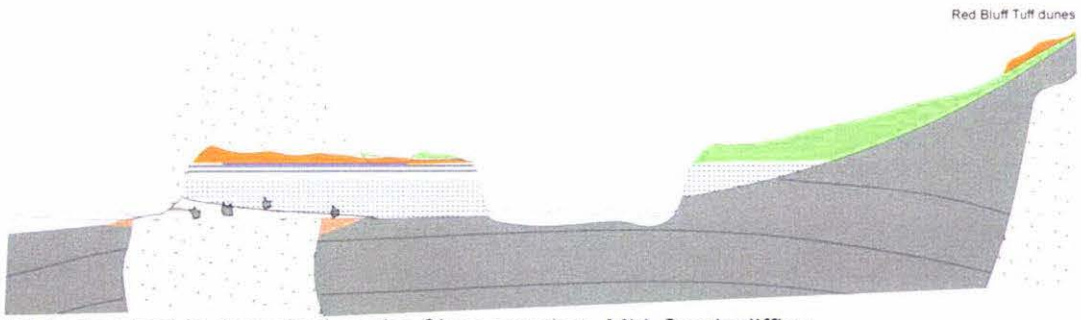

7A tephra bed is deposited on the Skua member. Mid-Castlecliffian.

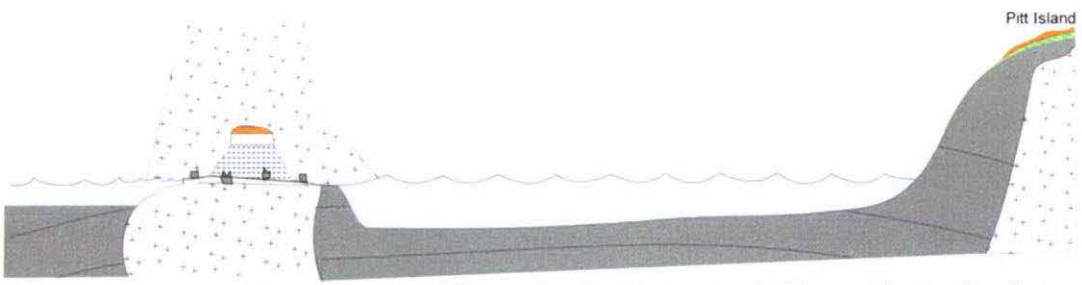

8. The poorly consolidated Tupuangi Formation has been eroded by marine action from around Mangere Island. The Mangere sedimentary sequence has been reduced to a remnant. Castlecliffian-Haweran?

Figure 78b. Diagrammatic summary of the history of the Mangere sedimentary sequence.

4.5.0 For further consideration:

4.5.1 Dating of the sequence.

The Mangere and Rangiauria Formations as a whole are rather vaguely dated with an upper limit for the Mangere Formation of Mangapanian on the strength of pollen grains whose position in the formation is not given.

It is frustrating that the Formation is so poorly time constrained (see Section 4.3.0). Even Rangiauria volcanism, is dated by only one radiometric date (6.1+-0.3Ma). The Whenuataru Tuff, which is reported to overlap the Rangiauria Breccia in age (Campbell.*et al.* 1993, p129), and may be contemporaneous with the Bag End Breccia, is given as 5-2.5Ma.

Perhaps the dating problem could be overcome by taking cores from the mudstones of the Basal and Cyclic Members at close intervals to match with known magnetic reversals. For Rangiauria volcanism the radiometric date might be verified by fission track dating of hornblende or augite. The Bag End Breccia might be time constrained by a close study of the macrofossils in this member.

The tephra does not contain zircons which might otherwise date it but rare earth elements might associate it with a Coromandel or TVZ tephra.

The thin sequence of strata at the southwestern end of the lower peninsula may repay study in case it once overlay the present Parakeet membera a possible complete sequence might be found if the tephra could be found under it. This sequence might also contain *Dracophyllum* pollen.

Chapter 5

Conclusions.

Tupuangi Formation is mapped as present on Mangere Island. It has the same lithology, heavy minerals, and pollen content as Tupuangi Formation on Pitt Island. Tupuangi Formation and its overlying strata extended subaerially from Pitt Island to at least Mangere Island at least as recently as the late Pliocene.

In the early Pliocene there were volcanic edifices centered approximately on northern Mangere Island and on southwest Mangere/Little Mangere Island

At this time there was an arm of the sea stretching toward Waihere Bay, Pitt Island between the Mangere Island northeastern and southwestern groups of Rangiauria volcanic vents. This sea arm was subsequently blocked to the seaward by a series of volcanic debris avalanches from the northeastern and southwestern groups of vents to form the Bag End breccia.

The result was the formation of an oligotrophic freshwater lake. Low energy conditions and vegetated slopes around the lake at this time resulted in the deposition of *ca.* 30 m of fine-grained sediment in the lake (the Basal Member of the Mangere Formation).This sediment was derived mainly from the Robin Bush Siltstone Member of the Rangiauria Breccia and also from the Tupuangi Formation and younger strata.

The Bag End breccia "dam" was then breached by the sea as a result of a rising sea level and/or land subsidence and the lake came under marine influence. The surrounding slopes were destabilized in severe storms resulting in the coarser sandstones being deposited. These storms alternated with low energy periods of mudstone deposition to produce the Cyclic Member, which conformably overlies the Basal Member of the Mangere Formation. Jointing in the sandstone units of the Cyclic member shows that the principal stress in the area was northwest-southeast. This was probably a result of thermal doming subsequent to the deposition of the Cyclic member and probably correlates with tectonic uplift in the Castlecliffian. Short wavelength ripples on the top of a number of the sandstone units of the Cyclic member indicate that the initial shallow marine conditions continued during its

deposition as a result of a rising sea level keeping pace with sedimentation in the lake.

This was followed by a sea level fall, plus tectonic uplift, which probably resulted in a period of subaerial erosion and a very low angular unconformity. A new freshwater lake developed on the ensuing surface with marginal mires, coastal small trees, shrubs, and herbs.

Continued marine erosion of the overlying strata of the Tupuangi Formation resulted in a deposit of Red Bluff Tuff (identified by a different population of hornblendes from those of the Rangiauria Breccia and Cyclic member) being exposed from which wind-blown material overwhelmed the lake, forming dunes. This formed the volcaniclastic yellow red unit, (Sk1 and 2 and possibly also Sk3 and 4) of the Skua member.

Volcanic activity, probably from the Taupo Volcanic Zone, deposited a layer of tuff (Sk 5) over the area. Continued marine erosion in the Quaternary separated Mangere Island from Pitt Island and reduced the Mangere sequence to the present-day remnant.

An attempt has been made in Fig. 79 to correlate the eustatic, tectonic, and depositional/ erosional events of the Mangere Formation to the 3rd order global sea level curve of Haq *et al.* (1987). If this correlation is correct the upper limit of the Parakeet formation is at least Castlecliffian.

Except for ostracods and a few small molluscs, the sequence is lacking in macrofossils, coccoliths, foraminifera, radiolarians, diatoms, and sponge spicules. Palynomorphs are relatively common in all units.

Throughout the sequence the coastal climate around Mangere Island appears to have been fairly equable, giving rise to a coastal association of small trees, shrubs, and herbs that changed little during its formation. A notable feature of the palynology of the sequence is a total lack of *Dracophyllum* pollen which suggests that *Dracophyllum* did not reach the Chatham Islands until the Pleistocene. It was probably introduced to the Chatham Islands from mainland New Zealand and/or the subantarctic islands by ocean-going birds.

The sequence could not be definitively dated from pollen or other fossil evidence. The best hope for dating it is to take a close series of siltstone samples

from the Mangere Formation to obtain their magnetic signature. A much closer study of the pollen of the Skua member and the mineralogy of its tephra cap may give information on their ages which may well be Pleistocene.

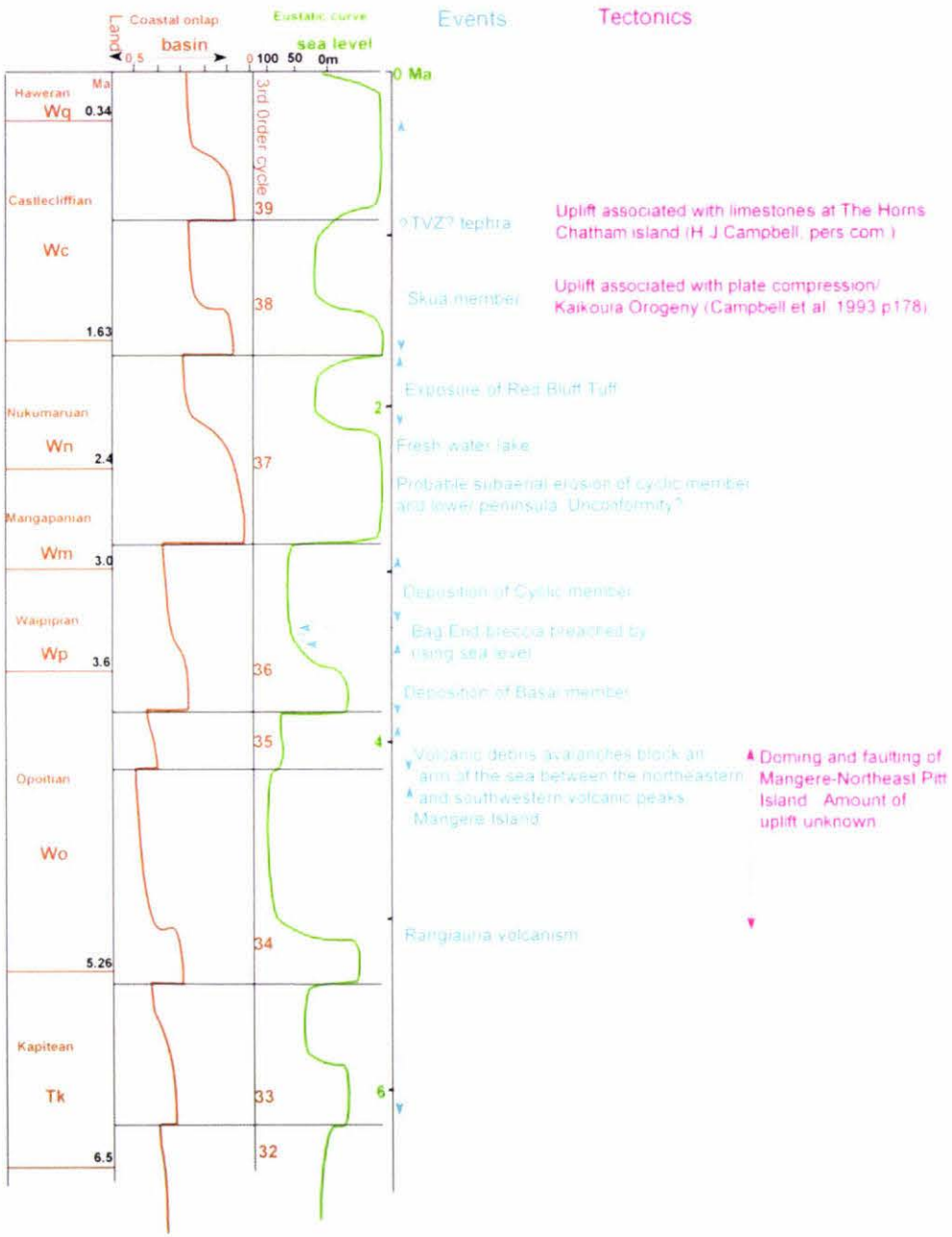

Figure 79. Correlation of the eustatic, tectonic, and depositional/erosional events of the study to the 3rd order global sea level curve of Haq *et al.* (1987).

REFERENCES.

Adams, C.J.D.; Robinson, P. 1977: Age of metamorphism of schists, Chatham Islands, New Zealand Plateau, southwest Pacific. *New Zealand Journal of Geology and Geophysics* 20: 287-301.

Allen, S.R. 2004: The Parnell grit beds revisited: are they all the products of sector collapse of western subaerial volcanoes of the Northland Volcanic Arc? *New Zealand Journal of Geology and Geophysics 47*: 509-524.

Andrews,P.B. 1982: Revised guide to recording field observations in sedimentary sequences. *Department of Scientific and Industrial Research, New Zealand.*

Austin, P.M.; Sprigg, R.C.; Braithwaite, J.C. 1973: Structure and petroleum potential of eastern Chatham Rise, New Zealand. *American Association of Petroleum Geologists.Bulletin 57*: 477-497.

Atkinson, I.A.E. 2003: A Restoration plan for Mangere Island, Chatham Islands group *New Zealand Department of Conservation.*

Ballance. P.; Gregory, M.R. 1991: Parnell Grits- large subaqueous volcaniclastic gravity flows with multiple particle-support. *SEPM (Society for Sedimentary Geology) Special Publication No. 45*: 189- 200.

Ballance, P.; Tappin, D.R.; Wilkinson, I.P: 2004: Volcaniclastic gravity flow sedimentation on a frontal arc platform: the Miocene of Tonga. *New Zealand Journal of Geology and Geophysics 47*: 567- 587.

Blackford, J.J. 2000: Charcoal fragments in surface samples following fire and the implications for interpretation of subfossil charcoal data. *Paleogeography Paleoclimatology, Paleoecology 164*: 33-42.

Boggs, S. 2001: Principles of sedimentology and stratigraphy. 3rd ed. Upper Saddle River.Prentice Hall.

Boyd, W.E. 1982a: Subsurface formation of charcoal and its possible relevance to the interpretation of charcoal in peat. *Quaternary Newsletter 37*: 5-8.

Bradshaw, J.D.; Andrews, P.B.; Adams C.J.D: 1981. Carboniferous to Cretaceous on the Pacific margin of Gondwana: the Rangitata phase of New Zealand. *Fifth International Gondwana Symposium, Wellington, New Zealand:* 217 - 221.

Brasier, M.D. 1980: Microfossils. London, Allen & Unwin.

Butler, K. R. (in press): Interpreting charcoal in New Zealand's paleoenvironment- what do the charcoal fragments really tell us? *Quaternary International.*

Campbell, H.J.; Andrews, P.B.; Beu, A.G.; Edwards, A.R.; Hornibrook, N de B.; Laird, M.G.; Maxwell, P.A.; Watters, W.A. 1988: Cretaceous-Cenozoic lithostratigraphy of the Chatham Islands. *Journal of the Royal Society of New Zealand 18*: 285-308.

Campbell, H.J.; Andrews, P.B.; Beu, A.G.; Maxwell, P.A.; Edwards,A.R.; Laird, M.G.; Hornibrook, N. de B.; Mildenhall, D.C.; Watters, W.A.;Buckeridge, J.S.; Lee, D.E.; Strong, C.P.; Wilson, G. J.; Hayward, B. W: 1993. Cretaceous-Cenozoic geology and biostratigraphy of the Chatham Islands, *New Zealand. Institute of Geological and Nuclear Sciences* Monograph 2.

Clark, J.S.; 1988: Particle motion and the theory of charcoal analysis: source area export and sampling. *Quaternary Research. 30*: 67-80.

Collinson, J. D.; Thompson, D. B. 1989: Sedimentary Structures. 2nd ed. New York, Harper Collins Academic.

Department of Lands and Survey: RNZAF (sortie 197), Aerial Plan 1074, 1974, 1:12000, Photogrammetric Branch.

Faegri,K.; Iveson J. 1964: Textbook of pollen analysis. 2nd ed. Oxford. Blackwell.

Folk, R. L.; Ward, W. C. 1957: Brazos river bar: a study in the significance of grain size parameters. *Journal of Sedimentary petrology 27*: 3-26.

Froggatt, P R. 1983: Toward a comprehensive upper Quaternary tephra and ignimbrite stratigraphy of New Zealand using electron microprobe analysis of glass shards. *Quaternary Review 19*: 188-200.

Grindley, G.W.; Adams, C.J.D.; Lumb, J.T.; Watters, W.A. 1977: Paleomnagnetism, Kr dating and tectonic interpretation of Upper Cretaceous and Cenozoic volcanic rocks of the Chatham Islands New Zealand. *New Zealand Journal of Geology and Geophysics 20*: 425-467.

Glicken, H. 1991: Facies architecture of large volcanic- debris avalanches. *SEPM (Society for Sedimentary Geology) Special Publication No. 45:* 99- 108.

Hay, R.; Mutch,A.R.; Watters, W.A. 1970: Geology of the Chatham Islands. *New Zealand Geological Survey Bulletin 83:* 1-86.

Hornibrook, n. de B. 1968: A handbook of New Zealand microfossils (foraminifera and ostracoda). *New Zealand Geological Survey handbook, information series 62*:1-136.

Jian Qin. 2005: Bio-hydrocarbons from algae- impacts of temperature, light and salinity on algae growth. *http://www.geo.arizona.edu/palynology/ppalgal.html*. Site accessed 19 Sept, 2005.

King, P.R. 2000: Tectonic reconstructions of New Zealand: 40 Ma to the present. *New Zealand Journal of Geology and Geophysics 43*: 611- 638.

King, M 1990: A land Apart: The Chatham Islands of New Zealand. Auckland, New Zealand. Random Century.

Knox, G.A. 1957: General account of the Chatham Islands 1957 expedition. *New Zealand Department of Scientific and Industrial Research. Bulletin 122.*

Krumbein, W.C. ;Petttijohn, F. J. 1961: Manual of sedimentary petrography. New York. Appelton-Century-Crofts.

Large, M. F.; Braggins, J.E. 1991: Spore atlas of New Zealand. *Supplement to New Zealand Journal of Botany.*

Land Information Topographic map 260 Ed 1, 1981, 1:50000. Chatham Islands, Sheet 2.

Mildenhall, D.C. 1976: Exotic pollen rain on the Chatham Islands during the late Pleistocene. *New Zealand journal of geology and geophysics 19*: 327-333.

-1983: Late Cretaceous in situ and Permian to Jurassic recycled palynomorphs from the Waihere Formation and Kahuitara Tuff, Chatham Islands, New Zealand. *XV Pacific Science Conference Dunedin, New Zealand. Programme abstracts and congress information: 165.*

-1994:Palynological reconnaissance of Early Cretaceous to Holocene sediments, Chatham Islands. *New Zealand. Institute of Geological and Nuclear Sciences. Monograph 7.*

Mildenhall, D.C.; Crosbie, Y.M.; 1981: Remanie Permian and ? Triassic spores and Pollen from the Waihere Formation and Kahuitara Tuff (late Cretaceous),Pitt Island, Chatham Islands New Zealand. (Abstract) *New Zealand Geological survey Conference, Turangi*: 22-23.

Mildenhall, D.C.; Wilson, G.J. 1976: Redeposited lower and upper Cretaceous palynomorphs from Mangere Formation, Mangere Island, Chatham Islands,New Zealand. *New Zealand journal of geology and geophysics 21*: 661-662.

-1978. Cretaceous palynomorphs from The Sisters islets, Chatham Islands, New Zealand. *New Zealand journal of geology and geophysics 1*:121-6.

Moar, N.T. 1993: Pollen grains of New Zealand dicotyledenous plants. Manaaki Whenua Press. Landcare Research New Zealand.

Morris, P.A. 1985a: Petrology of late Cretaceous alkaline rocks from the Chatham Islands, New Zealand. *New Zealand Journal of Geology and Geophysics 28*:253-266.

Munsell Soil Colour Charts. 1994: Revised edition, Macbeth Publications.

Neall, V.E., Davies, G., Wallace, R.C. 2005. Twin Peaks: The pre-Mangere formation sequence on Mangere Island, Chatham Islands. *Geological Society of New Zealand Abstracts*, 2005.

Palmer, B.A.; Alloway, B.V.; Neall, V.E. 1991: Volcanic-debris-avalanche deposits in New Zealand- lithofacies organization in unconfined wet avalanche flows *SEPM (Society for Sedimentary Geology) Special Publication No. 4:* 89-98.

Patterson III, W.A.; Edwards, K.J.; Maguire, W.J. 1987: Microscopic charcoal as a fossil indicator of fire. *Quaternary Research 6*: 3-23.

Pettijohn, F.S.; Potter, P.E.; Siever, R. 1972: *Sand and sandstone.* New York, London. Springer Verlag.

Phillips, F.C. 1972: Stereographic projection in structural geology. London. Edward Arnold.

Reineck, H.E.; Singh, I.B. 1980: Depositional sedimentary environments. 2nd Ed. Berlin, New York.Springer-Verlag.

Shane, P.A.R.; Froggat, P.C. 1994: Discriminant function analysis of glass chemistry of New Zealand and North American tephra deposits. *Quaternary Research. 41*:70-81.

Shane, P.A.R. 2000: Tephrochronology: a New Zealand case study. *Earth Science Review. 49*: 223- 259.

Shane, P.A.R.; Black, T.M.; Alloway, B. V.; Westgate, J.A. 1966 Early to middle Pleistocene tephrochronology of North island, New Zealand: Implications for volcanism, tectonism, and paleoenvironments. *Geological Society of America Bulletin 108*: 915-925.

Strong, C.P.; Edwards, A.R. 1979: Late Haumurian (Maastrichtian) microfossils from Chatham Islands, New Zealand. *New Zealand Journal of Geology and Geophysics 22*: 613-619.

Watters, W. A. 1978: Notes on the geology of Mangere and South East Islands, Chatham Islands. *New Zealand Geological Survey report G22*: 1-32.

Whitton, J.S.; Churchman, G.J. 1987: Standard methods for mineral analysis of soil survey samples for characterization and classification in NZ Soil Bureau. *New Zealand Soil Bureau report 79.*

Wood, R.A.; Ingham, C.E. 1981: Chatham Islands refraction survey. *New Zealand Survey Report G48*: 1-17.

Wood, R.A.; Anderson, H.J. 1989: Basement structure at the Chatham Islands. *Journal of the Royal Society of New Zealand 19*: 269-282.

Wood, R.A.; Andrews, P.B.; Herzer, R.H.; and others, 1989: Cretaceous and Cenozoic geology of the Chatham Rise. *New Zealand Geological Survey basin studies 3.*

Bibliography

Adams, A.E.; McKenzie, W.S.; Guilford, C. 1984: *Atlas of sedimentary rocks under the microscope.* Burnt Mill, Harlow.Longman Group.

Allan, R.S. 1925: Preliminary account of the geology of the Chatham Islands. *New Zealand Journal of Science and Technology B7*: 290-294.

-1929: Chatham Islands: The physical features and structure. *Transactions of the New Zealand Institute 59*: 824-834.

Allen, J.R.L. 1982: Sedimentary structures their character and physical basis vol. 1. Amsterdam, New York. Elsevier Scientific Publications.

Barber, H.G.; Haworth, E.Y. 1981: A guide to the morphology of the diatom frustule. *Fresh Water Biological Association scientific publication no. 44.*

Berner, R.A. 1980: Early diagenesis- a theoretical approach. Princeton Press.

-1982b: Subsurface formation of charcoal: an unexplained event in peat. *Quaternary Newsletter 38*: 15-16.

Boyd, W.B.1982b: Subsurface formation of charcoal: an unexplained event in peat. *Quaternary Newsletter* 38: 15-16.

Bush, M.B. Piperno, D.R.; Colvineau P.A.; Oliviera, P.E.; Krissick, L.A.; Miller, M.C.; Rowe W.E. 1992: A 14300 yr paleoecological profile of a lowland tropical lake in Panama. *Eclogical Monographs. 63 (2):*251-275.

Chen, J. K.; Taylor, F. W.; Edwards, R.L.; Hai Cheng; Burr, G.S. 1955:Recent emerged reef terraces of the Yenkahe resurgent block, Tanna. Vanuatu: implications for volcanic, landslide and Tsunami Hazards. *Journal of Geology 103*: 577-590.

Clarke, J.S. 1988: Particle motion and the theory of charcoal analysis: source area. *Quaternary Research 30* 67-80.

Clark, R.L. 1982: Point count estimation of charcoal in pollen preparations and thin sections of sediments. *Pollen et Spores 24*: 523-535.

-1984. Effects on charcoal of pollen preparation procedures. *Pollen et Spores 26*:559-579.

Collinson, J.D.; Thompson, D.B. 1989. *Sedimentary structures.* London. Unwin Hyman.

De Lange, P.J.; Saywer, J.W.D.; Ansell,R. 1999: Checklist of indigenous vascular plant species recorded from Chatham Islands. Wellington. Department of Conservation.

Dodson, J.R. 1976: Modern pollen spectra from Chatham Island, New Zealand. *New Zealand Journal of Botany 14*: 341-347.

Eliot, M.B.; Flenley, J.R.; Sutton, D.J. 1998: A Late Holocene pollen record of deforestation and environmental change from the Lake Tauanui catchment, Northland, New Zealand. *Journal of Paleolimnology 19*: 23-32.

Figueral,I.; Mosbrugger,V. 2000: A review of charcoal analysis as a tool for assessing Quaternary and Tertiary environments: achievements and limitations. *Paleogeography, Paleoclmatology, Paleoecology 4*: 397-407.

Fisher, R.V.; Smith, G.A. 1991. Sedimentation in volcanic settings. *SEPM (Society for Sedimentary Geology) Special publication No 45.*

Guy-Ohlson, O. 1992: Botryococcus algae as an aid in the interpretation of paleoenvironmental and depositional processes. *Review of Paleobotany and palynology. 71*: 1-15.

Hector,J. 1869: Notes on the Geology of the outlying islands of New Zealand. Chatham Islands. *Transaction of the New Zealand Institute 2*: 183.

Kear, D. 1957: Erosional stages of volcanic cones as indicators of age. *New Zealand Journal of science and technology B38*: 671-682.

Land Information New Zealand, 1998: Chatham Islands. Sheet 2, 1:50000.

Lewis, D.W.; McConchie, V.D. 1994: Analytical sedimentology. Chapman Hall.

McMinn, A.; Howard, W.R.; Roberts, D. 2001: Late Pliocene dinoflagellate cyst and diatom analysis from a high resolution sequence in DSDP Site 594, Chatham Rise, south west Pacific. *Marine micropaleontology 3-4*: 207-221.

Moss, B.1998. Ecology of fresh water. 3rd Ed. Blackwell Science Ltd.

Smale, D. 1982: Heavy minerals from Cretaceous sandstones of Pitt Island, Chatham Islands. *New Zealand Geological Survey report SL3*: 1-6.

Potts, P.J.; Bowles, J.F.W.; Reed, S.J.B.; Cave, M.R. 1995: Microprobe techniques in the earth sciences. Ch 2 *The mineralogical Society Series.* Chapman & Hall.

Scott, A.C.; Cripps J.A.; Collinson M.E.; Nicholls G.J. 2000: The taphomony of charcoal following a recent heathland fire and some implications for the interpretation of fossil charcoal deposits. *Paleogeography, Paleoclimatology, Paleoecology 164* (1-4): 1-31.

Shelley, D. 1985: Optical Mineralogy. 2nd Ed. Department of Geology, University of Canterbury. Christchurh, New Zealand.

Sewell, R. J. 1988: Late Miocene volcanic stratigraphy of central Banks Peninsula, Canterbury, New Zealand. *New Zealand Journal of Geology and Geophysics, 31*: 41-64.

Telford, R.J.; Barker, P.; Metcalf, S.; Newton, A. 2004: Lacustrine responses to tephra deposition: examples from Mexico. *Quaternary science reviews Vol.23: nos.23-24,* 2337-2353.

Thompson, C.S. 1983: The weather and climate of the Chatham Islands. New Zealand Meteorological Service.

Tucker, M. 1998: Techniques in Sedimentology. Blackwell Scientific Publications.

Van der Lingen, G.J.; 1968: The turbidite problem. *New Zealand Journal of Geology and Geophysics 12:* 7-50.

Wardle, P. 1987: Dracophyllum (Epacridaceae) in the Chatham and subantarctic islands of New Zealand. *New Zealand journal of botany 25*: 107-104.

-1990. Cambridge. Vegetation of New Zealand.

Winkler,M.G. 1985: Charcoal analysis for paleoenvironmental interpretation: a chemical assay. *Quaternary Research 23*: 313-326.

White, J.D.L. 1992: The depositional record of small, monogenetic volcanoes within terrestrial basins. *SEPM (Society for Sedimentary Geology) Special Publication No. 45:*155-174.

Wood, R.A.; Ingham, C.E. 1981: Chatham Islands refraction survey. *New Zealand Geological Survey Report G48*: 1-17.

Appendix 1.

Grain size data for Cyclic member.

Basal member. Grain size distribution for samples 1b, 3b, 5b.

	Weight in grams			Weight %		
Sample	1b	3b	5b	1b	3b	5b
>63um	3.193	0.789	2.311	28%	10%	19%
63-4um	2.037	2.088	5.192	18%	26%	44%
<4 um	6.058	5.192	4.369	54%	64%	37%
	11.288	8.069	11.872	100%	100%	100%

Cyclic Member, unit 13c

µm	Weight in grams, Top	Weight %	Weight in grams, Base	Weight %	Cumulative %	
500-1000	1.45	12%	5.39	26%	12%	26%
250-500	1.55	13%	4.36	21%	25%	48%
125-250	2.06	17%	3.6	18%	42%	65%
63-125	1.85	15%	2.73	13%	57%	78%
32-63	2.3	19%	2.37	12%	76%	90%
<32	2.83	24%	2.037	10%	100%	100%
Total	12.04	100%	20.487	100%		

Cyclic Member, unit 20c

µm	Weight in grams, Top	Weight %	Weight in grams, Base	Weight %	Cumulative %	
500-1000	0.877	9%	5.479	22%	9%	22%
250-500	1.356	14%	4.502	18%	24%	41%
125-250	2.068	22%	5.38	22%	45%	63%
63-125	1.296	14%	3.944	16%	59%	79%
32-63	1.73	18%	3.02	12%	77%	92%
<32	2.132	23%	2.037	8%	100%	100%
Total	9.459	100%	24.362	100%		

Cyclic Member, unit 13c

um	Top (g)	Wt %	Base (g)	Wt %	Cumulative %	
500-1000	1.45	12%	5.39	26%	12%	26%
250-500	1.55	13%	4.36	21%	25%	48%
125-250	2.06	17%	3.6	18%	42%	65%
63-125	1.85	15%	2.73	13%	57%	78%
32-63	2.3	19%	2.37	12%	76%	90%
<32	2.83	24%	2.037	10%	100%	100%
Total	12.04	100%	20.487	100%		

Turbidite, unit 28c

	North end of unit				South end of unit			
µm	Top (g)	Wt %	Base (g)	Wt %	Top (g)	Wt %	Base (g)	Wt %
500-1000	2.22	9%	4.917	26%	1.23	7%	2.06	22%
250-500	2.56	11%	4.43	23%	1.64	9%	1.45	15%
125-250	4.24	18%	2.474	13%	2.493	14%	1.285	14%
63-125	3.96	17%	2.433	13%	3.2	18%	1.72	18%
32-63	4.8	20%	2.75	15%	3.74	21%	1.55	16%
<32	5.86	25%	1.85	10%	5.25	30%	1.35	14%
Total	23.64	100%	18.854	100%	17.553	100%	9.415	100%

Grain size analysis. Skua Member, units Sk3 and 4.

	Sk3 (g)	Wt %	Sk4 (g)	Wt %
>500µm	11.25	8%	18.3	12%
500-250	13.5	9%	22.2	15%
250-125	19.05	13%	19.95	13%
125-63	31.35	21%	28.8	19%
63-32	29.7	20%	30.3	20%
<32µm	44.85	30%	49.05	33%
	149.7		168.6	

Appendix 2

Electron microprobe analyses of glass shards from tephra sample Sk5.

	SiO2	TiO2	Al2O3	FeO	MnO	MgO	CaO	Na2O	K2O	Total
MF4-Ca glass 1	72.43	0.14	11.98	0.86	0.10	0.04	0.96	4.21	3.67	94.39
MF4-Ca glass 1b	72.43	0.14	11.98	0.86	0.10	0.04	0.96	4.21	3.67	94.39
MF4-Ca glass 2	72.43	0.14	11.98	0.86	0.10	0.04	0.96	4.21	3.67	94.39
MF4-Ca glass 3	72.43	0.14	11.98	0.86	0.10	0.04	0.96	4.21	3.67	94.39
MF4-Ca glass 4	72.43	0.14	11.98	0.86	0.10	0.04	0.96	4.21	3.67	94.39
MF4-Ca glass 5	72.43	0.14	11.98	0.86	0.10	0.04	0.96	4.21	3.67	94.39
MF4-Ca glass 6	72.43	0.14	11.98	0.86	0.10	0.04	0.96	4.21	3.67	94.39
MF4-Ca glass 7	72.43	0.14	11.98	0.86	0.10	0.04	0.96	4.21	3.67	94.39
MF4-Ca glass 8	72.43	0.14	11.98	0.86	0.10	0.04	0.96	4.21	3.67	94.39
MF4-Ca glass 9	72.43	0.14	11.98	0.86	0.10	0.04	0.96	4.21	3.67	94.39
MF4-Ca glass 10	72.43	0.14	11.98	0.86	0.10	0.04	0.96	4.21	3.67	94.39
MF4-Ca glass 11	72.43	0.14	11.98	0.86	0.10	0.04	0.96	4.21	3.67	94.39
	72.43	0.14	11.98	0.86	0.10	0.04	0.96	4.21	3.67	94.39
Normalised	72.43	0.14	11.98	0.86	0.10	0.04	0.96	4.21	3.67	94.39
MF4-Ca glass 1	72.43	0.14	11.98	0.86	0.10	0.04	0.96	4.21	3.67	94.39
MF4-Ca glass 1b	72.43	0.14	11.98	0.86	0.10	0.04	0.96	4.21	3.67	94.39
MF4-Ca glass 2	72.43	0.14	11.98	0.86	0.10	0.04	0.96	4.21	3.67	94.39
MF4-Ca glass 3	72.43	0.14	11.98	0.86	0.10	0.04	0.96	4.21	3.67	94.39
MF4-Ca glass 4	72.43	0.14	11.98	0.86	0.10	0.04	0.96	4.21	3.67	94.39
MF4-Ca glass 5	72.43	0.14	11.98	0.86	0.10	0.04	0.96	4.21	3.67	94.39
MF4-Ca glass 6	72.43	0.14	11.98	0.86	0.10	0.04	0.96	4.21	3.67	94.39
MF4-Ca glass 7	72.43	0.14	11.98	0.86	0.10	0.04	0.96	4.21	3.67	94.39
MF4-Ca glass 8	72.43	0.14	11.98	0.86	0.10	0.04	0.96	4.21	3.67	94.39
MF4-Ca glass 9	72.43	0.14	11.98	0.86	0.10	0.04	0.96	4.21	3.67	94.39
MF4-Ca glass 10	72.43	0.14	11.98	0.86	0.10	0.04	0.96	4.21	3.67	94.39
MF4-Ca glass 11	72.43	0.14	11.98	0.86	0.10	0.04	0.96	4.21	3.67	94.39

FeO:CaO;K2O ratios

FeO	CaO	K2O	Total	FeO%	CaO%	K2O%
0.91	1.02	3.88	5.81	15.7	17.5	66.8
0.98	1.03	3.79	5.80	16.8	17.7	65.4
2.45	1.78	3.11	7.33	33.4	24.2	42.4
2.61	1.85	3.28	7.74	33.7	23.9	42.4
2.66	1.62	3.37	7.65	34.7	21.1	44.1
2.38	1.28	3.86	7.52	31.7	17.0	51.4
2.67	1.74	3.16	7.57	35.3	23.0	41.8
1.63	1.26	3.33	6.23	26.2	20.2	53.5
2.70	1.84	3.26	7.80	34.6	23.6	41.8
1.48	1.24	3.57	6.29	23.5	19.8	56.8
1.78	1.14	4.00	6.92	25.8	16.4	57.8
2.68	1.93	3.14	7.74	34.6	24.9	40.6

FeO	Na2O	K2O	total	FeO%	Na2O%	K2O%
0.91	4.45	3.88	9.25	9.8	48.2	42.0
0.98	4.34	3.79	9.11	10.7	47.6	41.7
2.45	4.67	3.11	10.23	23.9	45.7	30.4
2.61	4.50	3.28	10.39	25.1	43.3	31.6
2.66	4.62	3.37	10.64	24.9	43.4	31.7
2.38	3.55	3.86	9.79	24.3	36.2	39.4
2.67	4.24	3.16	10.07	26.5	42.1	31.4
1.63	4.08	3.33	9.05	18.1	45.1	36.8
2.70	4.63	3.26	10.59	25.5	43.7	30.8
1.48	4.01	3.57	9.06	16.3	44.2	39.4
1.78	4.01	4.00	9.79	18.2	41.0	40.8
2.68	4.63	3.14	10.45	25.6	44.3	30.1

Appendix 3.

3. Electron microprobe analyses of hornblende from Rangiauria Breccia, Cyclic member sample 30c and Skua member samples Sk1 and 2.

Sample ID	Proportion of the cations based on 23 oxygens								
	Si	Ti	Al	Fe	Mn	Mg	Ca	Na	K
ID = 11373 R-Brec 1	11.80	1.07	3.78	1.19	0.03	2.90	1.76	0.33	0.14
ID = 11374 R-Brec 2	11.74	1.11	3.72	1.23	0.02	2.85	1.80	0.38	0.17
ID = 11375 R-Brec 3	11.72	1.16	3.78	1.15	0.04	2.90	1.75	0.30	0.16
ID = 11376 R-Brec 4	11.72	1.16	3.78	1.15	0.04	2.90	1.75	0.30	0.16
ID = 11377 R-Brec 5	11.71	1.13	3.85	1.10	0.02	2.91	1.77	0.33	0.16
ID = 11379 R-Brec 6	11.77	1.10	3.73	1.24	0.01	2.85	1.80	0.33	0.15
ID = 11381 R-Brec 7	11.75	1.08	3.63	1.46	0.02	2.66	1.85	0.39	0.15
ID = 11384 CM-30c 1	11.70	1.12	3.81	1.12	0.00	2.94	1.76	0.37	0.16
ID = 11385 CM-30c 2	11.90	0.79	3.88	1.44	0.01	2.81	1.70	0.34	0.11
ID = 11386 CM-30c 3	11.83	1.03	3.70	1.19	0.01	2.96	1.77	0.33	0.16
ID = 11387 CM-30c 4	11.80	1.08	3.71	1.30	0.01	2.77	1.78	0.33	0.17
ID = 11389 CM-30c 5	11.81	1.08	3.76	1.21	0.02	2.90	1.73	0.34	0.14
ID = 11390 CM-30c 6	11.81	1.08	3.78	1.16	0.01	2.88	1.77	0.34	0.15
ID = 11391 CM-30c 7	11.77	1.05	3.79	1.20	0.03	2.88	1.76	0.33	0.15
ID = 11392 Sk 3 SS 1	11.48	1.14	3.78	2.05	0.01	2.38	1.69	0.31	0.15
ID = 11394 Sk 3 SS 2	11.62	1.00	3.97	1.7	0.03	2.06	1.80	0.41	0.13
ID = 11396 Sk 3 SS 3	11.88	0.94	3.76	1.46	0.02	2.31	1.77	0.36	0.13
ID = 11397 Sk 1&2 SS 1	11.89	1.08	3.66	1.75	0.04	2.26	1.84	0.32	0.14
ID = 11398 Sk 1&2 SS 2	11.70	1.01	3.97	1.75	0.02	2.33	1.76	0.35	0.11
ID = 11399 Sk 1&2 SS 3	11.78	0.95	3.68	1.71	0.01	2.38	1.84	0.39	0.12

Sample	Mg	Fe	Na+K	Mg/Mg+Fe
Rbrec-1	2.9	1.19	0.47	0.71
Rbrec-2	2.85	1.23	0.55	0.69
Rbrec-3	2.9	1.15	0.46	0.72
Rbrec-4	2.9	1.15	0.46	0.72
Rbrec-5	2.91	1.1	0.49	0.72
Rbrec-6	2.85	1.24	0.48	0.7
Rbrec-7	2.66	1.46	0.54	0.65
CM-1	2.94	1.12	0.53	0.72
CM-2	2.81	1.44	0.45	0.66
CM-3	2.96	1.19	0.49	0.71
CM-4	2.77	1.3	0.5	0.68
CM-5	2.9	1.21	0.48	0.7
CM-6	2.88	1.16	0.49	0.71
CM-7	2.88	1.2	0.48	0.7
Sk3	2.38	2.05	0.46	0.54
Sk3	2.06	1.98	0.54	0.5
Sk3	2.31	1.7	0.49	0.57
Sk1&2	2.26	1.75	0.46	0.56
Sk1&2	2.33	1.75	0.46	0.57
Sk1&2	2.38	1.71	0.51	0.58